ABSTRACT

Title of Document: KINETICS IN INDIVIDUALS WITH
UNILATERAL TRANSTIBIAL
AMPUTATIONS USING RUNNING-
SPECIFIC PROSTHESES

Brian Svercauski Baum, Ph.D., 2012

Directed By: Associate Professor Jae Kun Shim, Department
of Kinesiology

Improvements in rehabilitation and prosthetic design are needed to help promote

activities such as running that increase physical activity levels of individuals with lower

extremity amputation (ILEA). However, effectively developing these improvements

requires a detailed understanding of prosthetic and ILEA running biomechanics.

Running-specific prostheses (RSPs) have been developed to improve running

performance for ILEA runners, but altered running kinetics may still be necessary to

accommodate for the loss of musculoskeletal function caused by lower extremity

amputation. The few studies investigating ILEA running with RSPs focus on maximal

performance, but our understanding of how ILEA using RSPs modulate kinetics to run at

submaximal velocities remains limited. The purpose of this study was to characterize

changes in kinetics and mechanical energy across a range of running velocities in ILEA

wearing RSPs. This dissertation investigated six specific aims through six corresponding

experiments that improve our knowledge of mechanical and anthropometric properties of

RSPs and the kinetic profiles of ILEA running at submaximal velocities. Four common RSP designs were tested for mechanical and anthropometric properties. ILEA with unilateral transtibial amputations who wear RSPs and an able-bodied control group participated in the running experiments. Mechanical and anthropometric results indicated that RSP marker placement had little effect on joint kinetic estimations proximal to the prostheses, and trifilar pendulums can measure moments of inertia with <1% error. The running experiments provided the first 3D kinetic descriptions of ILEA running. The prosthetic limb typically generated lower peak kinetic parameters and 50% lower total mechanical work than the intact and control limbs, indicating a greater reliance on the intact limb. To counter the prosthetic limb deficiencies, ILEA increased stride frequencies compared to control subjects. Additionally, the prosthetic limb demonstrated prolonged periods of anterior ground reaction force to increase propulsive impulse and prolonged hip stance phase extension moments that generated increased hip concentric work. The data indicated that ILEA wearing RSPs run differently than able-bodied runners and use several adaptive mechanisms to run at the same velocity and to increase running velocity. These mechanisms are discussed and future directions of research are suggested.

KINETICS IN INDIVIDUALS WITH UNILATERAL TRANSTIBIAL
AMPUTATIONS USING RUNNING-SPECIFIC PROSTHESES

By

Brian Svercauski Baum

Dissertation submitted to the Faculty of the Graduate School of the
University of Maryland, College Park, in partial fulfillment
of the requirements for the degree of
Doctor of Philosophy
2012

Advisory Committee:
Professor Jae Kun Shim, Chair
Dr. Arick Auyang
Professor Adam H. Hsieh
Professor John J. Jeka
Dr. Erik J. Wolf

Acknowledgements

No dissertation is completed entirely on one's own, and I wish to thank everyone who has helped me along the way. First, to Dr. Jae Kun Shim, my advisor, I thank you for your exemplary guidance and advice throughout the Ph.D. process. Your leadership and tireless work ethic have provided constant aspiration and have continued to drive me to reach as high as possible. To my dissertation advisory committee, Dr. Arick Auyang, Dr. Adam Hsieh, Dr. John Jeka, and Dr. Erik Wolf, I thank you all for your valuable critiques that have improved this dissertation and discussions that have challenged me and made me continue to examine questions from a multitude of angles. To the Department of Kinesiology at the University of Maryland, College Park, you have provided outstanding support and education with inspiring staff and graduate students. A huge thank you is deserved to the Neuromechanics Laboratory graduate students and post-doctoral associates, in particular Roozbeh Borjian, Kyung Koh, Alison Linberg, Dr. Hiroaki Hobara, Dr. You-Sin Kim, and Dr. Hyun Joon Kwon. You all have been instrumental in my success and learning through lively discussions, programming assistance, equipment building study subjects, and much needed lunch breaks. I hope that my contributions to your work have been equally valuable to you. To my undergraduate research assistants Andrea Tian and Melanie Schultz, thank you both for your incredibly hard work and help throughout data collection, analysis, and writing. Your contributions have been invaluable.

To my parents and sister, I thank you for being so supportive and for instilling in me my work ethic and drive. I have looked up to each of you as role models and

you have continued to motivate me through the peaks and valleys of life. I am so proud to be a part of our incredible family.

Finally, to Constance, thank you for your patience, your moral support, your emotional support, and for forcing me to keep my eye on the big picture and what matters most. I cannot thank you enough. I love you.

Table of Contents

List of Tables

List of Figures

Chapter 1: Introduction

1.1 Problem Statement

Locomotion eases our ability to perform our everyday activities at home, work, and in the community. It is imperative for individuals who undergo lower extremity amputations (ILEA) to achieve a locomotive level to maximize their quality of life. As of 2005, 1.6 million people in the United States were living with limb loss and this number is expected to increase to 3.6 million by the year 2050 (Ziegler-Graham et al., 2008). Each year, it has been reported that 80,000 to 90,000 lower-extremity amputation surgeries are performed in the United States (Feinglass et al., 1999; Mayfield et al., 2000). Limb loss, especially lower extremity amputation, often leads to a reduction in physical activity levels (Bussmann et al., 2004) and can lead to weight gain, depression, anxiety, increased risks of cardiovascular and other chronic diseases, and an overall reduction in quality of life (Naschitz and Lenger, 2008; Saris et al., 2003; Singh et al., 2007; Yap and Davis, 2008). Early studies on "functional capabilities" of ILEA found that the most difficult physical activities for ILEA were running, and walking long distances (Kegel, 1985; Kegel et al., 1978). New methods in rehabilitation and prosthetic design are needed to help promote increased physical activity levels of ILEA and thus promote healthier lifestyles for this group. However, developing improved rehabilitation techniques and prosthesis designs to promote running within this population requires a detailed understanding of ILEA running biomechanics and the biomechanical function of prostheses during this activity. The development of running-specific prostheses (RSPs) has yielded dramatic

improvements in biomechanical performance and sprinting times for elite athletes with amputation (Dyer et al., 2010; Laferrier and Gailey, 2010; Lechler and Lilja, 2008; Mokha and Conrey, 2007; Nolan, 2008; Pailler et al., 2004), suggesting that the running biomechanical performance of RSPs is superior to that of non-RSPs, or prostheses originally designed for walking. RSPs may therefore also provide improved performance for ILEA who wish to run or jog for recreation or exercise, making running a more accessible activity for a greater number of ILEA. However, due to the passive nature of RSPs and the different shape compared to the body parts they replace, RSPs likely function differently than intact feet and ankles. ILEA will therefore need to adapt their kinetic and joint mechanical energy profiles to accommodate to the altered biomechanics and function when running with an RSP. These adaptations are not well described or understood, and gaining this knowledge will identify areas of running and prosthesis performance that can be objectively targeted within rehabilitation and used to improve prosthetic designs.

Lack of scientific knowledge regarding biomechanics and physiology of ILEA using prostheses to run make providing appropriate rehabilitation to assist ILEA in adapting to new physical conditions and demanding physical activities difficult (Mensch and Ellis, 1986). For the purposes of this dissertation, the term "adaptation" will refer to changes or differences from healthy, able-bodied functioning. Our limited understanding of biomechanical adaptations ILEA must make when running to account for the loss of musculoskeletal function resulting from lower extremity amputation is mainly due to the lack of research on this topic. This lack of knowledge limits orthopaedic surgeons, physical therapists, and prosthetists in terms of

prescribing individualized prostheses and rehabilitation plans of care for this population. Considering the large number of ILEA in our society (Ziegler-Graham et al., 2008), the large number of amputation surgeries performed every year (Feinglass et al., 1999; Mayfield et al., 2000), and the negative effect amputation has on the daily living of ILEA (Wing and Hittenberger, 1989), one might have assumed that there would have been rigorous research in ILEA running, but that is not the case. For example, there are only 69 publications found through a PubMed search using "amputation" and "running" as keywords. Only 19 of these results relate to an ILEA's running biomechanics or physiology, and only three of these articles studied RSPs.

Problem 1: No Validated Models for ILEA Running

Due to the lack of running studies in ILEA and the dearth of information on RSPs, limited objective evidence exists to describe any potential advantages or disadvantages of RSPs. Extensive biomechanical testing is further warranted to determine potential risks or benefits of running for ILEA as well as to potentially optimize running performance in these individuals. During common three-dimensional running analyses, reflective markers are placed on anatomical landmarks to generate biomechanical models that estimate joint center positions, define body segment motions, and influence segment inertial property estimations. The distal segment motions and inertial properties, in combination with ground reaction force data from a force platform, can be used as inputs to inverse dynamics equations to estimate proximal joint kinetic values including joint force, moments, and powers. Since marker placements determine the limb segment definitions, they can affect the

immediately proximal joint kinetic estimations and all subsequent proximal joint kinetic data up the limb chain. The effect that marker placement on RSPs has on the proximal joint kinetic estimations has not been investigated. Current marker placement techniques for walking and running analyses were developed and validated using intact limbs, which have different anatomical landmarks, functional abilities, and inertial properties than RSPs. Consequently prosthesis-specific marker placement models along with accurately measured inertial properties are necessary to ensure accurate biomechanical data and subsequent interpretations during running. Upon identifying RSP marker placement influences on proximal joint kinetic estimations, studies of ILEA running biomechanics can be performed and interpreted with greater confidence. **Problem 1 is addressed in Chapters 3 and 6 of this dissertation**.

Problem 2: Limited Known Inertial Properties of RSPs

The development of valid biomechanical models for use with RSPs will allow researchers to study kinematic and kinetic adaptations that individuals with amputation must make in order to run. However, the kinetic data calculations will also rely on accurate segmental inertial properties. While intact limb segmental inertial properties have been determined through both cadaveric and body scanning methods, prosthetic component inertial parameters are not well established. Studies investigating walking prostheses generally provide a poor description of how inertial properties of the prostheses were estimated, and to our knowledge, inertial properties of only one design of RSPs for one individual (Brüggemann et al., 2009) are reported in the literature. Many RSPs have a standard design and may have uniform inertial

properties. These data would be valuable in providing researchers needed parameters for kinetic analyses. Detailed methods of measuring prosthesis moments of inertia and reports of inertial properties for commonly prescribed RSPs are needed to aid researchers in performing biomechanical analyses of amputee running. **Problem 2 is addressed in Chapter 4 of this dissertation**.

Problem 3: Limited Understanding of Amputee Running Kinetics

Individuals with lower extremity amputation have demonstrated significant differences between the prosthetic and intact limb ground reaction force profiles and stance phase knee and hip joint moments during running (Brüggemann et al., 2009; Buckley, 2000; Czerniecki et al., 1991; DiAngelo et al., 1989; Miller, 1987; Sanderson and Martin, 1996) suggesting altered joint control strategies. This data is limited to running at one or two speeds with non-RSPs or to elite runners using RSPs at or near top speed. Wearing RSPs may provide improved running function over wearing non-RSPs during running at submaximal and maximal speeds. However, these devices are still passive and most likely do not match the function of the intact foot/ankle complex. This functional discrepancy may therefore necessitate altered joint control strategies during stance compared to able-bodied runners. Furthermore, due to their reduced mass compared with the intact limbs they replace, RSPs may induce different swing phase joint moment control strategies. To date, no literature related to ILEA running with RSPs has reported swing phase mechanics. Studies examining ground reaction force and joint moment adaptations when running at different submaximal velocities with RSPs are needed to provide deeper

understanding of joint kinetic adaptations during amputee running. **Problem 3 is addressed in Chapters 5 and 7 of this dissertation**.

Problem 4: Limited Understanding of Amputee Running Energetics

The limitations in our understanding of joint kinetic control adaptations during ILEA running also limit our understanding of mechanical energy production by and flow through the lower limbs. Energy during ambulation is often investigated through joint power and mechanical work where work is the measure of energy flow from one body to another and joint power is the rate of work done over time. ILEA demonstrate significantly different joint power profiles and mechanical work generation as compared to healthy individuals when running (Buckley, 2000; Czerniecki and Gitter, 1992; Czerniecki et al., 1996; Czerniecki et al., 1991). Major compensatory patterns allowing ILEA with transtibial amputation to run include an increase in stance phase hip muscle work on the prosthetic limb and increased hip and knee muscle work on the intact limb during swing phase (Czerniecki and Gitter, 1992). This study was performed with non-RSPs and only at one running velocity. Increased residual knee work in two subjects wearing RSPs while sprinting has been suggested as an additional compensatory mechanism (Buckley, 2000). However, with only two subjects running near maximal speeds, it is unknown whether these compensations will be observed at submaximal running velocities or if the mechanisms may change as amputees run at different velocities. More encompassing running studies examining mechanical energy adaptations at different running velocities will provide

greater insights into adaptive mechanisms used by individuals with amputation while running. **Problem 4 is addressed in Chapter 8 of this dissertation**.

1.2 Study Objective, Specific Aims, and Hypotheses

The overarching objective of this dissertation was to characterize changes in kinetics and mechanical energy across a range of running velocities in ILEA wearing RSPs. This was investigated using a series of experiments with six specific but complementary aims that build to achieve the overarching objective. Each of the specific aims was examined successively in dedicated chapters. Chapter 2 provides a detailed review of the literature related to ILEA ambulation with a focus on running. Chapters 3-8 provide a progression of studies to investigate current gaps in the literature as defined by the six objectives.

Specific Aim 1: Investigate the effects of RSP marker placement on proximal joint kinetic estimations via material testing [Chapter 3]

Marker placement models currently used to analyze running with prostheses were originally developed and validated using intact limbs. A single marker is typically placed on either the same relative position as the intact limb's ankle joint or the most acute point on the prosthesis curvature, i.e. the point of greatest curvature. However, no information is available to support whether or not these marker placements validly represent an "ankle" joint or whether proximal joint kinetic data are affected by the choice in marker placement. Placing more markers on the

prosthetic keel will generate more subsegment definitions within the prosthesis and can account for deformation and accelerations at more points along its length. Consequently, more accurate kinetic estimations can be made as forces are transferred from distal subsegments to the proximal subsegments. However, placing more markers on the prosthesis can also inflate error as the number of assumptions in inertial estimations increases as does the possibility of measurement errors. An optimal tradeoff may exist between more accurately modeling the keel motion and increasing the assumption and measurement errors with greater numbers of markers placed on RSPs. Performing a controlled investigation using RSPs in a material testing system where the proximal applied force and torque are measured directly and can be compared to estimated force and torque values determined from inverse dynamics techniques will allow for the determination of marker placement influences on these variables. Therefore, Chapter 3 examines Specific Aim 1, to investigate how varying the number and position of markers on RSPs would affect kinetic estimations compared to directly measured values.

Specific Aim 2: Investigate the inertial properties of RSPs [Chapter 4]

Accurate kinetic estimations using link-segment models depend on accurate segment inertial property measurements including mass, center of mass position, and moments of inertia. Methods to measure inertial properties of prostheses, especially moments of inertia, are not well described in the literature. Physical pendulums that rely on a joint or bearing that is assumed to be frictionless (Hillery et al., 1997; Martin et al., 1989) are most commonly cited. In practice, however, friction in this

bearing does exist and along with air resistance, will slow the period of oscillation and impart error in the inertial estimations. Trifilar pendulums are reportedly more accurate than physical pendulums since they do not rely on bearings, which minimizes inaccuracies caused by friction (Genta and Delprete, 1994). However, aligning RSPs properly within trifilar pendulums is necessary, and the accuracy of moment of inertia measurements from these pendulums when misaligning RSPs is unknown. In conjunction with limited descriptions of methods measuring prosthesis moments of inertia, only one study to date has reported any inertial property values for RSPs. This included a description of two RSPs of the same design from one subject. Inertial property measurements from multiple RSP designs and different stiffness categories within each design can provide basic guidelines for use in ILEA running research. Detailed descriptions of measuring inertial properties for RSPs will provide researchers with guidelines for measuring inertial properties of subject-specific prosthetic components. Therefore, Chapter 4 examines Specific Aim 2, to investigate the inertial properties of RSPs. This specific aim was achieved through three sub-aims: (2a) to test the validity of a trifilar pendulum method in estimating the inertial properties for four common RSP designs, (2b) to provide inertial property values for RSPs that are readily available for use by the scientific community, and (2c) to develop a predictive equation to estimate RSP CM positions.

Specific Aim 3: Investigate temporal-spatial and ground reaction force adaptations during ILEA running [Chapter 5]

Adaptations in mechanical interactions between the feet and ground in ILEA alter running biomechanics to account for the loss of musculoskeletal function. When running, ILEA with transtibial amputation demonstrate reduced peak vertical and anteroposterior (AP) ground reaction forces (GRFs) in the prosthetic limb(s) and altered temporal-spatial profiles compared to able-bodied individuals. ILEA running with non-RSPs show increased peak vertical and AP GRFs on both limbs with faster velocities. ILEA running with RSPs exhibit increased vertical GRFs with velocity, but the anterior GRF component that governs forward acceleration of the whole body center of mass has not been examined. ILEA consistently demonstrate greater step and stride frequencies than able-bodied runners at the same velocities. However, the literature conflicts on how ILEA modulate temporal-spatial parameters to increase running velocity, either by primarily increasing step frequency or primarily increasing step length. Therefore, Chapter 5 examines Specific Aim 3, to investigate GRF and temporal-spatial adaptations to different running velocities when running with a passive RSP.

Hypothesis 3.1: ILEA running with RSPs would exhibit altered temporal-spatial and GRF profiles compared to a control group running at matched velocities.

Hypothesis 3.2: ILEA would exhibit greater loading on and propulsion generated by the intact limb compared to the prosthetic limb indicated by GRF parameters, but differences between limbs would not increase with velocity.

Hypothesis 3.3: ILEA would increase running velocity by increasing step frequency and reducing the related temporal parameters.

Specific Aim 4: Investigate the effect of RSP marker placement on joint kinetic estimations during overground running [Chapter 6]

The number of markers and their placement on RSP keels was shown to have little effect on kinetic estimations proximal to the prosthesis during an axial loading task. However, when ILEA run, RSPs are loaded three dimensionally, so the results from an axial loading task may not generalize to actual running motions. If marker placement effects are dependent on the 3D loading profile, then such effects must be examined during overground running or via a material testing system capable of applying loads in three dimensions. Therefore, Chapter 6 investigates Specific Aim 4, to investigate the effect of RSP marker placement on the estimations of lower extremity joint kinetics during overground running.

Hypothesis 4.1: The number of markers and their placement on the keel of RSPs would not affect the residual limb joint moment estimations.

Specific Aim 5: Investigate joint moment adaptations during ILEA running [Chapter 7]

Individuals with transtibial amputation demonstrate altered stance phase knee and hip joint moments and joint angle trajectories as compared to healthy individuals when running to compensate for physical deficiencies. Peak joint moments in the

prosthetic limb were typically lower than those in the intact limb and able-bodied limbs, and when increasing velocity peak magnitudes from both limbs increase similarly. These adaptations were either reported during running with non-RSPs or in elite runners using RSPs at sprinting speeds. However, many gaps exist in our knowledge of ILEA running mechanics and their lower extremity joint kinetic adaptations. Joint moments at submaximal running velocities, swing phase mechanics, and how ILEA adapt their joint mechanics to achieve different running velocities are not understood when subjects wear RSPs. A complete description of the 3D joint moment profiles would provide greater insights into how ILEA run and compensate for replacing an active limb with a passive prosthetic device. Therefore, Chapter 7 examines Objective 5, to investigate lower extremity joint moments in ILEA when running with RSPs under different velocity constraints.

Hypothesis 5.1: ILEA would demonstrate lower peak joint moment magnitudes in the prosthetic limb than the intact and control limbs throughout stance and swing phase at each velocity.

Hypothesis 5.2: Increased running velocity would be associated with similar increases in intact and prosthetic limb peak joint moments.

Specific Aim 6:   Examine mechanical energy adaptations during ILEA running [Chapter 8]

Individuals with transtibial amputation demonstrate different mechanical energy adaptations during running as quantified by joint power and mechanical work generation. Overall, the prosthetic limb performs less total mechanical work than the

intact limb during ILEA running. Major compensatory mechanisms allowing ILEA with transtibial amputation to run with non-RSPs include increased stance phase hip muscle work on the prosthetic limb and increased hip and knee muscle work on the intact limb during swing phase. It is unknown whether these compensations are similar when using RSPs or if they remain consistent at different running velocities. Therefore, Chapter 8 examines Objective 6, to investigate lower extremity joint power and mechanical work adaptations when running with a passive RSP at different running velocities.

Hypothesis 6.1: ILEA would exhibit lower mechanical energy in the prosthetic limb than the intact and control limbs at each velocity.

Hypothesis 6.2: Increased running velocity would be associated with similar increases in mechanical energy of the intact and prosthetic limbs.

1.3 Organization of Dissertation

In Chapter 2, the following issues of previous literature are reviewed and discussed related to ILEA running: kinematic adaptations, kinetic adaptations, work and energy adaptations, and effects of prosthetic inertial properties. The dissertation will be composed of a series of studies (Chapters 3-8) that are systematically linked (Figure 1.1).

CHAPTER 3
Marker Placement on Running-Specific Prostheses: Material Testing

⬇

CHAPTER 4
Determining Inertial Properties of Running-Specific Prostheses

⬇

CHAPTER 5
Temporal-Spatial and Ground Reaction Force Adaptations during ILEA Running

⬇

CHAPTER 6
Marker Placement on Running-Specific Prostheses: Overground Running

⬇

CHAPTER 7
Joint Moment Adaptations during ILEA Running

⬇

CHAPTER 8
Mechanical Energy Adaptations during ILEA Running

Figure 1.1. Systematic structure of the sub-studies of the dissertation.

Chapter 2: Background and Review of Literature

As of 2005, 1.6 million people in the United States were living with limb loss and this number is expected to increase to 3.6 million by the year 2050 (Ziegler-Graham et al., 2008). Limb loss, especially lower extremity amputation, often leads to a reduction in physical activity levels (Bussmann et al., 2004), and can lead to weight gain, depression, anxiety, increased risks of cardiovascular and other chronic diseases, and an overall reduction in quality of life (Naschitz and Lenger, 2008; Saris et al., 2003; Singh et al., 2007; Yap and Davis, 2008). Secondary pain issues are also quite prevalent among individuals with lower extremity amputation (ILEA). One survey of 255 ILEA reported 52% have persistent, bothersome back pain, and 25% of those individuals described the pain at the level of severely interfering with daily activities (Ehde et al., 2001). Back pain is also more prevalent after transfemoral than for transtibial amputation, but phantom limb pain is commonly reported regardless of the amputation level (Kulkarni et al., 2005).

Amputations can also cause significant biomechanical and physiological adaptations during ambulation. To examine these gait adaptations, a brief review of walking gait is presented followed by a review of the amputee running literature.

2.1 Amputee Walking Gait

2.1.1 Prosthetic Components

A variety of prosthetic components are available on the market. As technology advances, new materials and artificial control mechanisms are being implemented

within these devices that can improve function, although no prosthetic device is currently capable of replicating anatomic function (Laferrier and Gailey, 2010). For prosthetic foot components, the most basic designs are traditional, non-dynamic response feet, may be articulated at the ankle joint with single- or multiple-axis foot designs, or they may be non-articulated with a continuous, solid connection between the foot and shank as in the solid ankle, cushion heel (SACH) foot. The articulated feet allow for plantarflexion at the ankle joint after heel-strike, while the SACH foot utilizes a compressible material in the heel that simulates plantarflexion at heel-strike (Edelstein, 1988). Using nomenclature proposed by Hafner et al. (Hafner et al., 2002), energy-storage-and-return (ESAR) feet use a keel that deforms when loaded, absorbing energy, then returns the energy to assist gait as the keel bounces back to its original shape when unloaded. Non-ESAR feet can be appropriate for less dynamic patients while higher functioning walkers benefit from ESAR feet (Friel, 2005). For individuals with transfemoral amputations, the prosthetic knee units offer additional choices. Fixed-cadence knees have a fixed pendulum swing and may be appropriate for lower level ambulators while variable-cadence knees that control the swing rate via hydraulic, pneumatic, or microprocessor methods benefit higher functioning walkers. Each prosthetic component offers a myriad of designs from different companies, each with its own unique functional claims, making prescription a daunting task. Research has identified many functional differences between prosthetic componentry; however, regardless of these components, functional outcomes for individuals with transtibial amputations are better than those with transfemoral amputation (Perry, 2011).

The intact ankle generates considerably more work during walking than any other lower extremity joint (Czerniecki et al., 1991; Robertson and Winter, 1980; Winter, 1983a). Since all current prosthetic feet are passive in nature, they cannot completely replace the function of the lost ankle joint. This discrepancy in function causes asymmetries between the intact and residual limb joints in people with unilateral amputation and compensations by the remaining joints in individuals with both unilateral and bilateral amputations.

2.1.2 Kinematics of Amputee Walking

The loss of the ankle joint induces asymmetries between the intact and prosthetic limb in temporal-spatial parameters (Nielsen et al., 1989; Torburn et al., 1990). Comparisons between prosthetic components indicate a variety of functional results. Many temporal-spatial parameters are dependent on the prosthetic foot design. The energy-storing Vari-flex foot allowed subjects with transfemoral amputation to walk faster and take more symmetrical step lengths than with a conventional articulating foot, the Multiflex (Graham et al., 2007). In contrast, when comparing the SACH with the Carbon Copy II foot (a basic ESAR design), no differences were identified for step length, single and double limb support time, swing time, cadence or self-selected walking velocity (Barr et al., 1992). Furthermore, a repeated-measures design comparison of five different prosthetic feet revealed no temporal-spatial differences between the components, although differences were observed at the joint kinematic level (Torburn et al., 1990).

This and other studies indicate that prosthetic feet vary in their abilities to produce functional kinematic patterns. In some cases, few or no kinematic differences are observed between foot units (e.g. between the SACH and Carbon Copy II (Barr et al., 1992)). Other foot designs generated more obvious deviations. During barefoot walking, using a solid ankle cushion caused gait abnormalities such as knee hyperextension and loss of ankle plantar flexion in early stance phase, but gait patterns improved with the use of a single-axis prosthetic foot, which permitted a further plantar flexion after initial contact (Han et al., 2003). Kinematic patterns tend to improve when ILEA use more advanced ESAR prosthetic designs. Subjects were able to achieve greater peak ankle dorsiflexion at push-off with the Vari-Flex foot than with a conventional Multiflex foot (Graham et al., 2007). The Flex-Foot prosthesis also provides more dorsiflexion in terminal stance than the SACH and Seattle Light foot, increasing step length and allowing for a greater peak push-off power (Perry, 2011).

Prosthetic feet still tend to provide smaller ranges of ankle motion than either intact limbs or control subject ankles during gait (Nolan and Lees, 2000a; Postema et al., 1997; Powers et al., 1994), and the intact limb often compensates for the lack of prosthetic ankle function with increased ranges of motion relative to healthy gait (Nolan and Lees, 2000a). Compared to healthy gait, knee flexion during loading response (weight acceptance) of walking is reduced in ILEA with transtibial amputations (Isakov et al., 1996; Powers et al., 1998; Su et al., 2007) and is often absent in the residual knees of ILEA with transfemoral amputation (Segal et al., 2006). Reduced hip joint sagittal range of motion, primarily due to a lack of hip

extension at terminal stance, has been cited as a mechanism that ILEA with transfemoral amputation use to maintain speed (Rabuffeti et al., 2005). Hip hiking (increased pelvic range of motion in the frontal plane) is also prevalent in ILEA to assist with clearing the prosthetic limb during swing (Michaud et al., 2000; Su et al., 2007) and is generally more exaggerated in those with transfemoral amputation (Michaud et al., 2000). These kinematic deviations at each lower extremity joint show that ILEA have adapted their gait to overcome the loss of their joint function and/or the shortcomings of the prosthetic components. To elucidate the causes of these kinematic deviations, the joint kinetic and mechanical energy profiles of ILEA gait must be examined.

2.1.3 Kinetics of Amputee Walking

The kinematic differences observed between prosthetic foot designs also translate to kinetic differences. For example, the Carbon Copy II exhibits slower unloading in late stance, a later peak propulsive force, and performed greater work in both energy-storage and energy-return in the stance phase, returning energy with 57% efficiency as compared to the SACH foot, which had a 30% energy return (Barr et al., 1992). The energy-storing Vari-Flex foot generates three times greater prosthetic ankle power at push-off than the conventional Multiflex foot (Graham et al., 2007). Prosthetic feet also dissipate energy during heel ground contact with values ranging between 33 and 82% of the original energy input, depending on the foot (Klute et al., 2004). The afore-mentioned inadequacy of prosthetic components to mimic intact limb functions are more prevalent when comparing amputee kinetics with kinetic data

from a control group. In particular, knowledge of joint mechanical work provides insights into the energy generated to successfully ambulate.

In individuals with unilateral amputations, there is a discrepancy between the limbs in the amount of work performed. The intact limb knee performs more work than the residual knee throughout the gait cycle. Hip joint work does not appear to differ between limbs during walking (Beyaert et al., 2008; Grumillier et al., 2008). As compared to healthy, control subjects the residual limb knee joint performs significantly less concentric work during stance (Beyaert et al., 2008; Gitter et al., 1991) while the residual hip performs more concentric work (Beyaert et al., 2008; Grumillier et al., 2008) than control knees and hips, respectively. The intact leg of amputees performs more knee and hip work during stance than controls (Beyaert et al., 2008; Grumillier et al., 2008; Silverman et al., 2008). Despite lower work, no differences between peak power of the residual and intact limb joints are observed (Prinsen et al., 2011). One possible explanation provided was that similar peak magnitudes with shorter durations of power generation or absorption would lead to lower work in the residual limb (Prinsen et al., 2011). The reliance on the intact limb joints may help explain the greater incidences of osteoarthritis in the intact limb knee of ILEA with transtibial amputations (Norvell et al., 2005). During gait in individuals with transfemoral amputation, the residual limb hip performs significantly more work than the intact limb, which performs more work than reference hips of a control group (Seroussi et al., 1996). This may place the residual hip at much greater risk of developing degenerative joint diseases.

The difference between ILEA work profiles and those of healthy control subjects indicate adaptive strategies employed by ILEA to make up for the loss of joint function after amputation. Since current prosthetic components are unable to adequately mimic those lost functions, the remaining joints and surrounding musculature must compensate to generate propulsive energy and adapt limb control to perform the task of ambulating. These alterations in joint reliance may place the remaining joints at a greater risk of developing degenerative diseases since a greater, or different, burden is placed on them.

2.2 Able-Bodied Running Gait

Human running is defined by having a flight phase where a period of time exists that neither of the limbs are in contact with the ground. During the support phase, only one limb is ever in contact with the ground. This is in contrast to walking where at least one limb is in contact with the ground at all times and there is also a period of double support where both limbs contact the ground simultaneously. Running is a common form of cardiovascular exercise, a means of transportation, and a form of competition that is performed widely as a part of sporting events and every day activities.

Investigating running biomechanics can provide insights into control mechanisms used by the body to ambulate, reducing injuries, and improving maximal performance, and improving performance from a mechanical and metabolic efficiency standpoint. The kinematics of running provide descriptions of how the body is moving while running kinetics provide information on how and why the body

moves as it does. The ultimate goal of this review is to provide a description of our current knowledge on running biomechanics in individuals with lower extremity amputation; however, to achieve that goal, it is important to provide a description of uninjured, or able-bodied running biomechanics as a reference.

2.2.1 Kinematics of Able-Bodied Running

Ankle sagittal plane kinematics will depend on the running style of the individual. Heel-to-toe runners will exhibit an initial plantarflexion action just after footstrike and then the ankle will dorsiflex through midstance, while midfoot and forefoot runners will immediately dorsiflex the ankle at footstrike. The ankle is plantarflexed during the push-off phase and then dorsiflexed during swing to assist with toe clearance. With greater amounts of knee and hip flexion during running swing phase, ankle dorsiflexion is not as important as during walking since clearing the toe no longer becomes an issue. Sagittal plane knee motion during running exhibits a similar pattern to that of walking. The knee flexes to approximately 45° during early stance to absorb the shock from initial contact, then the knee extends to an average of 25° (of flexion) during the propulsion phase. During swing, the knee flexes to approximately 90° during running and to 105° or greater during sprinting. The hip extends during the second half of swing phase during running and sprinting in preparation for initial contact. This difference is to avoid the excessive deceleration that would occur at the time of initial contact if the foot were too far ahead of the center of mass of the body.

Coronal and transverse plane joint kinematics is quite small relative to sagittal plane motion in running, but these motions can assist with shock absorption and minimizing the motion of the upper body. The hip joint coronal and transverse plane motion is less restricted by stabilizing ligaments than the knee or ankle, and consequently the hip motion in these planes tends to be larger and more important to the tasks mentioned above. Generally, in walking, running and sprinting, the hip is adducted while the limb is loaded in stance phase to absorb shock from initial foot-ground contact and the joint is abducted during swing to assist with foot clearance. Hip motion in this plane mirrors the movement of the pelvis. This nearly reciprocal motion minimizes shoulder and head movement and is one of the most important mechanisms for decoupling the abundant lower extremity motion from the trunk and head (Novacheck, 1998b). This decoupling results in relatively minimal head and trunk motion that allow the body to maintain its balance and equilibrium (Novacheck, 1998b). In running and sprinting, the peak forward (internal) pelvic rotation occurs in midswing to lengthen the stride, but the pelvis rotates externally prior to footstrike in order to maximize horizontal propulsive forces (or to minimize horizontal breaking forces) (Novacheck, 1998b). This is in contrast to walking where the peak forward transverse rotation of the pelvis occurs near footstrike to assist with increasing step length but at the expense of horizontal velocity.

2.2.2 Kinetics of Able-Bodied Running

Novacheck's review of running biomechanics provided a detailed yet succinct description of joint moment profiles (Novacheck, 1998b). The following paragraph

summarizes that description. During heel-to-toe running, the ankle moment pattern is similar to that in walking with a short dorsiflexor moment phase just after footstrike with the ankle plantarflexion moment initiating at 5–10% of the running gait cycle. In contrast, during sprinting there is no initial dorsiflexor moment because initial foot contact is on the midfoot or forefoot which causes the ankle to immediately dorsiflex upon ground contact. The knee moment pattern is very similar in sprinting and running. To prepare for foot contact with the ground, the hamstrings dominate the second half of swing producing a knee flexor moment, which controls rapid knee extension by slowing it down. Shortly after foot-ground contact, the quadriceps become dominant producing a knee extensor moment to prevent the knee from collapsing. In swing phase very little power is generated by the knee musculature, rather the muscles absorb power to control the movement of the swinging leg. At the hip joint, the hip extensors are dominant just prior to and just after initial foot-ground contact. In contrast, the hip flexors dominate the second half of stance through the first half of swing. Both the hip flexors and extensors are responsible for increased power generation in running and sprinting.

A proximal-to-distal timing occurs in the generation of peak extensor power during stance at the hip, the knee and then the ankle. Major periods of hip extensor power generation occur in early stance (Bezodis et al., 2008) while the ankle plantarflexors generate the greatest peak powers during late stance (Bezodis et al., 2008; Johnson and Buckley, 2001). A moderate knee power generation peak towards toe-off may exist, but knee power is primarily negligible despite a large extensor moment throughout stance. Three main sources of power generation during able-

bodied running may then be summarized as 1) the hip extensors during the second half of swing and the first half of stance; 2) the hip flexors after toe off; and 3) ankle plantarflexors during stance phase generation (Novacheck, 1998b). The primary function of the knee joint during running thus appears to be maintaining the center of mass height and facilitating the power generated at the hip to be transferred to the ankle and to the ground (Bezodis et al., 2008; Johnson and Buckley, 2001).

Mechanical work can be calculated by integrating the joint power data across time to provide further insights into the generation, absorption, and transfer of mechanical energy during running. The body must absorb energy after initial contact with the ground (shock absorption) and generate energy to maintain a particular running speed. These tasks involve a complex interplay of energy transfers through the limb segments to share the burden of energy absorption and generation between the limbs and effectively. Two-joint muscles are proposed as mechanisms allowing the transfer of energy from one segment to the next (Jacobs et al., 1993; Jacobs et al., 1996; Wells, 1988). In the push-off phase of running, the two-joint muscles (rectus femoris and gastrocnemius) transfer mechanical energy from the proximal joints of the leg to the distal ones (hip-to-knee and knee-to-ankle transfers, respectively). This energy transfer can also occur in the opposite direction. During the shock-absorbing phase of running, the two-joint muscles transfer energy from the distal to proximal joints. Prilutsky and Zatsiorsky (Prilutsky and Zatsiorsky, 1994) identified that distal one-joint muscles produced less mechanical work than proximal one-joint muscles, and the proximal links compensate for this deficiency by distributing mechanical energy between the joints through the two-joint muscles. During the push-off phase

of running, the muscles of the proximal links helped to extend the distal joints by transferring part of the generated mechanical energy distally, and during the shock-absorbing phase, the proximal link muscles assisted the distal link muscles in dissipating the body's mechanical energy.

2.3 Running Injuries and Kinetics

Runners sustain high rates of injury that are reported between 19-79% during any one-year period (Jacobs and Berson, 1986; Lysholm and Wiklander, 1987; Macera et al., 1989; Marti et al., 1988; van Gent et al., 2007; Walter et al., 1989). A majority of running injuries can be categorized as overuse injuries (Hreljac, 2005). Overuse injuries can be defined as injuries of the musculoskeletal system that results from the combined fatigue effect over a period of time beyond the capabilities of the specific structure that has been stressed (Stanish, 1984). These injuries occur when several repetitive forces are applied to a structure (e.g., muscle or tendon); each is less than the acute injury threshold of the structure (Hreljac, 2005). The knee sustains a greater number of injuries than any other joint followed by the ankle, while the hip is injured less often (Hreljac, 2005; Marti et al., 1988; Taunton et al., 2002; van Gent et al., 2007). The etiology of these injuries is not clear as little empirical evidence exists linking potential causes, and few prospective studies are available that would provide stronger evidence of a cause and effect relationship.

Biomechanical variables are commonly investigated as a source of running injuries. In able-bodied runners, an initial impact spike is often observed in the vertical ground reaction profiles. Greater peak impact forces have often been

implicated as the cause of overuse running injuries (Hreljac, 2004; Hreljac et al., 2000) as these forces are typically high in magnitude and reach their peak quickly. Activities such as downhill running that increase the peak impact forces have therefore been suggested to increased the risk of injury to the limbs (Gottschall and Kram, 2005). Rather than just examining the peak of the impact spike, the loading rates calculated from the impact forces have also been identified as potential causes of running injury (Milner et al., 2006; Nigg et al., 1981). High loading rates suggest poor shock absorption, and the impact forces could be transferred nearly unattenuated to an at-risk structure that would lead to injury. In runners with a history of tibial stress fractures, these injuries were associated with increased instantaneous and average vertical loading rates and tibial shock (Milner et al., 2006).

However, some studies suggest that these forces loading rates are incorrectly associated as injury risk factors. High impact forces and high impact loading rates were independent of injury rates during running (Stefanyshyn et al., 2001) suggesting no relationship between these variables and injury. These authors concluded that the impact forces during running were most likely not a large factor in injury development. It has been further suggested that chronic injuries associated with jogging are most likely to be related to the forces at mid- and late-stance rather than to those occurring at the time of impact (Messier et al., 1991; Winter, 1983b) because of the much greater loads at these time points.

In addition to ground reaction forces, abnormal or increased joint moments are often implicated as risk factors for injury. The extensor mechanism of the knee is the most common site of chronic running injuries because it functions to absorb 42% of

the actively absorbed energy associated with ground contact (Novacheck, 1995; Novacheck, 1998a). The net knee extensor moment in stance phase is as much as five times greater in running than during walking (Novacheck, 1998a) placing a much greater amount of stress on the quadriceps muscles, tendon, and patellar ligament. Additionally, peak Achilles tendon forces reach approximately six to eight times body weight during running (Alexander, 1992). Peak ankle moments occur during mid-stance, caused by contraction of the gastrocnemius-soleus complex, not by the shock of the initial ground contact (Novacheck, 1998a). Consequently, injuries commonly seen in the Achilles tendon are caused by the active muscle forces in mid-stance rather than the passive impact forces that occur at initial foot contact (Novacheck, 1998a).

Injury risk has also been blamed on the coronal and transverse plane joint kinetics during running. High external rotation and abduction knee moments were identified as the strongest predictors of injury during running (Stefanyshyn et al., 2001). These non-sagittal moments would place greater stresses on the passive structures within and around the knee joint that would increase the risk of tearing or rupture.

Additional research is needed to continue to elucidate the primary causes of injuries during running. While it is generally agreed upon that acute injuries are caused by excessive forces, chronic and overuse injury etiology remains unclear. A majority of injury risk studies have been performed retrospectively, which makes it difficult for researchers to separate causative variables from adaptations from an

injury. More prospective studies into chronic and overuse injury etiology will be extremely valuable to better understanding injury risks and mechanisms.

2.4 Amputee Running Gait

Early studies on "functional capabilities" of ILEA found that the most difficult physical activities were running, and walking long distances (Kegel, 1985; Kegel et al., 1978). Running is one of the most convenient and cost-effective forms of cardiovascular exercise that can increase physical activity levels and decrease the risk of cardiovascular-related diseases. Running can also offer an opportunity for socialization and participation in many recreational or competitive sports. It has been reported that running can assist with weight loss (Poirier and Després, 2001), help manage stress (Singh et al., 2007), and reduce risks of chronic diseases by improving cardiovascular health (Kavanagh, 1983). All of these positive traits of running exercise can lead to an enhanced quality of life for both healthy individuals and those with lower extremity amputations.

Despite the prevalence of amputation, negative health consequences from reductions in physical activity, and difficulties with demanding dynamic activities like running that could ameliorate some of the negative health risks, surprisingly little research has investigated such activity in ILEA. Prostheses designed specifically for running have now been available for several years and these devices could make running easier than with a walking-specific prosthesis. This could attract more ILEA to running as a common method of exercise. However, to this point, ILEA running research has been minimal making directed improvements in technology and

rehabilitation techniques difficult. A PubMed search using "amputation" and "running" as keywords returned only 65 publications. Only 19 of these results relate to an ILEA's running biomechanics or physiology, and only three of these articles studied running-specific prostheses (RSPs). The following sections describe the current state of knowledge regarding the biomechanics of amputee running. This report aims to cover kinematic, kinetic, and mechanical energy adaptations by ILEA when running. Current methods of analysis, limitations in knowledge, and future directions of research will also be discussed.

2.4.1 Temporal-Spatial Parameters and Kinematics of Amputee Running

Enoka et al. (1982) were first to quantify the ability of amputees to run with clear alternating phases of single-support and non-support (flight) (Enoka et al., 1982), and at that time, considerable variability existed from subject to subject, which were in part attributed to a lack of proper training and a need to modify the prosthetic components for the biomechanical demands of running. The subjects in this study relied on step rate to maintain increasingly higher speeds while maintaining similar step lengths across speeds. The increase in step rate was primarily attributed to a decrease in single support duration. Flight time was similar for the intact step across speeds but flight time increased with speed for the prosthetic step. This indicates a progressively more active role of the residual limb at faster speeds (Enoka et al., 1982).

Running velocity is a function of step length and step frequency, and individuals may adjust either or both of these parameters to change velocity. This

seemingly simple relationship is governed by a complex interaction of many determinants governing these parameters (Hay, 1993; Hunter et al., 2004) producing an infinite number of possible ways to alter or maintain running velocity. Step frequency is a function of stance and swing time so velocity can be tuned by adjusting these parameters. Both step length and step frequency in part depend on the ground reaction forces (GRFs) generated when the foot contacts the ground. Swing time is the time it takes for the limbs to be repositioned for successive steps as faster swing times will shorten the overall step time thus reducing the time it takes for a step and increasing velocity (assuming constant step length). Vertical GRFs must therefore be applied that are large enough to provide an aerial time long enough to reposition the legs for the next running cycle. Step length is partly dependent on the anterior (propulsive) GRFs as greater anterior forces will allow an individual to generate a longer step length. Since posterior (braking) GRFs will slow or reverse the forward progression of the whole body center of mass, individuals could also modulate this parameter to control their average running velocity.

Able-bodied individuals tend to increase running velocity by increasing step length at lower velocities and by increasing step and stride frequency at greater velocities (Dillman, 1975; Ounpuu, 1994; Sanderson and Martin, 1996). At top speeds, however, studies have shown that step frequency or step length dominance may be an individual preference (Hunter et al., 2004; Salo et al., 2011). ILEA increase their running speed predominantly by increasing their step frequency as opposed to increasing step length (Enoka et al., 1982). Adult ILEA runners had greater stride frequencies than able-bodied runners at 2.7 and 3.5 m/s with shorter

stance and swing times in the ILEA limbs compared with the control group (Sanderson and Martin, 1996). In this study, the intact limb showed similar responses to increasing velocity as able-bodied individuals by maintaining similar stride frequencies indicating an increased step length, but the residual limb increased stride frequency to achieve the faster velocity. The residual limb step length tends to be shorter than the intact limb step length despite similar or longer step duration (Brouwer et al., 1989). Conversely, longer steps with the residual limb compared with the intact limb have been observed during the long jump approach with increased approach speeds achieved by increasing the intact limb step length (Nolan, 2008).

RSPs have been developed to improve the running performance of prostheses, and research is only beginning to evaluate the biomechanical responses of running with these devices. When wearing RSPs, ILEA with unilateral amputations still show some differences between limbs in temporal-spatial parameters. They show increased step frequency with velocity, but the intact limb has a greater increase at greater velocities (Grabowski et al., 2010). The differences in step frequency were attributed to a non-significant but meaningfully shorter aerial time following the intact limb push-off compared to that following the prosthetic limb push-off. Step lengths were not reported for this treadmill running study, so it is not known whether or not RSPs have improved this asymmetry noted in ILEA runners wearing non-RSPs. An elite bilateral ILEA, Oscar Pistorius, has been the subject of multiple tests to determine whether RSPs provide an advantage over intact limbs during running. These studies cannot be generalized to other ILEA runners, but different studies using the same subject have reported conflicting results relative to temporal-spatial parameters. At

top sprinting speeds, this subject's aerial times were consistently reported as shorter than those of able-bodied sprinters (Brüggemann et al., 2009; Weyand et al., 2009); however, in one study, stride lengths and contact times were determined to be no different than able-bodied runners (Brüggemann et al., 2009), while a second study indicated that he had shorter swing times and longer contact times (Weyand et al., 2009). More research is needed to determine the adaptations ILEA make when running with RSPs at submaximal and maximal velocities.

Comparing the intact limb to the prosthetic, or residual, limb, slower step speeds on the residual limb have been attributed to significantly lower vertical ground reaction forces (Brouwer et al., 1989). Longer step lengths with the residual limb have been observed during sprinting in the long jump approach for individuals with transtibial amputation (Nolan, 2008; Nolan and Patritti, 2008). These observations indicate that ILEA run asymmetrically with a reliance on the intact limb.

Kinematic analyses of ILEA running confirm the prevalence of asymmetrical limb movements, although joint kinematics are influenced by the prosthetic design. Ankle kinematics are largely affected by prosthetic design and marker placement. The SACH and single-axis foot designs were incapable of simulating natural foot-ankle function resulting in significant interlimb asymmetries (Brouwer et al., 1989). The stance phase prosthetic ankle range of motion is limited and angular velocity is reduced during running, although transtibial amputees were able to exhibit an "up on toes" running style with Flex-Foot Mod III prosthesis (Buckley, 1999). Currently there is no standard method to define the "ankle joint" in many prosthetic designs, especially in RSPs that do not resemble the intact foot and ankle complex. When

using prostheses designed primarily for walking, most studies place the malleoli markers on the prostheses at the same approximate point where malleoli would be if it were an intact limb.

The literature provides consistent information supporting altered residual limb knee kinematics during running; however, the intact limb knee kinematics behavior may be more dependent on the type of prosthesis worn during running. In children, the residual limb knee has marked reduction of initial flexion during stance (Brouwer et al., 1989), while in adults the residual knee appears more flexed than the intact limb knee both at foot contact (Buckley, 1999) and at toe-off (Buckley, 1999; Sanderson and Martin, 1996). These differences between children and adults could be attributed to prosthetic components or possibly development and coordination differences due to age. Adults also exhibit increased, sustained residual limb knee flexion throughout swing phase compared to the intact limb knee reducing the overall range of residual limb knee motion throughout the gait cycle (Buckley, 1999), while able-bodied subjects exhibit greater swing phase knee flexion than either of the ILEA subjects' limbs (Buckley, 1999; Sanderson and Martin, 1996). In some ILEA subjects, the intact limb knee joint also appears more extended during swing phase of running than those of able-bodied subjects and remains so throughout a range of velocities (2.7 – 3.5 m/s) (Sanderson and Martin, 1996) whereas other ILEA may run with intact limb knee kinematics comparable to able-bodied runners (Buckley, 1999). Residual limb knee overextension in late swing is also a commonly observed phenomenon while mean peak flexion and extension angular velocities are reduced compared to the intact limb (Buckley, 1999).

Discrepancies in hip joint behaviors during ILEA running are also prevalent in the literature. Intact limb hip kinematics may be comparable to able-bodied runners (Buckley, 1999), but decreased intact hip flexion prior to toe-off compared to able-bodied runners has also been observed (Brouwer et al., 1989). The residual hip demonstrates increased flexion at foot contact compared to the intact limb (Buckley, 1999; Sanderson and Martin, 1996) and maintains this relationship at push-off (Buckley, 1999; Sanderson and Martin, 1996).

2.4.2 Kinetics of Amputee Running

Distinct differences between limbs and kinetic adaptations are apparent during ILEA running, but the mechanisms underlying these adaptations are still poorly understood. The foot contact with the ground generates ground reaction forces that are reflective of the summation of the product of each body segments' mass and acceleration (Winter, 2005; Zatsiorsky, 2002). Muscle forces accelerate the body segments, but cannot move the whole body's center of mass to ambulate without the constraint of the ground and the resultant ground reaction force (Zatsiorsky, 2002). Since ILEA with transtibial and transfemoral amputations are missing at least part of their foot and ankle musculature, which provides a large portion of the overall power generation to accelerate the whole body during both walking (Robertson and Winter, 1980; Winter, 1983a) and running (Czerniecki et al., 1991; Winter, 1983a), it can be expected that ground reaction forces might differ in ILEA when stepping on the prosthetic limb. Studies have shown that the prosthetic limb generates reduced peak vertical and anteroposterior (AP) ground reaction forces compared with the intact

limb or able-bodied subjects when running (Brouwer et al., 1989; Sanderson and Martin, 1996). The inability of prosthetic feet, including RSPs, to assist in generating similar peak ground reaction forces to the intact limb has been suggested as a mechanism that limits top running speeds (Grabowski et al., 2010). Increased ambulation velocities result in greater peak ground reaction forces and peak joint moment values during both walking and running in healthy individuals (Collins and Whittle, 1989; Keller et al., 1996; Munro et al., 1987; Nilsson and Thorstensson, 1989). Increased velocities reportedly result in similar trends during ILEA ambulation (Nolan et al., 2003). Average ground reaction forces also increase with running velocity when running with RSPs but the intact limb always generates greater ground reaction forces than the prosthetic limb (Grabowski et al., 2010). These data suggest that increasing running velocity will also increase joint loads in ILEA using RSPs. However, the specific joint loads and adaptations to this ground reaction force discrepancy are not well understood.

With reduced ground reaction forces on the prosthetic limb compared with intact limbs, it is also expected that adaptations to the joint kinetics would occur during running and asymmetries between limbs in ILEA with unilateral amputations would be prevalent. Early studies showed that SACH and single-axis feet were incapable of simulating natural foot-ankle function resulting in significant interlimb asymmetries (Brouwer et al., 1989). Conflicting data exist regarding the ankle moment during ILEA running. Some studies report that the prosthetic ankle generates limited plantarflexor moments during running compared with the intact limb (Czerniecki et al., 1991; Miller, 1987), which is consistent with the previously

described reduced ground reaction forces. However, another study observed a substantially smaller peak ankle plantarflexion moment in the intact limb (Sanderson and Martin, 1996). Sanderson and Martin (Sanderson and Martin, 1996) explained that the ankle moment profile of the residual limb is directly related to the passive elastic properties of the prosthesis, running speed, and stride length and that the ILEA has little to no ability to modulate the ankle moment. Ankle moment profiles presented in ILEA sprinting with RSPs also show discrepancies. Buckley (Buckley, 2000) reported greater peak plantarflexor moments at the intact ankle in two subjects who wore both the Sprint Flex and Cheetah RSPs. Bruggemann et al. (Brüggemann et al., 2009) observed greater plantarflexion moments in a bilateral ILEA sprinter wearing Cheetah prostheses than an able-bodied control group. Buckley did not include a control group and the different running velocities of the two studies (Buckley: 6.81-7.05 m/s; Bruggemann et al.: 9.2-9.5 m/s) make comparing the data difficult.

At the knee, the prosthetic limb generates reduced peak knee extensor moments compared to the intact limb or able-bodied subjects when running (Brouwer et al., 1989; Czerniecki et al., 1991; Nolan and Lees, 2007; Nolan et al., 2006; Sanderson and Martin, 1996). To compensate for this reduction and to maintain upright support, a longer duration residual limb hip extensor moment is generated (Buckley, 2000; Czerniecki et al., 1991; Sanderson and Martin, 1996). At foot strike, the knee moment is near neutral in able-bodied runners and may exhibit a brief flexor moment (Sanderson and Martin, 1996). ILEA with unilateral transtibial amputations demonstrate a greater initial knee flexor moment at foot-strike on the residual limb

(Czerniecki et al., 1991; Miller, 1987). This phenomenon can in part be attributed to the type of prosthetic components as the flexor moment was reduced to normal (< 1 Nm) when subjects ran with a Flex foot compared to a SACH or Seattle foot (Czerniecki et al., 1991). However, since the intact limbs of some ILEA and some control subjects also exhibit small initial knee flexion moments during running, this pattern cannot be solely attributed to prosthetic componentry. Running style could also generate such a pattern. If the foot contacts the ground in an initially propulsive manner, a knee flexor moment might be produced to prevent hyperextension. Throughout stance phase, however, the knee moment is dominated by an extension moment. During the first half of stance, the moment is eccentric and serves to slow knee flexion and maintain upright body support, while a concentric extension moment exists in the second half of stance to aid in propulsion (Novacheck, 1998b). ILEA knee moments follow this pattern, but the residual limb knee peak extension moment is smaller in magnitude than that of the intact limb or for able-bodied runners (Brouwer et al., 1989; Czerniecki et al., 1991; DiAngelo et al., 1989; Miller, 1987). The smaller knee extension moment could be due to the reduced range of knee sagittal motion in the prosthetic limb throughout stance phase. Since the first half of the stance phase knee extension moment is eccentric to prevent the limb from collapsing, a lower peak moment would be required if the knee motion is limited. In swing phase, the knee demonstrates an eccentric flexor moment that slows knee extension in the second half of swing. ILEA running with non-RSPs showed similar knee moment profiles between the intact, residual, and able-bodied limbs (Sanderson and Martin, 1996). This suggests that the muscular demands to slow knee extension

between the prosthetic and intact limbs are similar. However, RSPs have much lower masses and moments of inertia than non-RSPs, so the muscular demands to resist knee extension at terminal swing may be reduced. Currently, no studies have published swing phase kinetic data on ILEA running with RSPs.

During the stance phase of able-bodied running, concentric hip extensor moment gives way to eccentric hip flexor moment which slows hip extension (Mann and Hagy, 1980; Winter, 1983b). Hip moment profiles of ILEA runners also show some substantial differences from typical running patterns. The intact hip often has an extensor moment during initial stance phase consistent with able-bodied runners, but the residual limb hip extensor moment is reportedly greater in magnitude and duration (Brouwer et al., 1989; Czerniecki et al., 1991; Miller, 1987). This increased extension moment is an adaptive mechanism that compensates for the reduced residual knee flexion moments to aid in controlling the knee flexion at the beginning of stance and assists with residual knee extension by rotating the thigh backward with respect to the hip (Czerniecki et al., 1991; Miller, 1987). In ILEA children, the intact limbs exhibited a net extensor moment near toe-off, which was inconsistent with able-bodied runners (Brouwer et al., 1989). This compensation was suggested at a strategy to limit the body's forward acceleration and was the only observed instance where the intact limb deviated from normal.

In conjunction with the reduced peak moments in the residual limb joints, peak ankle powers for ILEA with transtibial amputations during sprinting (6.8 − 7.1 m/s) are reportedly much lower in the prosthetic limb when wearing either a Flex-Sprint (870-1012 W) or Cheetah (307-637 W) RSPs than for the intact limb (1853-

2741 W) (Buckley, 2000). This reduced peak prosthetic power generation will limit running velocity in addition to inducing kinetic asymmetries between the limbs of ILEA with unilateral amputations.

The limitations in our knowledge of joint kinetic adaptations during ILEA running hinder advancements in both rehabilitation techniques and prosthetic designs. Continued research is necessary to more completely understand the biomechanical adaptations that ILEA make in order to run and to uncover control mechanisms that may guide these adaptations.

2.4.3 Mechanical Energy during Amputee Running

Energy cost during ambulation is affected by prosthesis type. For example, the VSP foot design improved energy cost by 5% during walking and 11% during running over the Flex-Foot and SACH foot (Hsu et al., 1999). The same study also observed similar improvements for "gait efficiency" (defined as energy cost per meter travelled) with no observed differences between the Flex-Foot and SACH foot. One bilateral and five unilateral ILEA with transtibial amputations running at 2.2 m/s had lower submaximal heart rate and VO_2 values when wearing RSPs compared to prostheses not specifically made for running, and their maximal heart rate (186 beats per minute, bpm) and peak VO_2 (50.7 ml/kg/min) with the RSPs were similar to an age, training status, and body composition-matched group of able-bodied subjects (182 bpm and 55.0 ml/kg/min, respectively) (Brown et al., 2009). Therefore, using RSPs gives no physiological advantage compared with nonamputee runners because the energy cost at their set speed was not significantly different (Nolan, 2008) but

they do appear to provide a physiological advantage over non-RSPs. An examination of a world-record holding ILEA with bilateral amputations also concluded that running at different velocities with RSPs is physiologically similar to but mechanically different from running with intact limbs (Weyand et al., 2009). The link between the mechanical differences and the physiological similarity is yet to be determined.

Prosthetic foot design has a dramatic effect on mechanical energy efficiency, but to date, all prostheses fall far short of the mechanical energy efficiency of the intact foot and ankle complex. The Mod III reportedly has a 95% energy efficiency when tested under static conditions and the Cheetah foot has 63% energy efficiency as measured by dynamic hysteresis (Nolan, 2008). During running at 2.8 m/s, the SACH foot has 31% energy efficiency and Flex-Foot has 84%, whereas the intact human ankle has a 241% energy efficiency while running at this speed (Czerniecki et al., 1991). Consequently, carbon fiber prostheses provide improved energy efficiency as compared to other types of prostheses, but not compared with the intact ankle (Nolan, 2008).

Czerniecki and colleagues have provided valuable advances in our understanding of mechanical work and energy adaptations during ILEA running. When running, both ILEA and able-bodied subjects rely primarily on the ankle joint to generate most of their energy followed by the knee and hip extensors. Comparing prosthetic (Flex-Foot) to intact limb, the prosthesis absorbed 28.6 J and generated 24.1 J while the intact ankle absorbed 26.1 J and generated 62.9 J of energy (Czerniecki et al., 1991). The prostheses provided similar power absorption to the

intact ankle, but were clearly unable to provide similar power generation, most likely due to the passive nature of the prostheses. As a result of the reduced power generation by the prosthetic ankle in addition to reduced power output by the residual limb knee extensors, amputee runners exhibit a reduction in total mechanical work done by the prosthetic stance phase limb (Czerniecki and Gitter, 1992). The major adaptation to offset this reduction in ankle and knee power output is that the prosthetic limb hip extensors increase their mechanical work during stance phase (Czerniecki and Gitter, 1992; Czerniecki et al., 1991). During swing phase, the mechanical work done by intact limb musculature is greater than normal with increased concentric hip flexor work in early swing and increased concentric hip extensor and eccentric knee flexor work at the end of swing (Czerniecki and Gitter, 1992). These authors suggested that the increased mechanical work by amputees' intact swing phase limb may be an important source of energy to accelerate the trunk and/or the prosthetic limb. Furthermore, transferring energy across the hip joint to the trunk during deceleration of the swing phase leg may be an important energy distribution mechanism to compensate for the reduced mechanical work done by the prosthetic limb during stance (Czerniecki et al., 1996). These studies were all performed with subjects running in non-RSPs. Similar studies are needed to confirm whether RSPs require different mechanical work/energy adaptations during ILEA running or if RSPs have improved upon the discrepancies identified in this earlier research.

In addition to biomechanical adaptations due to loss of the mechanical and physiological function of the active foot and ankle complex, the alignment of these

devices and the mechanical properties of the prostheses can affect the biomechanics of ILEA running. Shifting load line of prosthetic limb posteriorly increases plantarflexion (Buckley, 1999) and puts greater loading on the toe of the prosthesis (Lechler, 2005). Increasing the plantarflexion angle of Cheetah RSP resulted in reduced hip extensor moments and improved symmetry (Gailey, 2003). These data show that the prosthetic alignment can have positive effects on running biomechanics, but additional work is needed that would identify more objective methods to optimize prosthetic alignment for a particular task such as running at maximal speed, improving limb symmetry, or reducing loading at specific joints.

When running at 2.2 m/s, transtibial amputees with RSPs had similar metabolic cost to able-bodied runners (Brown et al., 2009) despite the much lower mass of the RSP. This implies that a running prosthesis must be lighter than intact limbs in order for an amputee to have similar energy cost to an able-bodied person (Nolan, 2008).

Extensive analyses have not been performed examining the effects of manipulating the center of mass or moment of inertia of prostheses during running. During walking gait, altering center of mass and moment of inertia have little effect on gait kinematics but do alter gait kinetics (Selles et al., 2004; Selles et al., 1999; Selles et al., 2003). A recent study reported that manipulating the moment of inertia of RSPs by adding up to 300g of mass at the distal end of the prosthesis did not affect swing time of either the residual or intact limb, average ground reaction force, or top running speed (Grabowski et al., 2010). More detailed kinematic and kinetic data were not reported.

Prostheses are manufactured in different stiffness categories that are generally prescribed based on an individual's body weight. A heavier person is typically prescribed a RSP with a higher category of stiffness (higher categories correspond to greater prosthesis stiffness). Studies investigating prosthesis stiffness indicate that stiffness affects performance. A stiffer forefoot, wider c-curve, and thinner lay-up resulted in ILEA running their fastest sprint times (Lechler, 2005), which suggests that sprint speed can be a function of stiffness and prosthetic foot shape (Nolan, 2008). Using a greater category of stiffness when running with the Cheetah RSP also improved symmetry for transtibial amputees (Gailey, 2003). These studies suggest that increasing prosthesis stiffness will improve top running performance; however, improving maximal performance often comes at the expense of other parameters. Indeed, increasing foot stiffness considerably may reduce energy efficiency (Hafner et al., 2002). It is also not known how prosthesis stiffness affects submaximal running biomechanics and energetics. The data available, however, suggest that factors other than body weight, such as running speeds and energy cost concerns (i.e. whether the patient aims to sprint or run longer distances), may also be important factors to consider when prescribing an appropriate RSP stiffness. These factors and their relationship with prosthesis stiffness warrant additional investigation to improve prescription practices.

2.4.4 Running after Transfemoral Amputations

Running biomechanics and energetics of ILEA with transfemoral amputations (TFA) are even less studied than ILEA with transtibial amputations. Not surprisingly,

running with TFA shows dramatic kinematic asymmetries. The prosthetic knee remains extended throughout swing phase, and in one study, the prosthetic limb had a running pattern similar to that of walking (Buckley, 1999). An additional study observed significantly different symmetry indices between running and walking speeds for ILEA with TFA with a majority of the parameters revealing improved symmetry at walking speeds (Burkett et al., 2003). However, this asymmetry may be partially attributed to prosthetic alignment, settings, and/or training. Lowering the knee joint in four ILEA subjects with TFA improved interlimb asymmetry across 28 different kinematic and kinetic parameters, in addition to increasing running velocity by 26% (Burkett et al., 2001).

ILEA with TFA may choose to run either with or without a knee joint. If running without a knee joint, a rigid pylon replaces the knee joint mechanism. This would necessitate employing hip circumduction strategy to clear the residual limb during swing phase, which could place additional stress on the hip joint. Since running biomechanics are poorly understood in ILEA with TFA either with or without a knee joint, much more research is needed to describe and understand compensation mechanisms and injury risk potential of the various running styles.

2.4.5 Gait Analysis Methods for Amputee Running

Little work has been done to improve the models and analysis methods needed for running biomechanical analyses. Models developed for gait analyses using inertial parameters and marker placements on the intact foot and ankle complex are commonly used with prostheses. Placing markers on the prosthetic equivalent of the

intact malleoli (either at the height of the intact limb landmarks or at the perceived "ankle joint center") have been shown to estimate an erroneous ankle joint center position compared to the functional joint center of walking prostheses and produces different ankle kinematic patterns during walking (Rusaw and Ramstrand, 2010). In RSPs, the ankle joint marker for the prosthetic limb has been placed at the height of the intact limb's lateral malleolus when subjects stood on their tip toes (Buckley, 1999). This method has several drawbacks in that it uses the intact limb in an arbitrary position to place a marker on a passive device that has different architecture and is independent from the intact foot. Further, the method cannot be used for individuals with bilateral amputation. In other studies, the "ankle" joint marker is placed on the most acute point on the prosthesis or the point of maximum flexion (Buckley, 2000; Nolan and Lees, 2000b; Nolan and Lees, 2007; Nolan et al., 2006). This offers an improvement over using an intact limb for guidance as it is a repeatable method that uses the specific prosthesis architecture to guide marker placement. However, no validation studies have been performed to date to verify the accuracy of measurements made using such estimations. Indeed, Nolan's review of carbon fiber prostheses and running indicated that considerable errors are associated with reporting prosthetic ankle angle, moment, power output, and energy due to poor assumptions of ankle marker placement on the prosthesis (Nolan, 2008).

2.5 Velocity Affects Running Biomechanics

Ambulating at different velocities may induce different movement strategies involving altered biomechanical and/or physiological outcomes. Ambulation velocity

is known to affect temporal-spatial, kinematic, kinetic, and metabolic parameters. How velocity affects these variables can provide insights into motor control and efficiency of movement paradigms. In individuals with lower extremity amputation, examining different gait velocities can identify adaptive techniques employed to compensate for the loss of limb architecture and function.

Temporally, less time is spent in stance as running velocity increases. During walking, toe-off occurs at 62% of the gait cycle, running toe-off occurs at 39%, and sprinting toe-off at 36% (Novacheck, 1998b) while elite sprinters toe-off occurs as early as 22% of the gait cycle (Mann and Hagy, 1980). Slower running velocities have significantly different stride characteristics and lower extremity kinematics than at maximal velocities (Kivi et al., 2002). The lower extremity joints achieve greater peak flexion values and overall ranges as ambulation speeds increase from walking to running to sprinting, although pelvic motion does not change much with speed in order to conserve energy and maintain efficiency (Novacheck, 1998b). Interestingly, stance phase knee flexion is greater in running than it is in sprinting. This phenomenon may stem from the knee attempting to immediately extend for power production in sprinting as opposed to allowing for a more effective shock absorption accommodation in slower running speeds. Pelvic and trunk anterior tilt do increase with speed, however, and the hip and knee kinematics are more variable at faster velocities (Kivi et al., 2002).

Kinetic examinations of velocity effects on gait show similar patterns to those seen kinematically in that increased velocity typically increases the peak magnitudes of kinetic variables. For example, ground reaction force maxima and minima are

47

velocity-dependent (Williams et al., 1987). The faster an individual walks or runs, the greater the peak reaction forces become. The increased accelerations of the body during faster ambulation directly result in the ground reaction force increases. With greater reaction forces being generated, the joint moments of the lower extremities can be expected to increase. The ankle joint provides a large amount of energy used in forward propulsion. The magnitude of peak ankle moments and of the ankle power generation is directly related to the individual's ambulation speed (Novacheck, 1998b). The total energy absorbed by the ankle also increases with running speed. The knee joint moment pattern is very similar in sprinting and running; however, the magnitude of the peak knee extensor moment during stance phase tends to be greater in running than in sprinting (Novacheck, 1998b). This is related to a greater degree of knee flexion as the limb is loaded during running than the knee flexion during sprinting. In swing phase very little power is generated by the muscles crossing the knee. Instead the muscles absorb power to control the movement of the swinging leg. The hip moment pattern is similar in all conditions of forward locomotion, but the peak values increase with gait speed. Both the hip flexors and extensors are responsible for increased power generation in running and sprinting, and their contribution increases with running velocity.

In the case of replacing a joint after amputation, the artificial limb would ideally mimic the function of the intact limb and adapt accordingly to changes in ambulation velocity. Human ankle joints could be replaced with a rotational spring and damper for slow to normal walking speeds, but as walking speeds increase, this simple replacement is no longer sufficient to mimic the characteristics of the human

ankle (Hansen et al., 2004). Augmentations are then necessary to adequately represent ankle function. The slopes of the moment versus ankle angle curves during loading appeared to change as speed was increased and the relationship between the moment and angle during loading became increasingly non-linear (Hansen et al., 2004). This suggests that the human body may need to adjust control parameters at faster speeds. This may involve simply scaling up the joint control parameters that are used or possibly changing to a different control paradigm once a certain speed threshold has been surpassed. It is possible that this threshold is the speed at which the walk to run transition occurs.

In a study investigating the swing phase control of walking, increases in walking speed were associated with increased ranges of motion and torque magnitude at each joint, but the ratio describing the relative torque magnitude at each joint remained constant (Shemmell et al., 2007). These authors concluded that control of leg swing during gait may be simplified in two ways: (1) the pattern of dynamic torque at each lower limb joint is produced by appropriately scaling a single motor command and (2) the magnitude of dynamic torque at all three joints can be specified with knowledge of the magnitude of torque at a single joint. Walking speed could therefore be altered by modifying a single value related to the magnitude of torque at one joint (Shemmell et al., 2007). This hypothesis is further supported by research of an isokinetic torque-production task at different velocities. Peak torques generated at 30 and 180 degrees/s had no effect on upper to lower extremity work and power ratios. Regardless of speed, the upper extremity produced 55% of the work and 39% of the power of the lower extremity (Charteris, 1999). This also suggests that the

joint torques are scaled together and could be modified by a single motor command and that such a control strategy can be generalized to different motor tasks.

However, if velocity continues to increase, this simple control strategy may not hold true or it may involve more complexity. Movement strategies change as one increases speed from walking to running to sprinting. This is more evident when considering the sources of power generation for forward propulsion. Hip joint powers have the greatest changes with increases in running velocity (Belli et al., 2002). The total amount of power generated across all joints increases as speed increases, but the relative contribution from each of the lower extremity muscle groups changes such that relatively more power is generated proximally as speed increases (Novacheck, 1998b). Modifying a single motor command as suggested earlier would maintain the relative contribution of the muscles at faster running velocities. It is possible that walking, running, and sprinting have different control strategies or that walking can be controlled in a simpler manner. Alternately, similar control strategies may govern ambulation; however, such a strategy may not be clear when investigating only one or a few parameters. In either case, a greater reliance on more proximal muscle groups as velocity increases may have positive implications for ILEA runners and sprinters. ILEA may be relatively less functionally impaired at faster running speeds since they are missing more distal musculature and must rely more heavily on proximal joint energy production at all speeds.

Increased gait velocities may have additional benefits for ILEA as greater ambulation velocities appear to assist with reducing asymmetry in some gait parameters. With increased walking speeds, temporal gait asymmetries are reduced,

however, loading asymmetries become larger (prosthetic temporal gait variables reduced while ground reaction forces of the intact limb increased) (Nolan et al., 2003). Increased loading of the intact limb may be a strategy to achieve greater temporal symmetry and faster walking speeds, but this may induce greater risks of injury or degenerative diseases as both increased joint loading and altered loading patterns are associated with osteoarthritis initiation and progression (Andriacchi et al., 2009; Andriacchi and Mündermann, 2006; Chaudhari et al., 2008). Despite the potentially negative consequences of the loading asymmetries, reducing the temporal asymmetries may improve stability and adaptability of limb coordination. Stability of coordination between the limbs was examined in ILEA with transfemoral amputation and control subjects (Donker and Beek, 2002). These authors found that the coordination stability was reduced in amputees because of the inherent asymmetry induced by the prosthetic components. Increasing walking velocity increased the coordinative stability in transfemoral amputees and uninjured controls suggesting that stability could be improved in ILEA by training them at faster ambulation velocities.

2.5.1 Sprinting and Maximal Running Velocities

Maximal running speed is limited by the mechanical interaction between the stance and swing phases of gait (Weyand et al., 2010; Weyand et al., 2000). Many mechanical variables have been proposed to constrain maximal running speeds, but which variables are most important remains debatable. Velocity is simply the distance covered divided by the time it takes to travel that distance. The time it takes for the limbs to be repositioned for successive steps (swing time) constrains running

velocity (Weyand and Bundle, 2010b) as faster swing times will shorten the overall step time thus reducing the time it takes for a step and increasing velocity (assuming constant step length). Ground forces, therefore, must be applied that are large enough to provide an aerial time long enough to reposition the legs for the next running cycle (Taylor, 1994; Weyand et al., 2009; Weyand et al., 2000). However, only greater vertical ground forces would produce greater aerial times, but these forces do not generate propulsive forces that assist running speeds. Vertical ground reaction forces need only be large enough to provide the minimal aerial time to swing the legs forward. Anteroposterior (AP) ground forces should be maximized to produce propulsive forces during pushoff while reducing the braking forces at footstrike.

The faster an individual runs, the less time is spent in contact with the ground, making the ability to generate maximal propulsive forces more difficult. Consequently, the stance phase limit to running speed is imposed not by the maximum forces that the limbs can apply to the ground but rather by the minimum time needed to apply the large, mass-specific forces necessary (Weyand et al., 2010). This idea is further supported by anthropometry of elite sprinters. Shorter plantarflexor moment arms and longer toes in this population permit greater forward impulse generation. Longer toes in particular extended the contact time, providing more time for the propulsive ground reaction force to accelerate the body forward (Lee and Piazza, 2009).

Additionally, the forward distance the body travels when the foot is in contact with the ground will constrain top running speeds (Weyand and Bundle, 2010b). The body is a projectile during the flight phase of running, so no forces can be generated

by the runner that could assist to increase speed. Increasing the distance the body travels forward during stance would then dictate a large portion of forward progression. However, increasing stance distance alone would not increase running velocity without maintaining or reducing the stance time.

Clearly, none of the constraints alone dictate top running velocities, rather a combination of them interact to limit top running speeds. In individuals with amputation, prostheses have long been considered a large limitation for both walking and running function due to their passive nature. However, the recent controversy over whether or not RSPs provide an advantage has provided a renewed interest in the mechanical running constraints. Weyand and colleagues have argued that RSPs provide an advantage over intact limbs as RSPs have reduced mass that allow for faster swing times and they can be longer than intact limbs, allowing for increased contact durations (Weyand and Bundle, 2010a; Weyand and Bundle, 2010b; Weyand and Bundle, 2010c). Kram and colleagues countered this argument citing insufficient evidence to support any claim of advantage or disadvantage (Kram et al., 2010). Ground reaction forces, stance time, and swing time data during amputee sprinting were limited to one subject, Paralympian Oscar Pistorius, at the time of the article. Those data showed that peak vertical ground reaction forces were lower for Pistorius than for a control group of able-bodied athletes with similar best running times (Brüggemann et al., 2009; Weyand et al., 2009). With only one subject, a convincing argument for the advantages of RSPs cannot be made. Furthermore, the reduced reaction forces would generally be considered a disadvantage. Kram et al. also argue that Pistorius' swing times are not abnormally fast compared with other Olympic

athletes, but the reduced swing times may be a compensatory mechanism to overcome the reduced ground reaction forces (Kram et al., 2010).

From a metabolic energy standpoint, RSPs do not appear to provide any advantage. A study of six amputees running with RSPs showed no statistical difference in VO_{2max} values compared with a control group, but the amputees did have higher maximal heart rates (Brown et al., 2009). An additional study of Oscar Pistorius reported that he had metabolic costs 3.8% less than elite distance runners, 6.7% lower than subelite distance runners, and 17% lower than elite 400m specialists with intact limbs (Weyand et al., 2009).

The debate on whether or not RSPs provide an advantage or disadvantage in producing top running speeds is far from over. Much more research is needed to provide sufficient evidence for either argument and more amputees need to be tested in order to generalize findings.

2.6 Prosthetic Stiffness Affects Gait Biomechanics

In addition to the different designs of RSPs, each of these devices are manufactured in different stiffness categories that are generally prescribed based on an individual's body weight and general activity level. A heavier person is typically prescribed a RSP with a higher category of stiffness (higher categories correspond to greater prosthesis stiffness). Studies investigating prosthesis stiffness indicate that the stiffness affects performance, so body weight and general activity level may be insufficient guidelines for prescribing a stiffness category. A stiffer forefoot, wider c-curve, and thinner lay-up resulted in ILEA running their fastest sprint times (Lechler,

2005), which suggests that sprint speed can be a function of stiffness and prosthetic foot shape (Nolan, 2008). Using a greater category of stiffness may also improve gait symmetry values for ILEA with transtibial amputation (Gailey, 2003; Wilson et al., 2009), but it has also been shown to reduce energy efficiency (Hafner et al., 2002). These data suggest that different prosthesis stiffness categories could affect the performance of the prosthesis and therefore the force and torque transfer through the device.

2.7 Limitations and Future Directions

Locomotion research investigating individuals with lower extremity amputations is still in its relative infancy, especially when considering running biomechanics. New prosthetic components are constantly being developed in hopes of attaining the lofty goal of matching or exceeding intact limb function. Additional research is required to validate functional improvements and guide areas of development to continue improving prosthetic designs and rehabilitation techniques.

In the realm of ILEA running, there is an immense need for studies investigating the biomechanical and physiological adaptations to running with RSPs. A first major milestone that has not yet been achieved is the development of valid models to appropriately study these prosthetic designs. Current biomechanical models were developed and validated using intact limbs, and these models are likely either not appropriate or not optimal for measuring RSP biomechanics. New models are necessary to improve the accuracy and consistency of biomechanical data from different prostheses. In conjunction with suitable models, accurate inertial properties

of the prostheses are needed to complete accurate kinetic analyses. Once these two seminal steps are completed, running studies of ILEA using RSPs can be confidently developed and interpreted.

Valuable information currently exists regarding adaptations made by ILEA while running. However, a vast majority of these studies were performed at one submaximal velocity or at top sprinting speeds. Most published studies of sprinting biomechanics with RSPs have a sample size of one, and nearly all of these studies have used the same single subject. In order to generalize findings, more diverse populations with sample sizes greater than one are necessary. Our understanding of joint kinetic control will greatly benefit from studies that systematically investigate running adaptations at multiple velocities. In this way researchers can better discriminate whether control scaling occurs or if different control paradigms might be implemented at different target running speeds. Studies investigating joint moment adaptations to different running velocities would provide valuable knowledge on the net muscular control at the intact and residual joints. Studies investigating joint powers and work adaptations at different running velocities would provide information regarding the energy generation, absorption, and flow by and through the limbs that allow ILEA to modulate their running speeds.

Chapter 3: Marker Placement on Running-Specific Prostheses Does Not Affect Proximal Kinetic Estimations

(Working draft, in preparation for submission to the Journal of Biomechanics)

3.1 Abstract

Gait analyses for individuals wearing running-specific prostheses (RSPs) are currently performed by placing reflective markers arbitrarily on the RSP; inverse dynamics techniques are then used to estimate joint kinetics. Marker placements on RSPs have not been validated for accuracy in estimating joint kinetic data, and estimation errors are unknown. This study examined how varying the number and position of markers on RSPs affect kinetic estimations compared to directly measured values. Reflective markers were placed every 2 cm on four commercially available RSP models with three different stiffness categories each (12 total RSPs). A 6-degree-of-freedom load cell was attached to a material testing system (MTS), and the RSPs were attached to the load cell. The MTS applied cyclical axial loading to 2500N simulating peak running loads, measured by the proximal load cell. Ground reaction forces were measured from a second load cell fixed to the ground. Inverse dynamics estimated force transfers from the ground to the proximal endpoint of the prostheses through segments defined by markers. Differences between estimated forces and moments and measured values at the proximal endpoint were considered error and were calculated for every combination of markers. Results showed that regardless of the number of markers or their placement on the RSPs, joint kinetic estimations resulted in errors less than 10 N (1% of peak force), 17.5 N (0.75%), and 2.5 Nm (1.6%) for AP force, vertical force, and flexion moment, respectively. Therefore, marker placement on RSPs does not appear to affect proximal kinetic estimations during stance phase.

3.2 Introduction

During three-dimensional gait analyses, reflective markers are placed on anatomical landmarks to estimate joint center positions and to define body segment motions. The distal joint motion data along with ground reaction force data from a force platform can be used as inputs to inverse dynamics equations to estimate proximal joint kinetic values. In locomotion studies using prostheses, markers defining the most distal joint axis, usually the ankle, are generally affixed to spots on the prosthetic foot that mimic the relative marker location on the intact foot and ankle complex(Buckley, 1999; Goujon et al., 2006; Sanderson and Martin, 1996; Selles et al., 2004; Silverman et al., 2008; Winter and Sienko, 1988). Prostheses are often modeled anthropometrically like an intact limb even though these devices may not have the same architecture or landmarks(Miller, 1987; Royer and Wasilewski, 2006; Su et al., 2007).

With the development of running-specific prostheses (RSPs), new prosthetic foot designs have emerged that resemble a "C" or "J" shape rather than the human foot. The shape allows the prosthesis to flex and return more energy for propulsion during running, similar to a spring. Placing multiple markers to model RSPs as multisegmented objects during amputee locomotion studies provides a great challenge since definitive joint axes may not exist within the prosthetic foot design. Yet modeling RSPs as single rigid objects may not be appropriate since these devices can deform throughout their length. In the face of these challenges, many researchers analyze these prostheses using similar biomechanical analysis methods as have been employed in intact feet and prosthetic feet designed for walking. Studies investigating

running with RSPs have estimated the prosthetic limb "ankle" joint to be either at the same relative position as the intact limb's ankle joint (Figure 3.1a) or the point of greatest curvature (Figure 3.1b)(Buckley, 1999; Buckley, 2000; Burkett et al., 2003). However, no information is available to support whether or not these marker placements validly represent an "ankle" joint or whether proximal joint kinetic data are affected by the choice in marker placement. Using the intact limb as a reference for marker placement excludes such a model from use on individuals with bilateral amputations. Consequently, researchers need to know how marker placement on RSPs affects proximal joint kinetic estimations so models can be created for different RSP designs and can be used with individuals with either unilateral or bilateral amputations. An accurate model will provide data that can be interpreted with confidence and is needed to produce biomechanical and physiological data necessary to identify optimal running techniques, prosthetic alignment, prosthetic designs, training regimens, and energy efficiency. Placing more markers on the prosthetic keel
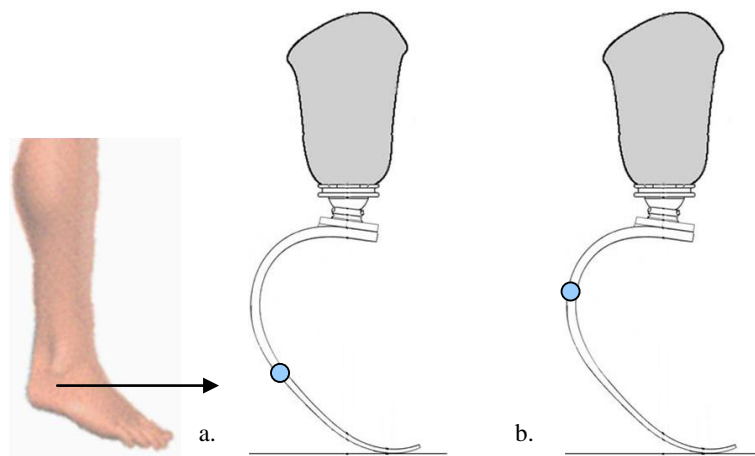
Figure 3.1. Literature has reported marker placement for running prostheses at (a) the height of the intact limb's lateral malleolus or (b) the point at which the radius of the prosthesis is most acute.

will allow for more subsegment definitions within the prosthesis. With more subsegments, the deformation and accelerations along the prosthetic keel can be more accurately modeled. Consequently, more accurate kinetic estimations can determined with more subsegments. On the other hand, each subsegment will inherently include errors due to system inaccuracy (Richards, 1999; Riemer et al., 2008). As the number of subsegments increases, the inaccuracies associated with each subsegment definition and with the elemental variables in the subsegmental kinetic estimations can accumulate to increase the overall error of the kinetic estimations proximal to the prosthesis. There may be an optimal tradeoff that allows for accurate modeling of keel motion while minimizing the errors in proximal kinetic estimations.

In addition to different RSP designs, each of these devices are manufactured in different stiffness categories that are prescribed based on the user's body weight and general activity levels(Lechler, 2005; Nolan, 2008). A heavier person is typically prescribed a higher stiffness category corresponding to greater prosthesis stiffness. Research indicates that the stiffness affects performance; therefore, body weight and general activity level may be insufficient guidelines for prescribing a stiffness category. A stiffer forefoot, wider c-curve, and thinner lay-up resulted in individuals with lower extremity amputation (ILEA) running their fastest sprint times(Lechler, 2005), which supports that sprint speed can be a function of stiffness(Hobara et al., In Press) and prosthetic foot shape(Nolan, 2008). Using a greater stiffness category may also improve running gait symmetry values for ILEA with transtibial amputation(Gailey, 2003; Wilson et al., 2009), but it has also been shown to reduce energy efficiency(Fey et al., 2011; Hafner et al., 2002). These data suggest that

different prosthesis stiffness categories could affect the performance of the prosthesis and therefore the force and moment transfer through the device.

The aim of this study was to investigate how varying the number and position of markers on RSPs would affect kinetic estimations compared to directly measured values. These effects were examined across four different RSP designs with three stiffness categories each.

3.3 Methods

Four of the most commonly prescribed RSPs currently available on the market were tested including the 1E90 Sprinter (OttoBock Inc.), Flex-Run (Ossur), Cheetah (Ossur) and Nitro Running Foot (Freedom Innovations) (Figure 3.2). Three different stiffness categories were also tested for each prosthetic design to identify whether prosthetic stiffness affects marker placement results. Stiffness categories, presented in Table 3.1, were chosen to reflect a common range of stiffnesses that might be prescribed. OttoBock does not use the term "category" to reflect stiffness, rather RSP stiffness is reflected by the target weight and activity level of the person using the device. Prostheses were aligned neutrally with their proximal ends attached to a six-degree-of-freedom load cell (Bertec PY6, Columbus, OH) that was connected to the

Table 3.1. Stiffness categories tested in this study for each prosthesis. The body mass range recommended by the manufacturers for each stiffness category is shown in parentheses.

Prosthesis Model	Stiffness Category (body mass range)		
Freedom Innovations Nitro	3 (60-68 kg)	6 (89-100 kg)	7 (101-116 kg)
Ossur Cheetah	3 (60-68 kg)	5 (78-88 kg)	7 (101-116 kg)
Ossur Flex-Run	3 (53-59 kg)	5 (69-77 kg)	7 (89-100 kg)
Otto Bock 1E90	140 lb (63.6 kg)	185 lb (84.1 kg)	235 lb (106.8 kg)

a. Freedom Innovations Nitro   b. Ossur Flex-Run   c. Ossur Cheetah   d. Ottobock Sprinter 1E90

Figure 3.2. Prostheses used for mechanical testing. Images from a) www.freedom-innovations.com, b-c) www.ossur.com, and d) www.ottobock.com.

arm of a material testing system (MTS, Eden Prairie, MN). A second load cell was secured to the base of the MTS (Figure 3.3). The prostheses were cyclically loaded for ten cycles with axial forces up to 2,500 N to simulate peak vertical forces commonly observed during running(Ferris et al., 1998; Grabowski et al., 2010; Weyand et al., 2000) (approximately three times the body weight of a 75 kg person). The load cells sampled data at 1000 Hz and measured the forces and moments at the point of load application proximal to the prostheses (applied load) and the reaction forces distal to the prostheses (ground reaction forces).

Reflective markers were placed at 2 cm intervals along the lateral aspect of the keel of each RSP (see Figure 3.3). Reflective markers were also placed orthogonally on the anterior, lateral, and medial aspect of the "head" of the prosthesis, at the point of connection to the socket or pylon, in order to define the prosthesis' local coordinate system. Three additional markers were placed along the midline of each prosthesis to define a plane to which the keel markers were projected for further analysis. An 8-camera motion capture system (Vicon, Oxford, UK) with a capture frequency of 500 Hz was used to collect marker 3-D positional data during each trial.
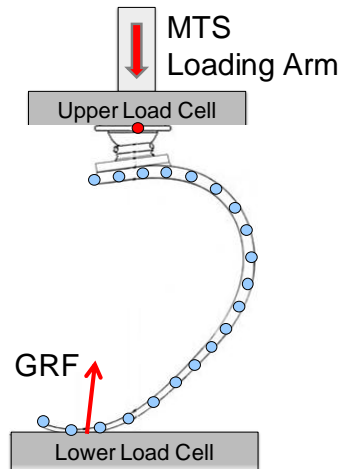
Figure 3.3. Marker placement on a RSP (Flex-Run shown) and its position in an MTS machine between two load cells. Fewer markers than actual are shown in the illustration for clarity. The most proximal dot indicates the load application point, measured by the upper load cell. The lower load cell measured ground reaction force (GRF). The arrows represent the input and GRF force vectors.

Two consecutive projected midline markers defined individual segments of the prosthesis (assumed to be rigid) and consecutive segments shared a common marker. The joint between these segments was assumed as a hinge joint. Standard inverse dynamics calculations(Zatsiorsky, 2002) were made to estimate the force and torque transfer from the ground reaction force, through the defined prosthesis segments, and to the load application point proximal to the prosthesis.

Prosthesis thickness was measured at each marker position using digital calipers, and prosthesis width at each position was calculated as twice the distance between the marker and its midline projection. Prosthesis segments were considered as rigid trapezoidal cuboids (see Figure 3.4). The center of mass (CM) along the width and thickness of each segment were determined from half the average width and thickness, respectively. CM position along the long axis (length, CM_z) of each segment was determined by Equation 1:

64
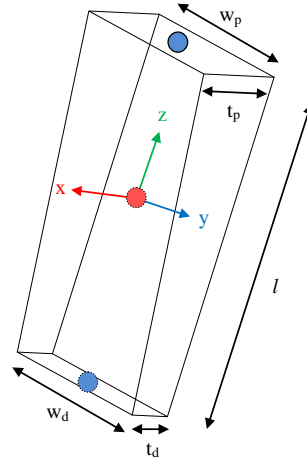
Figure 3.4. Schematic of segment definitions within each prosthesis. Circles at each end represent projected markers, the central circle represents the segment center of mass. The axis defines the segment local coordinate system with its origin at the center of mass. Segment length (*l*) is also shown along with the width (w) and thickness (t) at the proximal (p) and distal (d) ends.

$$CM_z = \frac{w_d + 2w_p}{3(w_p + w_d)} * l \qquad\qquad [1]$$

where w_d and w_p are the distal and proximal end widths and *l* is the segment length.

Segment volumes were estimated as a trapezoidal cuboid volume and the total volume of each prosthesis was estimated by summing all segment volumes. Mass was assumed to be evenly distributed throughout each RSP such that the ratio of segment volume to total volume equaled the ratio of segment mass to total mass, and segment masses were determined accordingly. The inertial properties of each prosthesis segment were estimated using assumptions based on a trapezoidal cuboid. Each segment length was integrated across 200 subsegments. Principal axis moments of inertia of each segment were estimated by Equations 2-4:

65

$$I_{xx} = \sum_{1}^{i} [\frac{1}{12} m_i (l_i^2 + w_i^2) + m_i r_i^2] \qquad \text{[2]}$$

$$I_{yy} = \sum_{1}^{i} [\frac{1}{12} m_i (l_i^2 + t_i^2) + m_i r_i^2] \qquad \text{[3]}$$

$$I_{zz} = \sum_{1}^{i} [\frac{1}{12} m_i (w_i^2 + t_i^2)] \qquad \text{[4]}$$

where m_i is the mass, l_i is the length, w_i is the width, t_i is the thickness, r_i is the distance between the subsegment CM and the segment CM for each integral subsegment i, respectively.

The angles between each set of three consecutive markers were calculated throughout the cyclic loading and the range of angle change was determined at each marker "joint". Markers representing joints that had an angular change of less than one degree were removed from further analyses as they were considered as part of a larger rigid segment. The one degree threshold was determined from the marker position error of the motion capture system. The remaining markers were used for the model analysis.

The difference between force and moment values at the load application point from the estimated inverse dynamics calculations and the directly measured values from the top load cell was considered model error. Force and moment estimations were made with every combination of remaining markers giving a resultant error value for each combination. Error was calculated for each loading cycle using Equations 5 and 6 for root mean squared error (RMSE) and normalized RMSE (NRMSE), respectively.

66

$$RMSE = \frac{\sum(K_m - K_c)^2}{n} \qquad\qquad [5]$$

$$NRMSE = \frac{RMSE}{(K_{m_{max}} - K_{m_{min}})}\% \qquad\qquad [6]$$

where K_m represents the directly measured kinetic values (force or moment) from the upper load cell, K_c represents the calculated kinetic values from inverse dynamics equations, n is the number of data points in the loading cycle, and *max* and *min* represent the maximum and minimum values within the loading cycle, respectively.

3.3.1 Uncertainty Analysis

Uncertainty refers to the maximum possible error in the inverse dynamics estimation (Riemer et al., 2008). The effects of input variable uncertainties were used to estimate the uncertainty of the resultant joint force and moment variables via an error analysis method. The upper bound of uncertainty in the result u_R was calculated according to Equation 7 (Riemer et al., 2008; Taylor, 1997):

$$u_R = \pm\sqrt{\sum_{i=1}^{n}\left(\frac{\partial R}{\partial x_i}\Delta x_i\right)^2} \qquad\qquad [7]$$

where R is the resultant value (e.g. joint force or joint moment), x_i is the ith input variable in predicting R, and Δx_i is the error associated with input variable x_i. Primary sources of error (Δx_i) included errors related to force measurement and marker noise which affects segmental kinematic parameters. The uncertainties

Table 3.2. Uncertainty (U) estimates for each prosthesis when calculating AP force (F_x), vertical force (F_z) and flexion moment (M_y).

Prosthesis	Cat	UF_x (N)	UF_z (N)	UM_y (Nm)
Freedom Innovations Nitro	3	0.208	0.255	0.030
	6	0.323	0.244	0.022
	7	0.227	0.336	0.019
Ossur Cheetah	3	0.225	0.174	0.333
	5	0.300	0.141	0.316
	7	0.384	0.344	0.685
Ossur Flex-Run	3	0.232	0.232	0.017
	5	0.441	0.261	0.016
	7	0.168	0.288	0.014
Otto Bock 1E90	140lb	0.312	0.198	0.023
	185lb	0.119	0.172	0.043
	235lb	0.129	0.288	0.029

Cat = stiffness category

estimated for anteroposterior (AP) force, vertical force, and flexion moment for each prosthesis are shown in Table 3.2.

3.4 Results

Calculated values and error data are presented for AP forces, vertical forces, and flexion moments during the cyclical loading trials for each prosthesis. Mediolateral (ML) forces, ML rotational moments, and internal/external rotational moments are not presented since the axial loading of the prostheses produced minimal forces and moments along and about these axes, respectively.

Regardless of the number of markers or their placement on the various RSPs, force and moment calculations using inverse dynamics techniques resulted in errors of less than 1.6% as compared to the directly measured values (Table 3.3). Directly measured and estimated AP force, vertical force, and flexion moment values are
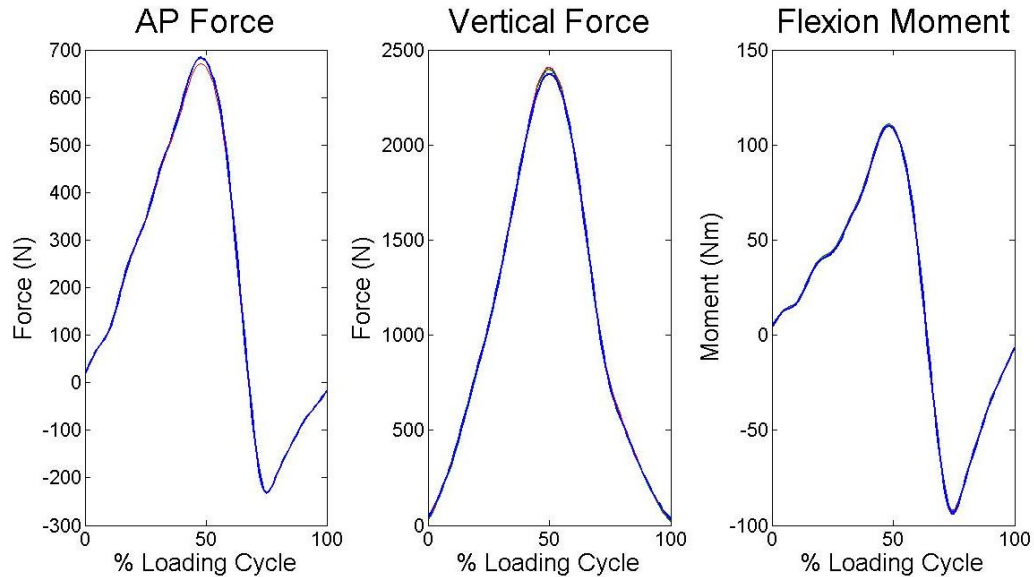
Figure 3.5. Anteroposterior (AP) force, vertical force, and flexion moment curves for cyclical loading. Thick lines represent the directly measured values from the upper load cell. Thin lines overlaid on the curves (showing nearly identical patterns) represent calculated values from each different combination of markers. Exemplar data are from the Flex-Run category 3 prosthesis. Other tested prostheses and stiffness categories showed similar results.

presented in Figure 3.5. Raw errors between the directly measured and calculated forces and moments are presented in Figure 3.6.

Across all stiffness categories and all tested combinations of markers, the Freedom Innovations Nitro prosthesis had a maximal RMSE range of 0.26 N (AP force), 4.45 N (vertical force), and 1.02 Nm (flexion moment) and a maximal NRMSE range of 0.02%, 0.17%, and 0.86% for AP force, vertical force, and flexion moment, respectively. The Ossur Flex-Run prosthesis had a maximal RMSE range of 0.98 N (AP force), 5.88 N (vertical force), and 1.05 Nm (flexion moment) and a maximal NRMSE range of 0.03%, 0.28%, and 0.56% for AP force, vertical force, and flexion moment, respectively across all stiffness categories and all tested combinations of markers. The Ossur Cheetah prosthesis had a maximal RMSE range
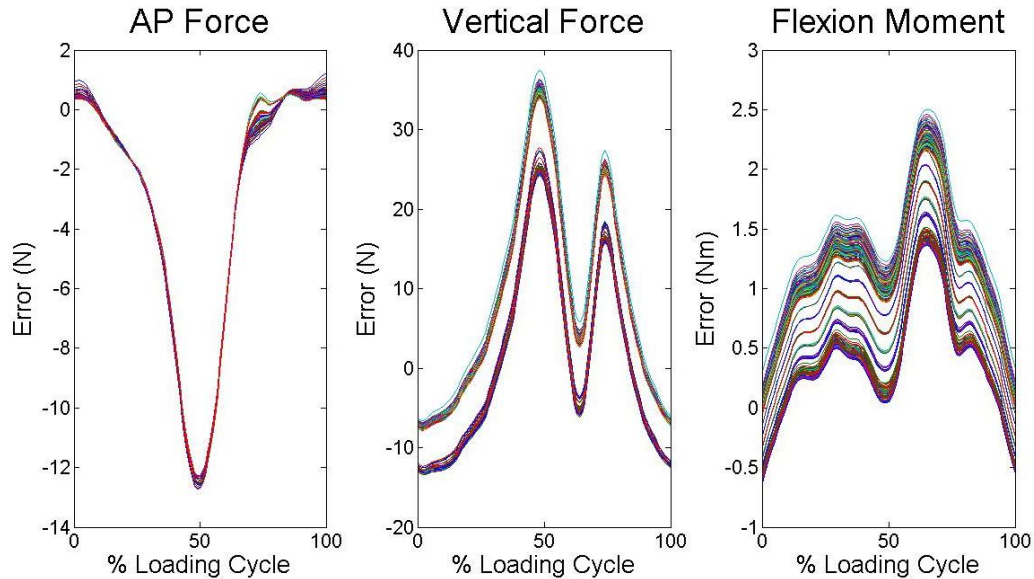
Figure 3.6. Average anteroposterior (AP) force, vertical force, and flexion moment error curves for the loading cycle. Each curve represents the difference between the directly measured values from the upper load cell and calculated values for one combination of markers on the prosthesis. Differences for all combinations of markers are shown. Exemplar data are from the Flex-Run category 3 prosthesis. Other tested prostheses and stiffness categories showed similar results.

of 0.99 N (AP force), 9.38 N (vertical force), and 0.73 Nm (flexion moment) and a maximal NRMSE range of 0.12%, 0.44%, and 0.53% for AP force, vertical force, and flexion moment, respectively across all stiffness categories and all tested combinations of markers. The Ottobock 1E90 prosthesis had a maximal RMSE range of 0.48 N (AP force), 7.54 N (vertical force), and 0.54 Nm (flexion moment) and a maximal NRMSE range of 0.07%, 0.35%, and 0.31% for AP force, vertical force, and flexion moment, respectively across all stiffness categories and all tested combinations of markers.

Table 3.3. Error ranges (minimum to maximum RMSE and NRMSE) of all combinations of markers for the estimated kinetic values from inverse dynamics equations.

		Freedom Innovations Nitro			Ossur Flex-Run			Ossur Cheetah			Ottobock 1E90		
Stiffness Category:		Cat 3	Cat 6	Cat 7	Cat 3	Cat 5	Cat 7	Cat 3	Cat 5	Cat 7	140 lb	185 lb	235 lb
AP Force	RMSE (N)	6.78-6.92	4.32-4.50	5.66-5.92	5.17-5.39	9.39-9.54	3.23-4.21	2.17-2.27	1.36-1.59	2.46-3.45	0.29-0.77	6.27-6.46	5.28-5.56
	NRMSE (%)	0.68-0.69	0.61-0.63	0.54-0.56	0.56-0.59	0.92-0.94	0.35-0.45	0.31-0.32	0.34-0.40	0.29-0.41	0.05-0.12	1.43-1.47	0.90-0.95
Vertical Force	RMSE (N)	16.37-16.80	11.55-16.00	14.39-15.85	11.05-16.93	10.19-11.95	11.85-14.18	10.27-17.41	7.57-16.95	9.22-17.49	6.88-11.93	7.17-9.61	7.16-14.70
	NRMSE (%)	0.64-0.66	0.45-0.62	0.50-0.55	0.44-0.72	0.41-0.48	0.49-0.59	0.30-0.50	0.36-0.80	0.28-0.53	0.41-0.71	0.47-0.63	0.33-0.68
Flexion Moment	RMSE (Nm)	0.98-1.36	0.81-1.83	1.27-1.99	0.63-1.59	0.78-1.09	0.89-1.94	0.91-1.13	0.87-1.14	0.66-1.39	2.02-2.32	0.98-1.52	1.03-1.38
	NRMSE (%)	0.52-0.71	0.67-1.53	0.72-1.14	0.31-0.78	0.37-0.51	0.48-1.04	0.67-0.83	0.53-0.70	0.46-0.99	0.75-0.86	0.58-0.89	0.38-0.51

*Notes: RMSE = root mean square error, NRMSE = normalized root mean square error
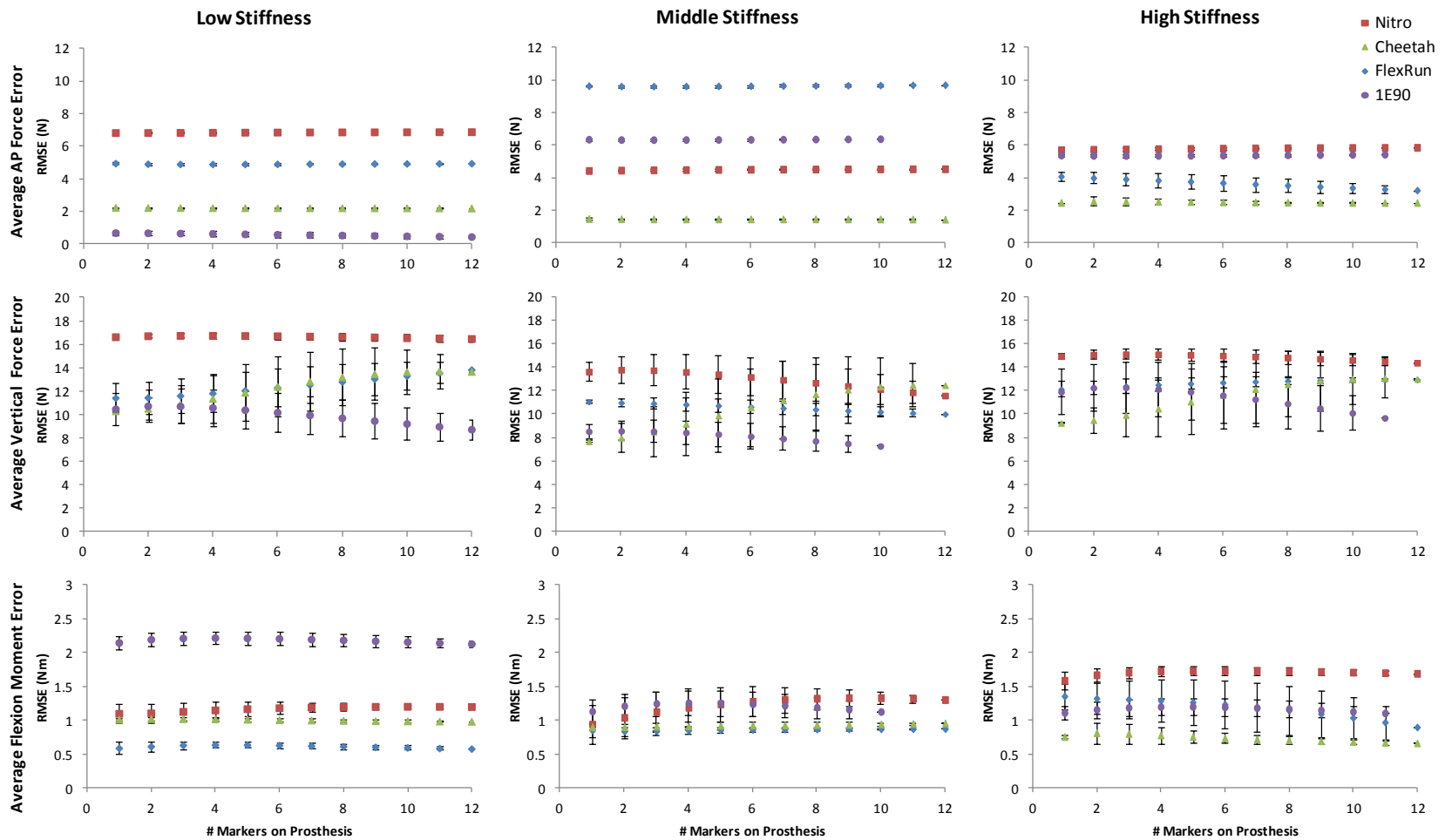
Figure 3.7. Average anteroposterior (AP) force, vertical force, and flexion moment root mean square error (RMSE) for each prosthesis across the number of markers on the prosthesis. All tested combinations with the number of markers indicated were averaged to generate each data point. Error bars represent ±1 standard deviation of all marker combinations tested for the number of markers shown.

The average AP force, vertical force, and flexion moment RMSE values for each combination according to the number of markers on the prostheses are shown in Figure 3.7. These data show little difference in RMSE values in kinetic variables regardless of the number of markers on a prosthesis.

3.5 Discussion

This study examined the effects of marker placement on proximal kinetic estimations using inverse dynamics during a cyclic loading task with RSPs. The results of this study indicated that RMSE between the directly measured and calculated kinetic variables were less than 18N for vertical forces, 10N for AP forces, and 2Nm for flexion moments regardless of the number of markers or their placement on the RSP. Considering peak values of approximately 2500N, 700N, and 120Nm, respectively, NRMSE values were less than or equal to 1.6% for all combinations of marker placements across all prostheses investigated. These low errors indicate that using any combination of markers would result in proximal joint kinetic estimations with reasonable errors for a running analysis.

To investigate whether placing a particular number of markers on a prosthesis would have an effect on the outcome variables, the average RMSE values were calculated for all combinations of a particular number of markers. For example, errors were averaged for all combinations of one marker placed on a prosthesis, all combinations of two markers, of three markers, etc. This data showed similar average RMSE values for all combinations of particular numbers of markers placed on the prostheses (see Figure 3.7). This information combined with the relatively small range of errors across all tested marker combinations suggest that the number and

placement of markers on any of the tested RSPs does not greatly influence the estimation of force and moment transfer through the prostheses. The estimated uncertainty values for AP force, vertical force, and flexion moment were less than 1% of the peak force and moment values. The range of RMSE across marker combinations for any prosthesis was similar to the uncertainty values for that prosthesis indicating that all marker combinations had similar RMSE values.

One explanation for the small change in error across different marker positions is that the magnitudes of the ground reaction forces during running are very large in comparison to the accelerations and inertial properties of the RSPs. During force transfer from the ground through the prostheses, the centers of mass of the prosthesis subsegments do not change dramatically, i.e they have low accelerations. Therefore, the ground reaction force transfers nearly unattenuated through the prosthesis, and generates torques that account for nearly all of the estimated proximal joint moments. The moments of inertia and the angular velocities of the prosthetic segments contribute relatively little to stance phase kinetics.

Several limitations exist in this study. First, only axial loading was performed on the prostheses, whereas when running, the prostheses are loaded while rolling forward, which would produce different loading patterns and potentially different prosthetic bending. This could affect the recommended marker placements on the prostheses. However, the overall ground reaction forces during running are still much larger than the inertial properties of the prostheses, so it is anticipated that for kinetic analyses, the results presented in this study would generalize to overground running. However, due to the axial loading, this study only presented AP force, vertical force,

and flexion moment results. Validation of the marker models is still needed for mediolateral forces, varus/valgus moments, and internal/external rotational moments. Additional studies are warranted to investigate these kinetic parameters using either a 6-degree-of-freedom material testing system that could mimic the prosthetic roll-over during running or direct load measurements at the proximal end of the prosthesis during running. An additional limitation of this study is that only stance phase loading was investigated. The inertial effects of the running prostheses during swing phase are most likely not trivial, so accurate measures of mass, center of mass position, and moments of inertia are needed to accurately estimate the joint kinetic values proximal to the prostheses. Future studies are needed to accurately measure and predict the inertial properties and effects of RSPs during the running swing phase.

Overall, these data suggest that kinetic data calculated from prior research with RSPs may be interpreted with greater confidence. Placing markers at the same relative position as the intact limb's ankle joint or the most acute point on the prosthesis curvature(Buckley, 1999; Buckley, 2000; Burkett et al., 2003) should yield similar results in resultant kinetic values proximal to the prosthesis. However, kinetic estimations at the prosthetic "ankle" joint representation will depend on the marker positioning(Brüggemann et al., 2009). For consistency and flexibility in modeling, it is recommended that markers are placed according to the prosthesis architecture rather than intact limb architecture. This will allow markers to be placed on the same location of a particular prosthesis from subject to subject and will allow for the study of ILEA with bilateral amputations and comparison of these individuals with those with unilateral amputations.

Utilizing a minimal marker set for RSPs will enable widespread use of such a model regardless of the number of cameras available to a laboratory and will allow for both overground and treadmill data collections while using the same model. Fewer markers on a prosthesis also makes setup less tedious and saves testing time. Additionally, fewer markers could also reduce the intra-observer and inter-observer variability in identifying the RSP keel landmarks, which are often a significant source of error. This will allow more uniform marker applications and consistency in results between and within research laboratories.

Chapter 4: Determining the Inertial Properties of Running-Specific Prostheses

(working draft for submission to Archives of Physical Medicine and Rehabilitation)

4.1 Abstract

Objectives: To (1) test the validity of a trifilar pendulum method in estimating moment of inertia (MOI) for running-specific prostheses (RSPs), (2) provide RSP inertial property values for use by the scientific community, and (3) develop a predictive equation to estimate RSP center of mass (CM) positions.

Design: Testing measurements were verified using an aluminum block with known inertial properties. Errors in MOI were investigated by systematically misaligning principal axes of the block and pendulum.

Setting: University biomechanics laboratory.

Specimens: Freedom Innovations Nitro, Ossur Cheetah, Ossur Flex-Run, Otto Bock 1E90. Three stiffness categories for each RSP were examined.

Interventions: Not applicable.

Main Outcome Measures: Mass, CM positions, principal axis MOI for RSPs; MOI error due to misalignment of principal axes of RSPs and the pendulum's platform.

Results: Inertial properties for each RSP are presented. The predictive CM equation produced errors between 0.010-0.028 m when using average input values across prostheses for a specific design. The trifilar pendulum estimated MOI within -6.21 $\times 10^{-5}$ kg·m² ($\leq 1\%$ error) of a block with known MOI. Misalignments of the RSPs' CM with the pendulum's CM between 1cm - 5cm yielded errors from 0.00002 to 0.00113 kg·m² ($0.3 - 59.2\%$). MOI about any axis varied ≤ 0.0038 kg·m² within the tested RSPs due to different stiffness categories, although MOI differed more substantially between different designs.

Conclusions: Inertial estimation errors from the pendulum measurements were less than or equal to errors associated with various methods for predicting intact limb inertial properties. This suggests that the methods and values presented are within currently accepted tolerances for inertial property estimations for gait studies.

<u>**4.2 Introduction**</u>

Joint kinetics and energetics (e.g. forces, moments, powers, and work) can provide insights into how individuals ambulate and how individuals control their movements. Link-segment models used in inverse dynamics calculations allow the estimation of proximal joint kinetics from distal link joint kinetics. This is achieved through knowledge of segment kinematics, inertial and anthropomorphic properties of segments, and external force and torque. Accurate kinetic calculations using link-segment models depend on accurate segment inertial property estimations including mass, center of mass (CM) position, and moments of inertia (MOI)(Winter, 2005).

Intact limb inertial properties and regression equations have been established through cadaveric studies(Chandler et al., 1975; Clauser et al., 1969; Dempster, 1955) and body scanning methods(de Leva, 1996; Zatsiorsky et al., 1990a; Zatsiorsky et al., 1990b). However, in individuals with lower extremity amputation (ILEA), prosthetic components replace lost limbs, and the inertial properties of the resultant limb-prosthesis are altered. It is common practice for researchers to approximate the inertial properties of walking prostheses by using the values of intact limbs even though the inertial properties may differ(Lehmann et al., 1998; Mattes et al., 2000). Some researchers suggest that modeling prosthetic feet using the same marker placements and inertial properties as intact limbs produces reasonably acceptable error levels in gait parameters during stance phase(Miller, 1987; Royer and Wasilewski, 2006; Su et al., 2007). However, other research supports the notion that the inertial properties of prosthetic feet significantly impact the resultant joint kinematic and kinetic estimations during both stance and swing(Mattes et al., 2000;

Selles et al., 2004; Selles et al., 1999; Selles et al., 2003) suggesting that more accurate estimations of prosthetic inertial properties are required. With the advent of running-specific prostheses (RSPs), these prosthetic components no longer resemble the intact foot and ankle complex, and they have much smaller masses than the anatomical parts they replace. It is therefore reasonable to assume that RSPs also have substantially different CM positions and MOIs than intact limbs. Currently there is very limited information on the inertial properties of RSPs, measurements of these properties, and the effects that these properties have on joint biomechanics. While RSP mass is relatively easy to measure using a scale, the CM position and MOIs require additional equipment and can be more difficult to determine. To our knowledge, only one study to date(Brüggemann et al., 2009) has reported any inertial property values for running specific prostheses.

Multiple methods of measuring MOIs exist. Genta and Delprete examined these methods and broadly categorized them into acceleratory and oscillitory(Genta and Delprete, 1994). They reported that acceleratory methods rely on non-periodic motion such as a falling weight or rolling on a ramp and are more affected by the presence of damping. Oscillatory methods rely on periodic motion, and within this category, torsional and multifilar pendulums are the most accurate, capable of errors less than 1%(Genta and Delprete, 1994). Physical pendulums, also oscillatory, are most commonly used in the prosthetic literature to measure prosthesis MOIs. These pendulums generally rely on a joint or bearing that is assumed to be frictionless to make accurate MOI measurements(Hillery et al., 1997; Martin et al., 1989). In practice, however, friction in this bearing does exist and, along with air resistance,

will slow the period of oscillation and impart error in the inertial estimations. One solution to this problem is to perform multiple oscillation trials with the pendulum and use only the first period under the assumption that it best represents the true period of oscillation(Hillery et al., 1997; Smith, 2008). An alternative solution is to use other pendulum designs that do not rely on bearings, such as multifilar pendulums, which minimize the issues caused by friction and allow for measurements of more periods of oscillation. A trifilar pendulum is a form of multifilar pendulum that utilizes a frame or platform suspended from three equidistant wires about which rotation occurs.

This study was designed to (1) test the validity of a trifilar pendulum method in estimating the inertial properties for four common RSP designs, (2) provide inertial property values for RSPs that are readily available for use by the scientific community, and (3) develop a predictive equation to estimate RSP CM positions.

4.3 Methods

Four commonly available RSPs were evaluated. The tested models included the Freedom Innovations Nitro, Ossur Cheetah, Ossur Flex-Run, and Otto Bock 1E90. Three different stiffness categories were investigated from each prosthesis model to identify whether inertial differences exist within each model type. The stiffness categories are typically prescribed according to user body mass and activity level, with greater categories corresponding to greater weight and activity intensity. Stiffness categories are not standardized across manufacturers, so a comparable range of stiffness categories for each prosthesis was tested. Stiffness categories tested in this study and the corresponding body mass ranges recommended by the manufacturers

Table 4.1. Stiffness categories tested in this study for each prosthesis. The body mass range recommended by the manufacturers for each stiffness category is shown in parentheses.

Prosthesis Model	Stiffness Category (body mass range)		
Freedom Innovations			
Nitro	3 (60-68 kg)	6 (89-100 kg)	7 (101-116 kg)
Ossur Cheetah	3 (60-68 kg)	5 (78-88 kg)	7 (101-116 kg)
Ossur Flex-Run	3 (53-59 kg)	5 (69-77 kg)	7 (89-100 kg)
Otto Bock 1E90	140 lb (63.6 kg)	185 lb (84.1 kg)	235 lb (106.8 kg)

are presented in Table 4.1. These stiffness categories were chosen to reflect a common range of population masses.

4.3.1 Mass and Center of Mass

Prosthesis masses were measured using a standard scale with a resolution of 0.001 kg (Digital Food Scale, The Sharper Image, New York, NY). Each RSPs CM position in the sagittal plane (x-y plane) was measured using a reaction board method(Groves, 1950; Hay, 1985; McIntosh and Hayley, 1952; Payne and Blader, 1970) and the principal axes were defined to originate at the CM (Figure 4.1). Each prosthesis design contained a linear "arm" section at its proximal end that was used as a reference to define the principal axes. For the Nitro and Flex-Run models, the most proximal linear segment was used to define the x-axis (antero-posterior). For the Cheetah and 1E90 models, the proximal end was used to define the y-axis (superior-inferior). In all prostheses, the z-axis was parallel to the width of the prosthesis, and orthogonal to the previously defined axis. The final principal axis was defined as orthogonal to both existing axes. The trifilar pendulum's platform CM was determined as the centroid of the triangle with the axis of rotation vertical, orthogonal to the ground.

a. Freedom
Innovations Nitro

b. Ossur Cheetah

c. Ossur Flex-Run

d. Otto Bock
Sprinter 1E90
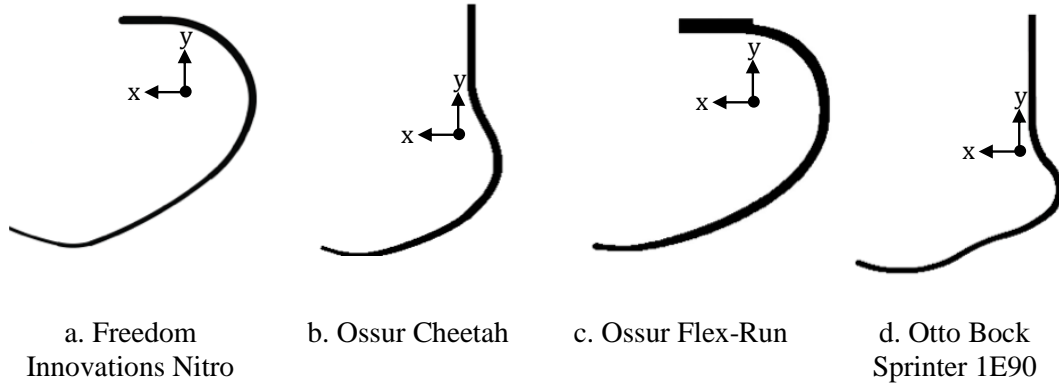
Figure 4.1. The coordinate systems used for moment of inertia estimation originating at the measured centers of mass for each prosthesis. The z-axis is orthogonal to the sagittal plane, with the positive direction pointing away from the reader. Details on defining all three axes are included in text. See Table 2 for center of mass position values.

An equation was developed to estimate the CM position for each RSP model relative to the most proximal ("head") and most distal ("toe") point on the prosthesis. Both of these markers were positioned on the midlines of the RSPs. The equation can be used to estimate the CM of a prosthesis in the absence of a reaction board or other equipment needed to directly measure a prosthesis' CM. The CM position of any RSP relates to the head and toe via Equation 1:

$$\overrightarrow{P_{CM}} = r[R]\overrightarrow{P_T} \qquad\qquad [1]$$

where $\overrightarrow{P_{CM}}$ is the head-CM position vector, $\overrightarrow{P_T}$ is the head-toe vector, r is the ratio of $\left|\overrightarrow{P_{CM}}\right|$ to $\left|\overrightarrow{P_T}\right|$, and $[R]$ is the rotation matrix with angle θ between $\overrightarrow{P_{CM}}$ and $\overrightarrow{P_T}$. Figure 4.2 shows a schematic of the relationship between the CM, head, and toe of an RSP with respect to Equation 1.
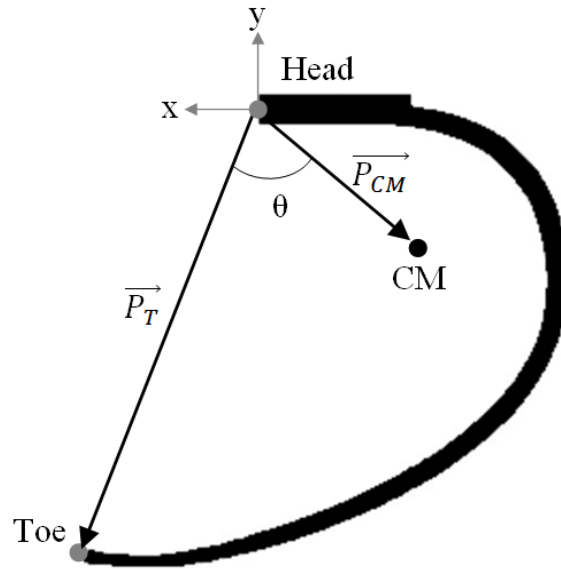
Figure 4.2. Relationship between the center of mass (CM), Head, and Toe of a running-specific prosthesis. $\overrightarrow{P_T}$ is the Head-Toe vector, $\overrightarrow{P_{CM}}$ is the Head-CM vector, and θ is the angle between these vectors. Equation 1 in the text may be used to estimate the CM position based on a known θ value and ratio between $\overrightarrow{P_{CM}}$ and $\overrightarrow{P_T}$ for a particular running-specific prosthesis design. x and y represent the 2D coordinate system, originating at the Head, used for the CM estimation.

4.3.2 Moment of Inertia

The MOI of each prosthesis was estimated by placing the prosthesis on a trifilar pendulum (see Figure 4.3) and measuring the periods of oscillation, as described by du Bois et al(du Bois et al., 2008). The pendulum consisted of a plexiglass equilateral triangle suspended from its corners by equidistant wires. A custom-built aluminum frame served to support the trifilar pendulum. A laser sensor (model BJN50-NDT, Autonics, Mundelein, IL) measured the pendulum's period of oscillation. The sensor was aligned such that the laser would be interrupted when a corner of the trifilar plate passed the sensor. Two consecutive passes determined one full period of oscillation of the pendulum.
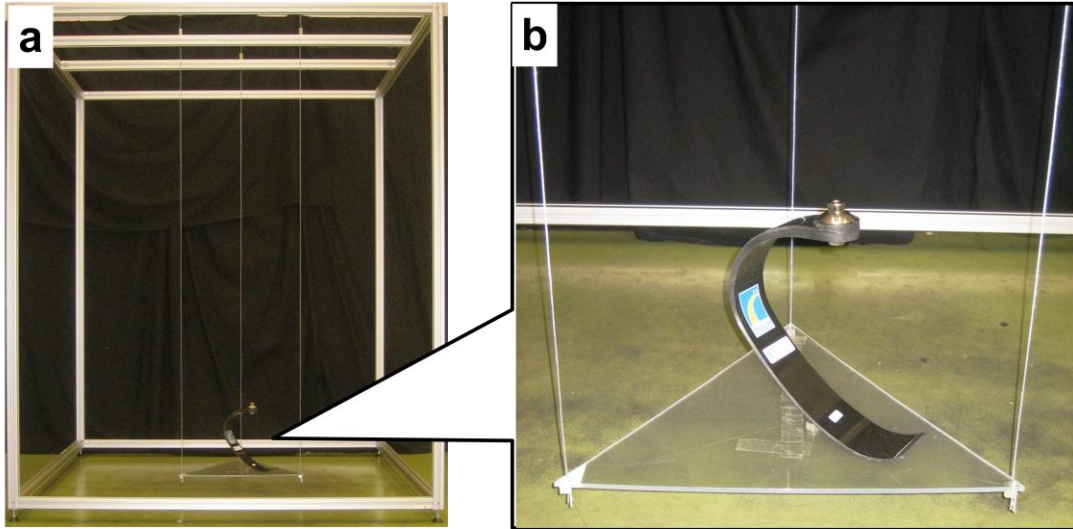
Figure 4.3. Custom-built trifilar pendulum. a) A large frame suspends b) a triangular platform by three equidistant wires that allow rotation about the platform's center of mass. The moments of inertia of a prosthesis may be calculated directly from the period of oscillation of the pendulum, measured when one corner of the platform passes a laser sensor (not shown).

Each prosthesis' principal axis MOIs were calculated from the period of oscillation measured by the trifilar pendulum. Prostheses were placed on the pendulum platform by aligning the platform's CM with the RSP's CM. Additionally, the RSP's principal axis of interest was aligned with the pendulum platform's axis of rotation (Figure 4.4). The platform-prosthesis system was then oscillated about the primary axis of rotation. Two trials of 25 oscillations were collected for each principal axis, and the resultant periods of oscillation were averaged for estimation of MOI. The period of oscillation, τ, was measured and the MOI about each principal axis originating at the CM was calculated via Equation 2 (du Bois et al., 2008).

$$I_{yy} = \frac{R^2 m g \tau^2}{4 \pi^2 L} \qquad\qquad [2]$$
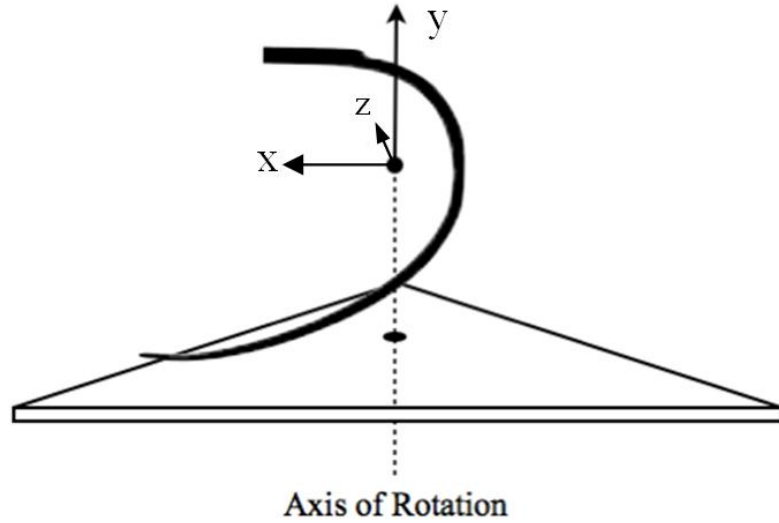
Figure 4.4. Experimental setup. Primary axes of rotation, shown here aligned with the y-axis, of the prosthesis is aligned with the trifilar pendulum platform's center of mass and axis of rotation.

where I_{yy} is the MOI about the oscillating axis of the pendulum, R is the distance from each wire connection to the center of the axis of rotation, m is the mass of the object, g is acceleration due to gravity, L is the length of the wires, and τ is the period of oscillation. When adding an object of unknown inertia, the mass and inertia from Equation 2 can be split into components of the frame and object:

$$m = m_P + m_{RSP} \qquad\qquad [3]$$

$$I_{yy} = I_{Pyy} + I_{RSPyy} \qquad\qquad [4]$$

where subscripts P and RSP represent the platform and RSP, respectively. Therefore, the MOI of the RSP can be calculated using Equation 5(du Bois et al., 2008):

$$I_{RSPyy} = \frac{R^2 g \tau^2}{4\pi^2 L}(m_P + m_{RSP}) - I_{Pyy} \qquad\qquad [5]$$

4.3.3 System Validation

To validate the system set-up, a rectangular aluminum block with a known mass (2.450 kg) and known MOI about its horizontal and vertical axes was tested in both positions using the same protocol that was used to test the RSP's. Data was collected, and MOIs were calculated and compared to the object's known MOIs. Estimation error was defined as the difference between the measured and known inertial value about that axis.

One criticism of the trifilar pendulum method is that it can induce errors in MOI estimations if the CM of the pendulum's platform and the CM of the object of interest are not aligned on top of each other(du Bois et al., 2008). These translational misalignments will cause a shift in the system's CM and the pendulum will no longer oscillate about the intended axis of rotation. Rotational misalignments will estimate the MOI about an axis different than the axis of interest. In trifilar pendulums, it is often impossible to ensure exact alignment of the centers of mass and axes of interest of the system, especially when using non-uniformly shaped objects such as prostheses. Mathematically, MOI error, ε_D, due to translational misalignment can be expressed by(du Bois et al., 2008)

$$\varepsilon_D = -\frac{m_{RSP} D^2}{m_P + m_{RSP}}\left(m_P + \frac{m_{RSP} g \tau^2}{4\pi^2 L}\right) \qquad\qquad [6]$$
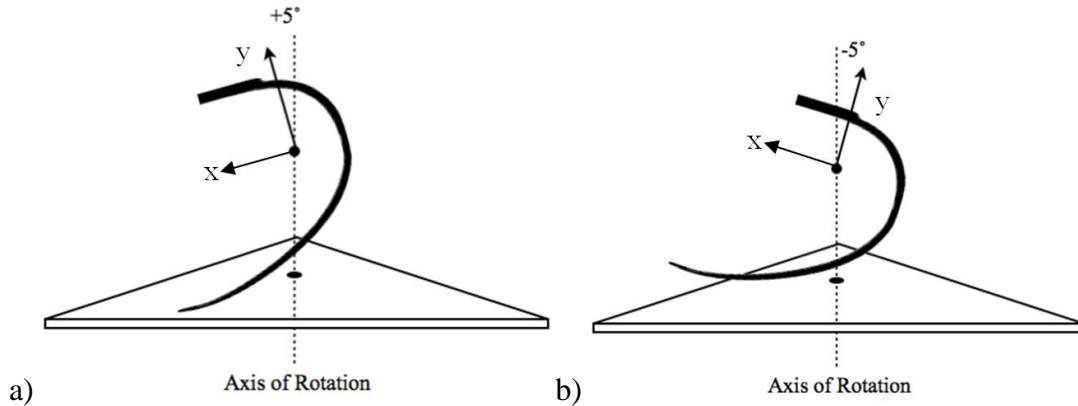
Figure 4.5. Inducing a) +5˚ and b) -5˚ rotational misalignment between the pendulum platform's axis of rotation and the prosthesis' principal axis (y-axis shown here).

where m_{RSP} is the RSP mass, m_P is the pendulum platform's mass, D is the misalignment distance between the platform and RSP CMs, g is acceleration due to gravity, τ is the period of oscillation, and L is the wire lengths suspending the platform. ε_D is influenced both by the increased inertia of the system (first term) and the change in weight distribution and center of rotation due to the new resultant CM position (second term, in parentheses) caused by the misalignment of the platform and RSP's centers of mass.

Rotational misalignment can also affect the accuracy of inertial calculations when oscillating the prosthesis about its principal axes. Each RSP's curved design prevented it from naturally balancing with its principal axes aligned with the platform's axis of rotation. Double-sided tape and light-weight foam were used to secure the prostheses. Levels and drop-lines were aligned with marked principal axes to ensure the desired alignment. To test the effects of rotational misalignment, the middle category of each type of RSP was re-tested with its x- and y-axes tilted ±5° (Figure 4.5). MOI was calculated following the same protocol and compared to the MOI of the prosthesis with its principal axes aligned to vertical.

4.4 Results

Each prosthesis' measured and estimated CM positions, including the predicted *r* and *θ* values are presented in Table 4.2.   Principal axis MOIs are presented in Table 4.3. For all prosthesis designs, the z-axis MOI corresponding to the anatomical flexion/extension axis resulted in the largest MOI whereas the y-axis (anatomical internal/external rotation) had the smallest MOI. RSPs resembling a "C" shape, e.g. the Freedom Innovations Nitro and Ossur Flex Run, had the lowest mass

Table 4.2. Center of mass (CM) positions, in cm, along the principal axes measured with a reaction board in the sagittal plane (x-y plane) relative to the "head" position (most proximal point on the prosthesis) compared to CM estimated using Equation 1 in the text. The z-position of the CM is aligned with the midline of the prosthesis and thus has a zero value. The r and θ values specific to each prosthesis exactly predicted the measured CM. The average r and θ values measured across stiffness categories for a particular prosthesis design were used as the input variables to predict the estimated CM positions.

Prosthesis Model	Cat	r	Avg r	θ (rad)	Avg θ (rad)	Measured CM (m) x	y	Estimated CM (m) x	y	Error (m) x	y
Freedom Innovations Nitro	3	0.366		-1.128		-0.053	-0.069	-0.062	-0.054	0.009	-0.015
	6	0.359	0.362	-1.091	-1.185	-0.051	-0.069	-0.063	-0.053	0.012	-0.016
	7	0.362		-1.336		-0.058	-0.063	-0.054	-0.061	-0.004	-0.002
Ossur Cheetah	3	0.504		-0.328		0.025	-0.264	0.018	-0.292	0.007	0.028
	5	0.589	0.556	-0.377	-0.360	0.019	-0.304	0.022	-0.286	-0.003	-0.018
	7	0.574		-0.374		0.021	-0.300	0.024	-0.290	-0.003	-0.010
Ossur Flex-Run	3	0.398		-0.951		-0.065	-0.072	-0.069	-0.070	0.004	-0.002
	5	0.418	0.404	-1.044	-0.999	-0.065	-0.079	-0.059	-0.079	-0.006	0.001
	7	0.395		-1.003		-0.058	-0.078	-0.059	-0.080	0.001	0.003
Otto Bock 1E90	140lb	0.597		-0.441		0.017	-0.307	0.019	-0.286	-0.002	-0.021
	185lb	0.538	0.562	-0.452	-0.429	0.029	-0.278	0.037	-0.287	-0.008	0.009
	235lb	0.537		-0.392		0.032	-0.278	0.023	-0.289	0.009	0.011

Cat = stiffness category

r = ratio of measured prosthesis head-CM to head-toe vector magnitudes

θ = angle, in radians, between measured head-CM and head-toe vectors

Error = difference between measured and estimated CM positions, in m

Table 4.3. Mass and moments of inertia calculated about each prosthesis' measured principal axis. Category represents the stiffness category of the prosthesis according to the manufacturer.

Prosthesis Type	Category	Mass (kg)	Moment of Inertia (kg·m²)		
			x - axis	y - axis	z - axis
Freedom Innovations Nitro	3	0.307	0.0021	0.0010	0.0029
	6	0.349	0.0024	0.0012	0.0033
	7	0.366	0.0026	0.0012	0.0036
Ossur Cheetah	3	0.492	0.0123	0.0021	0.0139
	5	0.511	0.0127	0.0023	0.0143
	7	0.539	0.0136	0.0022	0.0152
Ossur Flex-Run	3	0.416	0.0037	0.0014	0.0047
	5	0.437	0.0037	0.0017	0.0051
	7	0.466	0.0040	0.0017	0.0054
Ottobock 1E90	140lb	0.543	0.0116	0.0027	0.0130
	185lb	0.605	0.0131	0.0035	0.0152
	235lb	0.677	0.0144	0.0042	0.0168

x-axis = anatomical ab/adduction
y-axis = anatomical internal/external rotation
z-axis = anatomical flexion/extension

and MOI, while RSPs resembling a "J" shape, e.g. the Ossur Cheetah and Otto Bock 1E90, had greater masses and MOI values.

System validation with the aluminum block with known MOI showed that the trifilar pendulum was accurate. The error in MOI was -6.21 x10^{-5} kg·m² for the horizontal and -2.65 x 10^{-6} kg·m² for the vertical position of the aluminum block, which represent a 1% and 0.1% error in the results respectively. Figure 4.6 shows that the period of oscillation had minimal degradation across 25 consecutive oscillations.

Figure 4.7 shows errors in MOI due to translational misalignment between the RSP CM and the pendulum platform CM. The Nitro Category 3 y-axis had the lowest
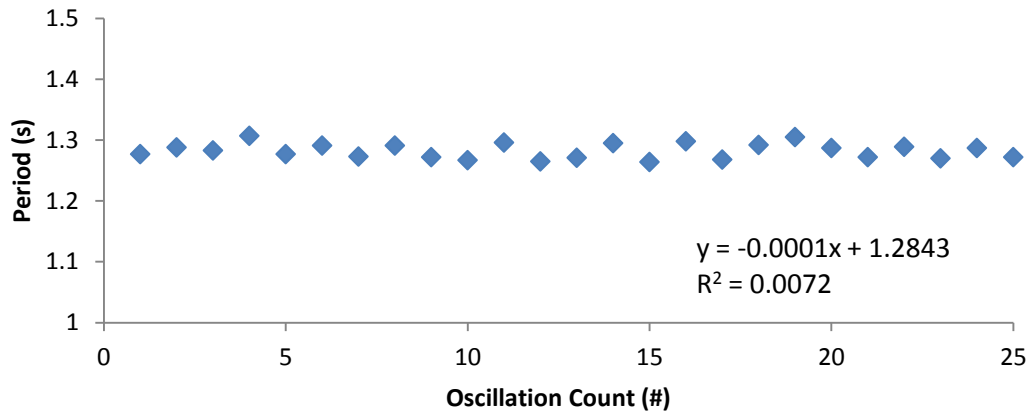
Figure 4.6. Exemplar period of oscillation measurements for a running-specific prosthesis using the trifilar pendulum. The graph shows low cycle-to-cycle variability and minimal degradation of the measured period across 25 consecutive oscillations.

mass and CM of any tested prosthesis and axis. Misalignment between the CM of this RSP and the platform's CM of 1cm yielded 0.00002 kg·m^2 (2.4%) error from MOI measured with CMs aligned. 5cm misalignment yielded 0.00038 kg·m^2 (59.2%) error and 10cm misalignment yielded 0.00236 kg·m^2 (237.0%) error. The Otto Bock 1E90 Category 235lb z-axis had the greatest mass and CM of any tested prosthesis and axis. Misalignments of 1cm, 5cm, and 10cm resulted in errors of 0.00005 kg·m^2 (0.3%), 0.00113 kg·m^2 (6.7%), and 0.00451 kg·m^2 (26.8%), respectively. As the mass and MOI of the RSP increased, the magnitude of the errors induced by misalignment increased. However, the error as a percent of the expected MOI was inflated more in RSPs with lower mass and MOI. Effects of rotational misalignment about the x- and y-axes are presented in Table 4.4. For each RSP, misaligning the y-axis resulted in a greater percentage error than misaligning the x-axis since the y-axis had a lower MOI.

Error in Moment of Inertia due to Misalignment
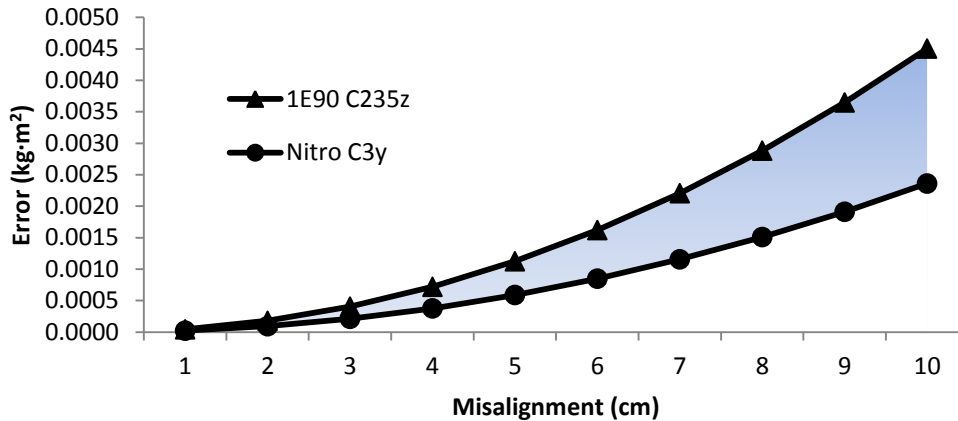
Figure 4.7. Error in moments of inertia due to misaligning the centers of mass (CM) of the tested running-specific prostheses (RSPs) and the CM of the pendulum's platform by up to 10cm, calculated by Equation 6. The Nitro C3y (Freedom Innovations Nitro, Stiffness Category 3, y principal axis) had the lowest mass and moment of inertia of the tested prostheses. The 1E90 C235z (Otto Bock 1E90, Stiffness Category 235lb, z principal axis) had the greatest mass and moment of inertia of the tested prostheses. The shaded area indicates the range of the errors in moment of inertia for all tested prostheses and principal axes due to CM misalignment.

4.5 Discussion

Mass, CM positions, and MOIs were estimated from three different stiffness categories for each of four different RSP designs. Variations in each of these parameters were identified in different prosthesis designs and stiffness categories.

Each prosthesis' CM position was calculated using a reaction board, and a predictive equation was developed to estimate these positions using the relationship between the most proximal point, most distal point, and the CM position of a particular prosthetic design. Using the ratio between the $\overrightarrow{P_{CM}}$ and $\overrightarrow{P_T}$ vectors along with the angle between these vectors, as illustrated in Table 4.3, the equation exactly

Table 4.4. Error values of rotational misalignment of ±5° orientation. Values represent the difference between the prosthesis' measured moment of inertia with the principal axis aligned properly and misaligned by ±5° rotation. Exemplar data are presented for the middle stiffness category for each prosthesis and include the raw error (kg·m²) and percent error (%).

Prosthesis Model	x-axis Error				y-axis Error			
	-5°		**+5°**		**-5°**		**+5°**	
	kg·m²	**%**	**kg·m²**	**%**	**kg·m²**	**%**	**kg·m²**	**%**
Freedom Innovations Nitro	0.00065	27.1	0.00071	29.6	0.00086	71.7	0.00051	42.5
Ossur Cheetah	-0.00030	2.4	0.00077	6.1	0.00046	20.0	-0.00050	21.7
Ossur Flex-Run	-0.00001	0.3	0.00012	3.2	0.00018	10.6	0.00014	8.2
Otto Bock 1E90	0.00030	2.3	0.00165	12.6	0.00076	21.7	-0.00075	21.4

predicted the centers of mass when the category-specific ratio and angles were used. When using the average ratio and angle for each prosthesis, a majority of the centers of mass were predicted to within less than one centimeter of error along the x- and y-axes. Several of the predictions, however, resulted in greater than 1 cm of error with a maximum error of 2.8 cm. The larger errors were a result of a greater range of ratio and angle values across the stiffness categories of a particular prosthetic design. Using different body segment parameter models (e.g. cadaveric vs. body scanning-based regression equations) to predict the intact foot CM position are shown to vary by greater than 2 cm in the predicted positions(Rao et al., 2006). This suggests that CM predictions within the range reported in this study are reasonable; however, it is recommended that direct measurements of the CM position within prostheses be used when possible to ensure the most accurate data and to reduce the possible errors these data will induce in joint kinetic estimations from inverse dynamics equations.

The high accuracy and minimal degradation in the period of oscillation measurement across multiple oscillations support the use of the trifilar pendulum

method for estimating MOI for prostheses. Trifilar pendulums measure more accurate periods of oscillation and MOI estimations than physical pendulums(Genta and Delprete, 1994) commonly used in prosthetic studies(Brüggemann et al., 2009; Hillery et al., 1997). In part this is due to the ability of trifilar pendulums to generate consistent periods of oscillation across multiple consecutive measurements while physical pendulums typically rely on bearings that impart friction that quickly degrades the period of oscillation(Hillery et al., 1997; Smith, 2008).

The errors reported herein also correspond well compared to errors reported for intact limb inertial estimations that can vary substantially depending on the method used to measure these parameters. Rao et al. (2006) compared segment inertial property estimations using six methodologies including one geometric model, two cadaveric-based models, and three mass scanning models from live subjects(Rao et al., 2006). They identified significant differences between methods in all inertial properties for each of the foot, shank, and thigh segments. Estimated MOIs for intact limbs are reported to differ by between 0.0025-0.0031 kg·m^2 for the foot, depending on the calculation method(Goldberg et al., 2008; Kingma et al., 1996). In the current study, it took an 8cm misalignment between the platform CM and CM of the RSP with the greatest MOI to induce an error (Figure 4.7) within this range. Misalignments of 5cm or less for any RSP resulted in errors less than 0.0012 kg·m^2, 50% lower than differences in intact foot MOIs due to measurement technique differences. This indicates that using a trifilar pendulum to estimate MOIs of prosthetic components will yield errors less than those currently accepted in the

literature for intact limbs, as long as the CM of the prosthetic device is aligned within 8cm of the pendulum's CM.

The CM and MOI measurements are limited to the prostheses in their uncompressed form (with no load as in running swing phase). Inertial parameters will change when the prosthesis is compressed, e.g. during running stance phase. However, since the loads required to compress the prosthesis are very large relative to the changes in inertial properties during loading, it is likely that these inertial changes would have a negligible effect on the resultant inverse dynamics estimations of joint kinetic values. Rather the external loads (i.e. ground reaction forces) would dominate the inverse dynamics predictions. Additional studies are needed to determine these effects and to discriminate between the effects of inertial changes and the loads required to produce those changes.

A limitation of the trifilar pendulum method is that it does not account for the effect of air resistance. With RSPs and low accelerations during oscillation, the effect of air resistance is most likely negligible, so these results are not anticipated to change. Additionally, this study only included inertial property estimations for RSP keels. Inertial properties for sockets were not investigated nor were any pylons or connecting hardware. The mass and MOI for sockets may not be trivial and could affect kinetic estimations during running. The methods described in this study can be used to measure inertial properties of sockets and pylons/hardware either separately or as a combined unit along with an RSP. Predictive equations for socket CM and MOI would be a valuable addition to the literature in the future, although since

sockets are subject-specific, large variability in inertial properties between subjects should be anticipated.

4.6 Conclusions

The inertial properties of four commonly prescribed RSPs were measured using a scale, reaction board, and trifilar pendulum. The trifilar pendulum demonstrated accuracy $\geq 99\%$ with low period of oscillation degradation across consecutive oscillations. Inertial parameters were shown to vary slightly between stiffness categories within a prosthetic design, and they varied more substantially between different prosthetic designs. A predictive equation was presented to estimate the CM position of a prosthesis when direct measurements are not possible. These data may be used for predicting inertial parameters of similar prostheses. The predictive equation and trifilar pendulum measured inertial properties with errors equal to or less than those found in commonly used predictive methods for intact limb inertial parameters. This suggests the presented methods and values presented are within or below currently accepted tolerances for inertial property estimations for gait studies.

Chapter 5: Amputees with Running Prostheses Adapt Ground Reaction Forces and Temporal Variables

(working draft for submission to Medicine and Science in Sports and Exercise)

5.1 Abstract

Adaptations in mechanical interactions between the feet and ground in individuals with lower extremity amputation (ILEA) alter running biomechanics to account for the loss of musculoskeletal function. Inability of ILEA to generate large ground reaction forces (GRFs) is proposed as a factor limiting top speeds, but how ILEA modulate GRFs and temporal-spatial parameters to achieve different submaximal velocities is unknown. PURPOSE: The aim of this study was to investigate GRF and temporal-spatial adaptations to different overground running velocities when wearing running-specific prostheses (RSPs). METHODS: Eight ILEA with unilateral transtibial amputations and eight control subjects ran overground around a 100m track at 2.5 m/s, 3.0 m/s, and 3.5 m/s. Ten forceplates measured GRF data and a motion capture system quantified temporal-spatial data. Temporal-spatial variables, peak 3D GRFs, and impulses were compared between limbs and groups. RESULTS: ILEA had shorter intact limb step lengths, greater stride frequencies, and shorter stance times than controls. ILEA increased velocity by increasing both stride frequency and step length. Stride frequencies were modulated by decreasing stance time but not swing time. Intact limb peak anteroposterior (AP), mediolateral (ML), and vertical GRFs were greater than prosthetic limb peaks. Intact limb peak vertical GRFs were greater than control limbs. Intact limb peak AP propulsive GRF, peak vertical GRF, and AP braking impulse increased with velocity more than those generated by the prosthetic limb. CONCLUSIONS: These data indicate that when running with RSPs, ILEA intact limbs experience elevated mechanical loading compared to the prosthetic limb that increases with velocity.

ILEA adapted for reduced intact limb step lengths and prosthetic limb peak GRFs by reducing stance times and increasing the prosthetic limb AP propulsive impulse period.

5.2 Introduction

Using running-specific prostheses (RSPs), individuals with lower extremity amputation (ILEA) have been able to approach the top running speeds of elite able-bodied runners. The controversy of whether or not RSPs provide a performance advantage to elite ILEA sprinters has led to a recent focus of research efforts. However, little to no attention has been given to the potential advantages that RSPs might provide the recreational ILEA runner or to the adaptations that ILEA must make in order to run with these devices at sub-maximal velocities.

Running velocity may be controlled by modulating a large number of factors including ground reaction forces and temporal-spatial parameters. The anteroposterior (AP), mediolateral (ML), and vertical ground reaction force (GRF) vector maxima and minima are velocity-dependent in able-bodied individuals (Collins and Whittle, 1989; Keller et al., 1996; Munro et al., 1987; Nilsson and Thorstensson, 1989; Williams et al., 1987). ILEA subjects with unilateral amputations have demonstrated similar increases in peak vertical and anterior GRFs between the limbs during both walking (Nolan et al., 2003; Silverman et al., 2008) and running with non-RSPs (Sanderson and Martin, 1996) suggesting that ILEA do not increasingly rely on the intact limb to ambulate faster. When running with RSPs, ILEA show similar increases in average vertical GRFs from the intact and prosthetic limbs (Grabowski et al., 2010) but the AP forces that influence running velocity have not been reported with respect to changes in velocity. Additionally, ILEA with unilateral amputations may demonstrate altered ML GRF profiles as the mechanical interactions between the

intact or prosthetic foot and the ground can be expected to differ. However, no reports of ML GRFs exist in ILEA running literature to confirm or refute this presumption.

Studies have shown that the prosthetic limb generates reduced peak vertical and AP GRFs compared with the intact limb and able-bodied subject limbs when running (Brouwer et al., 1989; Miller, 1987; Sanderson and Martin, 1996). An ILEA sprinter with bilateral amputations wearing RSPs also generated lower peak AP and vertical GRFs with both prosthetic limbs compared to able-bodied athletes (Brüggemann et al., 2009; Weyand et al., 2009). This inability of prosthetic feet, including RSPs, to assist in generating similar peak ground reaction forces to the intact limb has been suggested as a mechanism that limits top running speeds (Grabowski et al., 2010). AP and vertical GRF impulses during ILEA running follow similar patterns to the peak GRF values. The intact limb generates significantly greater AP and vertical GRF impulses than the prosthetic limb when running with non-RSPs (Prince et al., 1992). When running with SACH feet, the intact limb vertical impulse was also significantly greater than a control group, while no difference existed between the intact and control limb impulses when wearing prostheses with a flexible keel. The normalized vertical and horizontal braking impulses of the GRF were significantly lower during sprinting of an ILEA with bilateral transtibial amputations than those of control athletes (Brüggemann et al., 2009; Weyand et al., 2009). These data indicate that prosthetic limbs provide less braking but do not generate equivalent propulsive impulses to intact or control limbs. How propulsive impulses change with velocity and whether ILEA rely on the intact

limb more than the prosthetic limb to generate propulsion to increase velocity when wearing RSPs have not been examined.

With altered GRF profiles, ILEA runners must modulate temporal-spatial parameters in order to achieve a desired velocity. Able-bodied individuals tend to increase running velocity by increasing step length at lower velocities and by increasing step and stride frequency at greater velocities (Dillman, 1975; Ounpuu, 1994; Sanderson and Martin, 1996). But at top speeds stride frequency or step length dominance may be an individual preference (Hunter et al., 2004; Salo et al., 2011). Literature differs in how ILEA increase their running speed with respect to step/stride frequency and step length though ILEA consistently demonstrate greater stride frequencies than able-bodied runners at comparable velocities (Enoka et al., 1982; Grabowski et al., 2010; Sanderson and Martin, 1996). ILEA have been reported to predominantly increase their step frequency as opposed to increasing step length (Enoka et al., 1982), but they have also been observed to increase velocity by primarily increasing stride length (Sanderson and Martin, 1996). These differences may be due to different ranges of running velocities employed by both studies. ILEA running with RSPs on a treadmill have shown greater prosthetic limb step frequencies at slower velocities but greater intact limb frequencies at faster velocities (Grabowski et al., 2010), but this study did not report step or stride lengths. When running with non-RSPs, the prosthetic limb step length tends to be shorter than the intact limb step length despite similar or longer step duration (Brouwer et al., 1989), and ILEA runners also tend to have shorter stance and swing times compared to able-bodied limbs (Sanderson and Martin, 1996). These data suggest that ILEA may have more

difficulty in modulating their step length, possibly due to the functional impairment of pushing off with a passive prosthetic limb.

To date, little is currently known about how ILEA wearing RSPs adapt their temporal-spatial and GRF parameters to achieve different overground running velocities. The purpose of this study was to investigate GRF and temporal-spatial adaptations to different running velocities when running with a passive RSP. It was hypothesized that (1) ILEA running with RSPs would exhibit altered temporal-spatial and GRF profiles compared to a control group running at matched velocities; (2) ILEA would exhibit greater loading on and propulsion generated by the intact limb compared to the prosthetic limb indicated by GRF parameters, but differences between limbs would not increase with velocity; and (3) ILEA would increase running velocity by increasing step frequency and reducing the related temporal parameters.

5.3 Methods

5.3.1 Subjects

Eight male subjects with unilateral transtibial amputation (mean age = 32.0 ± 10.2 years, height = 1.80 ± 0.07 m, mass = 82.3 ± 13.0 kg; see Table 5.1) and eight healthy male control subjects (mean age = 29.0 ± 6.9 years, height = 1.84 ± 0.05 m, mass = 79.3 ± 7.9 kg) between 18 and 50 years of age volunteered to participate in the experiment. To maintain a uniform study population and reduce the potential data variability due to bilateral amputations and/or different design and function of prosthetic knee components, only ILEA with unilateral transtibial amputations were recruited. ILEA ran in their own prescribed RSPs to reduce variability due to using a

Table 5.1. ILEA subject characteristics. Total mass includes prosthesis mass.

Subject	Age (years)	Height (m)	Total Mass (kg)	RSP model	Amputated Limb	Running Experience (months)	Cause of Amputation
1	48	1.75	73.4	Flex-Run	Right	46	Congenital
2	31	1.71	67.9	Flex-Run	Left	48	Trauma
3	34	1.72	110.2	Flex-Run	Left	60	Trauma
4	27	1.80	73.8	Cheetah	Left	9	Trauma
5	23	1.88	85.3	Cheetah	Right	9	Trauma
6	27	1.84	85.3	Flex-Run	Left	3	Trauma
7	46	1.81	84.3	Catapult	Left	256	Trauma
8	20	1.89	78.0	Catapult	Right	12	Trauma
Mean	*32.0*	*1.80*	*82.3*			*55.4*	
(SD)	*(10.2)*	*(0.07)*	*(13.0)*			*(84.0)*	

new prosthetic design and to ensure proper alignment. ILEA had at least 3 months of running experience (range: 3-256 months) and the causes of amputation were either congenital (1) or trauma (7). Prior to participating, all subjects gave informed written consent, which was approved by the University of Maryland Institutional Review Board. Subjects with amputation were excluded if they had comorbidities on the intact limb that would affect gait.

5.3.2 Experimental Procedures

Subjects ran overground around a 100m long track at constant, prescribed velocities. Prior to beginning the experiment, retroreflective markers were placed on anatomical and prosthesis landmarks to define temporal-spatial parameters and to assist with defining footstrike events. Ten six-degree-of-freedom force platforms (Kistler, Amherst, NY) embedded in the track in series collected ground reaction forces sampled at 1000 Hz. Subjects completed at least five successful trials for each leg at each of three running velocities (2.5 m/s, 3.0 m/s, and 3.5 m/s) for averaging

purposes. A successful trial was defined as the subject running within ±0.2 m/s of the prescribed velocity within the track section containing the force platforms and stepping within the boundaries of the force platforms during the trial. Predetermined velocities were governed using concurrent biofeedback. Six sets of laser sensors were evenly distributed around the track such that when the subject ran past the sensors, the average velocity over the track section was instantaneously calculated. Verbal feedback was given to subjects indicating whether or not they were running at the desired velocity. The order for prescribed running velocities was randomized. Subjects rested for as long as needed between velocity conditions to reduce the effects of fatigue with a minimum rest of five minutes between conditions.

Temporal-spatial parameters included cycle time (the inverse of stride frequency), stance time, step time, swing time, step length, aerial time, and step frequency. Cycle time was calculated as the time for one full gait cycle to occur, from foot strike to ipsilateral footstrike. Stance time was defined as the time from footstrike to toe-off. Step time and step length were defined as the time and distance from footstrike to contralateral footstrike, respectively, and were named according to the contralateral (stepping) foot. Swing time was defined from toe-off to footstrike of the same leg. Aerial time was defined as the time between toe-off and contralateral footstrike and was named according to the contralateral (stepping) limb. Anteroposterior (AP), mediolateral (ML), and vertical ground reaction forces (GRFs) were filtered using a fourth order, zero lag low pass Butterworth filter with a cutoff set at 30 Hz. Peak AP braking, AP propulsive, medial, lateral, and vertical GRFs were examined for each limb at each velocity. AP braking, AP propulsive, and vertical

106

impulses were calculated as the time integrals of the negative AP GRF, positive AP GRF, and vertical GRF curves, respectively. Sagittal plane GRF vector angles and magnitudes were determined at the time of peak AP braking and propulsive GRF. These variables were used as indicators of general leg loading and posture. The angles were calculated between the resultant sagittal plane GRF and the AP axis.

5.3.3 Statistical Analysis

This research was designed to determine the influence of group, leg, and running velocity on temporal-spatial parameters, peak ground reaction forces, loading rates, and total impulses. Statistical comparisons were performed in SPSS 19.0 (SPSS Inc.). A 2x2x3 three-factor repeated measures analysis of variance (ANOVA) was used to identify statistical differences between the dependent variables using Group (ILEA and Control), Leg (prosthetic/intact and left/right), and Velocity (2.5 m/s, 3.0 m/s, 3.5 m/s) as independent variables (IVs). Group was treated as a between-subjects variable while Leg and Velocity were treated as within-subjects variables. When significant differences were identified from the full factorial model, two-way ANOVAs and pair-wise comparisons with Bonferroni adjustments for multiple comparisons were used when appropriate to determine which conditions were significantly different from each other. Significance for all statistical tests were set at $\alpha = 0.05$.

5.4 Results

No differences were observed between the left and right control limbs for any variable. Consequently, the data were averaged to generate a representative control

Table 5.2. Average (± standard deviation) of temporal-spatial parameters for the prosthetic, intact, and control limbs across the tested running velocities.

	Velocity	Prosthetic Limb		Intact Limb		Control Limbs	
Cycle Time[vg] **(s)**	**2.5 m/s**	0.73[a]	(0.11)	0.73[a]	(0.04)	0.79[b]	(0.04)
	3.0 m/s	0.72[a]	(0.12)	0.72[a]	(0.04)	0.76[b]	(0.03)
	3.5 m/s	0.68[a]	(0.14)	0.69[a]	(0.03)	0.74[b]	(0.03)
Stance Time[vg] **(s)**	**2.5 m/s**	0.27[a]	(0.03)	0.27[a]	(0.02)	0.32[b]	(0.03)
	3.0 m/s	0.24[a]	(0.02)	0.25[a]	(0.01)	0.28[b]	(0.02)
	3.5 m/s	0.22[a]	(0.02)	0.23[b]	(0.02)	0.26[c]	(0.02)
Step Time[vg] **(s)**	**2.5 m/s**	0.37[a]	(0.03)	0.37[a]	(0.02)	0.40[b]	(0.02)
	3.0 m/s	0.36[ab]	(0.02)	0.36[a]	(0.02)	0.38[b]	(0.02)
	3.5 m/s	0.35[a]	(0.02)	0.34[a]	(0.02)	0.37[b]	(0.02)
Swing Time (s)	**2.5 m/s**	0.46	(0.04)	0.46	(0.04)	0.47	(0.02)
	3.0 m/s	0.48	(0.04)	0.47	(0.03)	0.47	(0.02)
	3.5 m/s	0.47	(0.03)	0.46	(0.03)	0.48	(0.02)
Step Length[vg] **(m)**	**2.5 m/s**	1.04[a]	(0.09)	0.86[b]	(0.08)	1.04[a]	(0.02)
	3.0 m/s	1.20[a]	(0.10)	1.00[b]	(0.07)	1.20[a]	(0.05)
	3.5 m/s	1.31[a]	(0.10)	1.11[b]	(0.08)	1.32[a]	(0.06)
Aerial Time[v] **(s)**	**2.5 m/s**	0.09[ab]	(0.03)	0.10[a]	(0.03)	0.07[b]	(0.02)
	3.0 m/s	0.11[ab]	(0.02)	0.12[a]	(0.02)	0.09[b]	(0.01)
	3.5 m/s	0.12[a]	(0.02)	0.12[a]	(0.02)	0.11[a]	(0.01)
Step Frequency[vg] **(steps/min)**	**2.5 m/s**	163.5[a]	(10.74)	164.4[a]	(8.51)	151.8[b]	(7.16)
	3.0 m/s	165.9[ab]	(9.17)	167.7[a]	(8.66)	157.9[b]	(6.51)
	3.5 m/s	174.3[a]	(8.92)	176.2[a]	(9.16)	163.2[b]	(7.36)

[v] indicates significant velocity effects for each limb.

[g] indicates significant group effects between the ILEA and control subjects.

[a, b, c] indicate homogenous subgroups for limb differences where group members are significantly different from non-group members.

limb for clearer presentation in the tables and figures. However, all statistical outcomes were based on the balanced statistical design that included both control limbs.

5.4.1 Temporal-Spatial Parameters

Temporal-spatial results and leg effects are presented in Table 5.2. Significant group differences existed for stance time, step time, cycle time, step length, and step

frequency (p≤0.011) where the ILEA group had shorter times and step lengths but greater step frequencies than the control group. Cycle time, stance time, and step time decreased with increasing velocity while step length, aerial time, and step frequency each increased with velocity (p≤0.001 for all). Velocity did not significantly affect swing time (p=0.087). Step length had a significant leg x group interaction (p=0.001) where the ILEA limbs had a greater difference than the control limbs at each velocity (p<0.001). Significant velocity x group interactions were observed for step time and step frequency (p≤0.042). For both parameters, the groups had greater differences between each other at 2.5 m/s and 3.5 m/s than they did at 3.0 m/s.

5.4.2 Peek Ground Reaction Forces

Peak ground reaction force values and leg effects are presented in Figure 5.1. Ground reaction force curves normalized to stance phase are presented in Figure 5.2. Significant velocity effects were evident for the peak braking, propulsive, medial, lateral and vertical ground reaction forces (p<0.020 for all). The peak mediolateral GRFs for the ILEA limbs did not significantly change with velocity, but all other peak GRF variables increased in magnitude with velocity. Significant leg x group interactions were identified for peak braking, propulsive, lateral, and vertical GRFs (p≤0.050). ILEA group limbs had greater differences than the control group limbs at each velocity. Significant speed x group interactions were observed for peak braking GRFs (p≤0.018). This interaction was due to the interaction between the prosthetic-control limb pairing and velocity where the control limbs had a greater increase in peak braking GRFs with velocity than the prosthetic limb peak values. Significant leg x speed interactions were identified for the peak propulsive and vertical GRFs
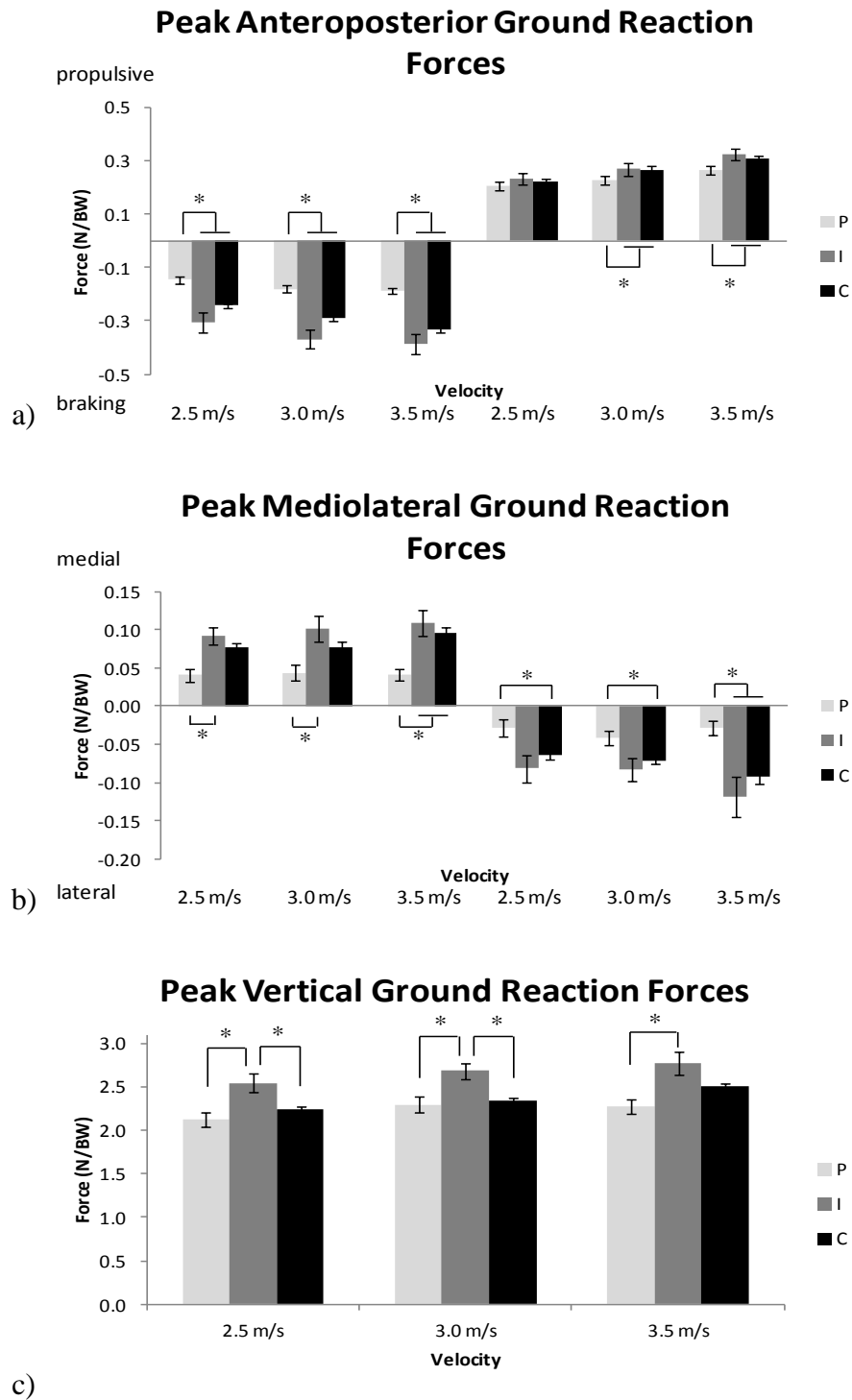
Figure 5.1. Peak a) anteroposterior (AP), b) medolateral (ML), and c) vertical ground reaction forces for the prosthetic (P), intact (I), and averaged control (C) limbs across the tested velocities. Error bars represent ±1 standard error. * indicates significant differences (p<0.05) between groups. Significant velocity effects were observed for each limb for peak AP and vertical GRFs and for the control limbs for peak ML forces.
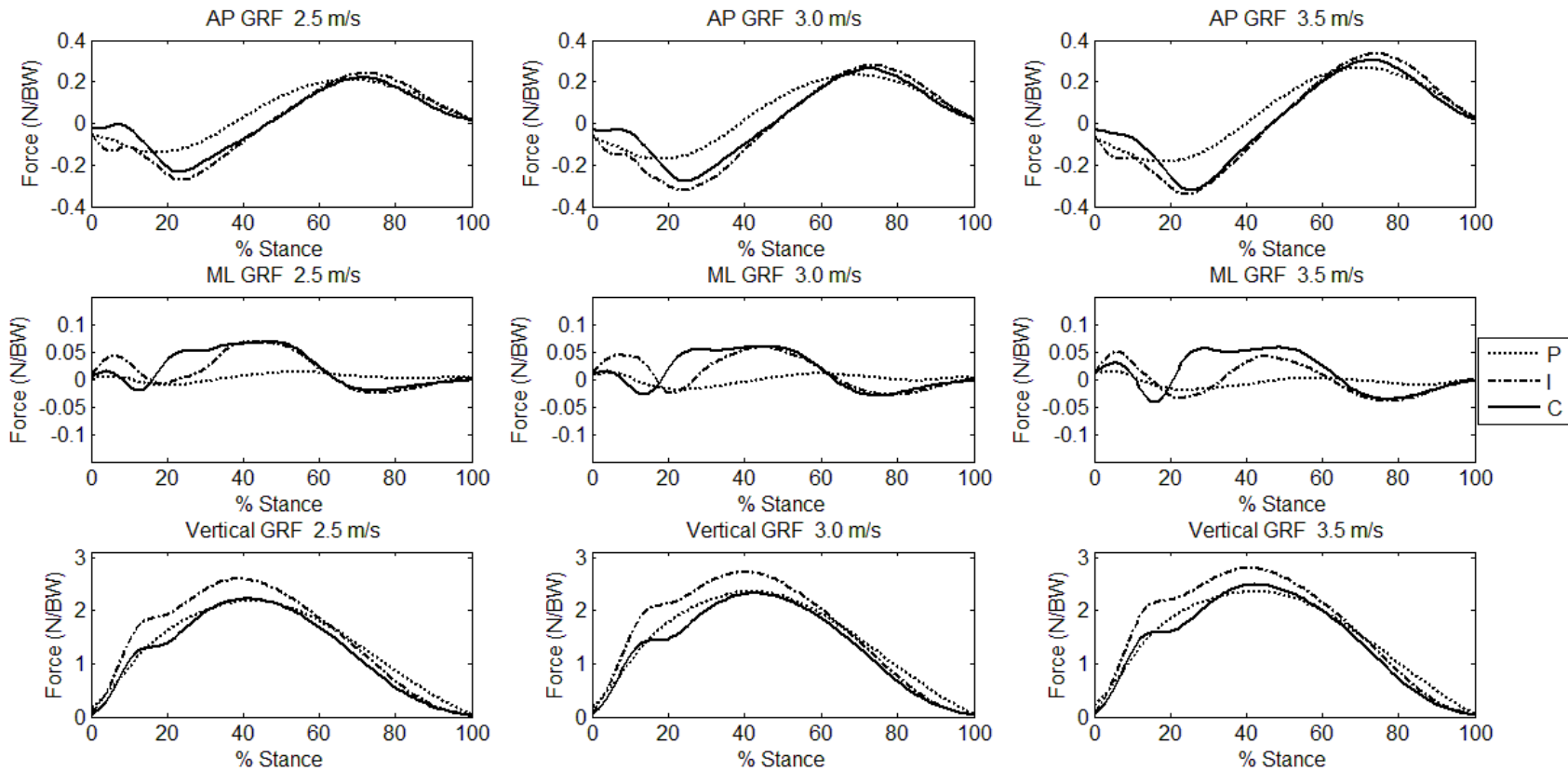
Figure 5.2. Mean ground reaction force profiles for the prosthetic (P), intact (I) and combined control (C) limbs across running velocities for each plane of force normalized to the running stance phase. AP and ML represent anteroposterior and mediolateral forces, respectively. Positive values indicate anterior, medial, and vertical ground reaction forces, respectively.

(p=0.042) where the intact and control limb peak magnitudes increased at a greater rate with velocity than the prosthetic limb peak magnitudes.

5.4.3 Ground Reaction Force Impulses

Total ground reaction force impulse data and leg effects are presented in Figures 5.3. Significant group effects existed for total vertical GRF impulse (p=0.011) where the ILEA group had lower total impulses than the control group. This difference was due to the lower prosthetic limb total impulse values compared to the control limbs at each velocity (p≤0.005). Significant velocity effects existed for braking impulse, propulsive impulse, and total vertical impulse (p<0.001 for all). Braking and propulsive impulse each increased with velocity while total vertical impulse decreased with increasing velocity for the intact and control limbs (p≤0.040). Braking (p=0.403) and propulsive (p=0.079) force impulses did not change significantly with velocity for the prosthetic limb. Significant leg x group interactions existed for AP braking and total vertical impulse (p≤0.023) where the differences between the ILEA limbs were greater than the differences between the control group limbs. AP braking impulse also had a significant leg x speed interaction (p=0.002). This full model interaction was due to the leg x speed interaction of the ILEA group where the intact limb braking impulse increased in magnitude with velocity while the prosthetic limb braking impulse remained similar in magnitude.

5.4.4 Ground Reaction Force Vector Angles and Magnitudes

GRF vector angles and magnitudes were examined at the time that the peak braking and propulsive GRFs occurred. The GRF vectors, angles, and magnitudes and

Anteroposterior Ground Reaction Force Impulse

a)

Vertical Ground Reaction Force Impulse

b)
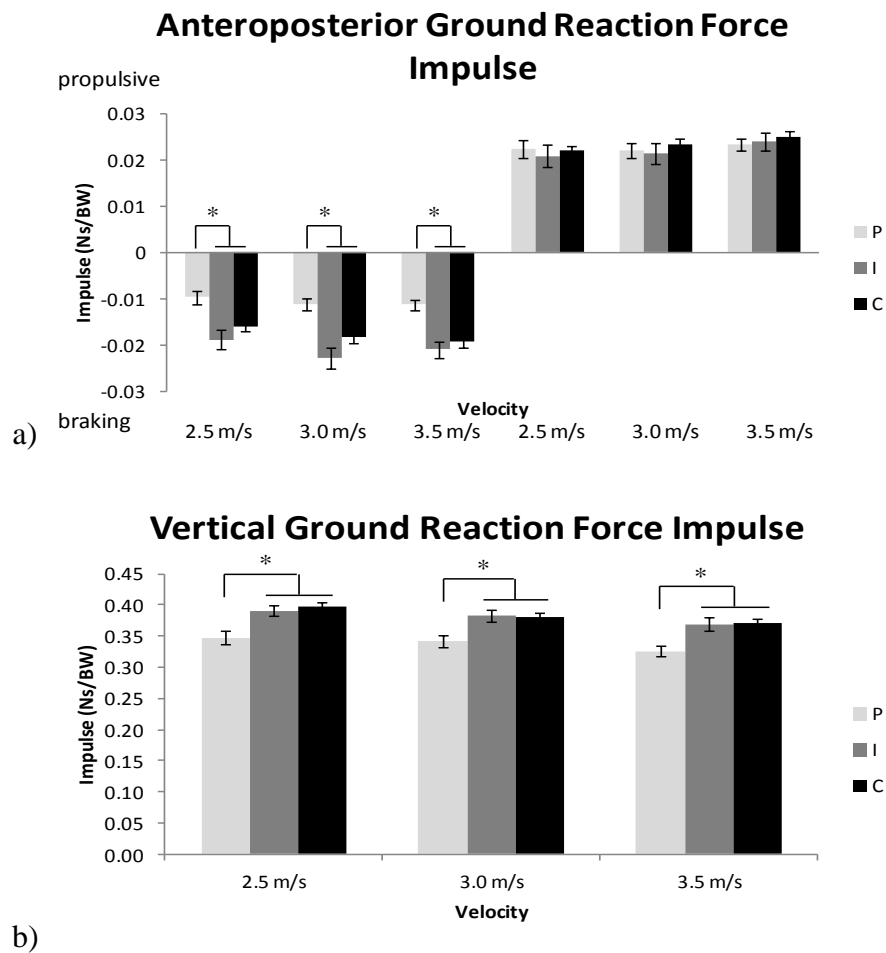
Figure 5.3. Total a) anteroposterior braking and propulsive and b) vertical ground reaction force (GRF) impulses for the prosthetic (P), intact (I), and averaged control (C) limbs across the tested velocities. Error bars represent ±1 standard error. * indicates significant differences (p<0.05) between groups. Significant velocity effects were observed for the braking and propulsive impulse values at the intact and control limbs. The prosthetic limb braking and propulsive impulses did not change with velocity. Significant velocity effects were observed for total vertical GRF impulses at each limb. No significant leg differences existed for total propulsive impulse.

their leg effects are presented in Figures 5.4-5.5. The prosthetic limb vector angle curves showed a lower overall range throughout stance phase compared to the intact and control limb vector angles. Significant velocity effects were observed for the braking and propulsive vector angles and magnitudes (p≤0.003). Control and prosthetic limb angles decreased with increasing velocity, while the intact limbs

113
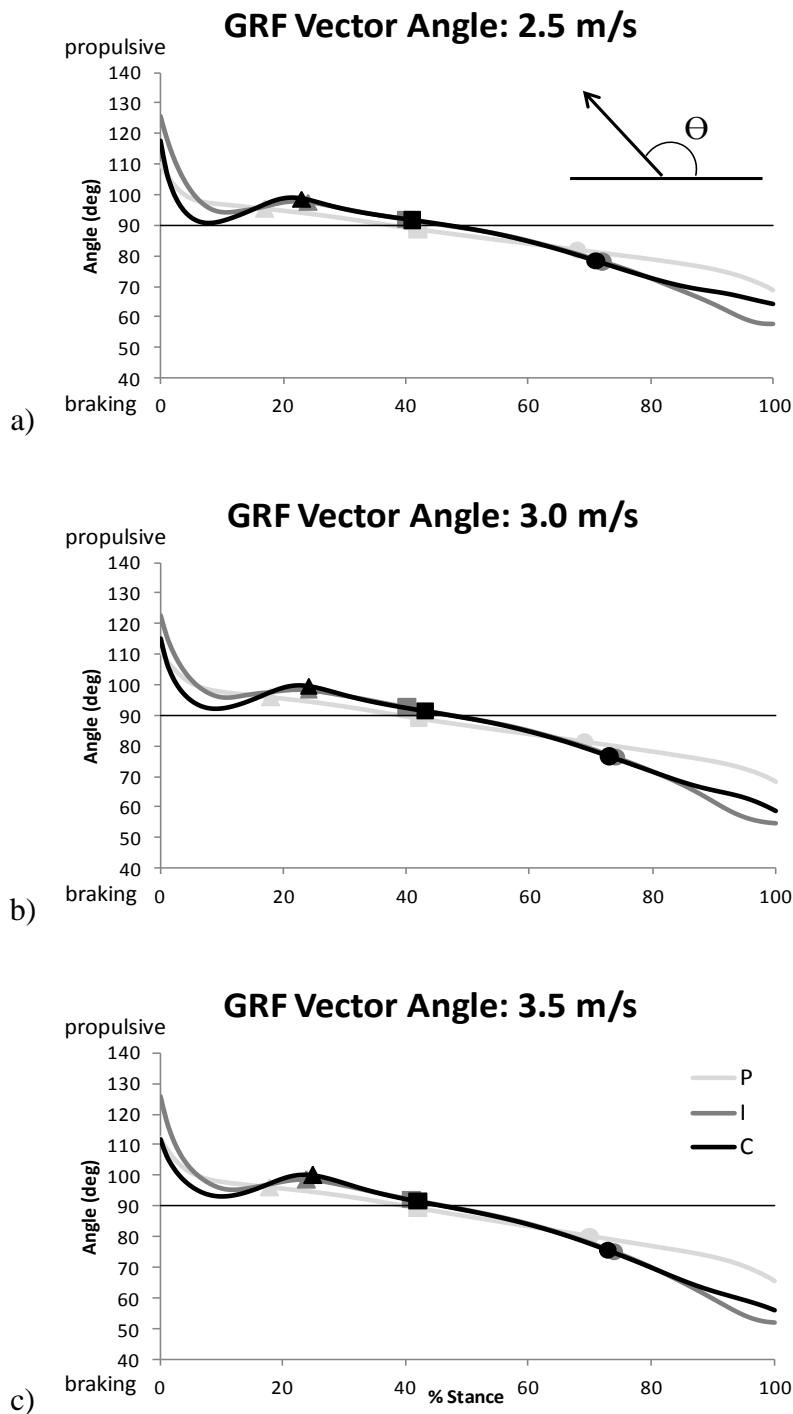
Figure 5.4. Sagittal plane ground reaction force (GRF) vector angles, Θ, for the prosthetic (P), intact (I), and averaged control (C) limbs normalized to running stance phase shown for a) 2.5 m/s, b) 3.0 m/s, and c) 3.5 m/s running velocities. Standard angle conventions are used such that 90° reflects a vertical force with no anteroposterior force component. Angles greater than or less than 90° indicate the presence of braking or propulsive forces, respectively. Triangles, squares, and circles indicate peak braking, vertical, and propulsive GRFs, respectively.

GRF Vector Angle

a)

GRF Vector Magnitude

b)
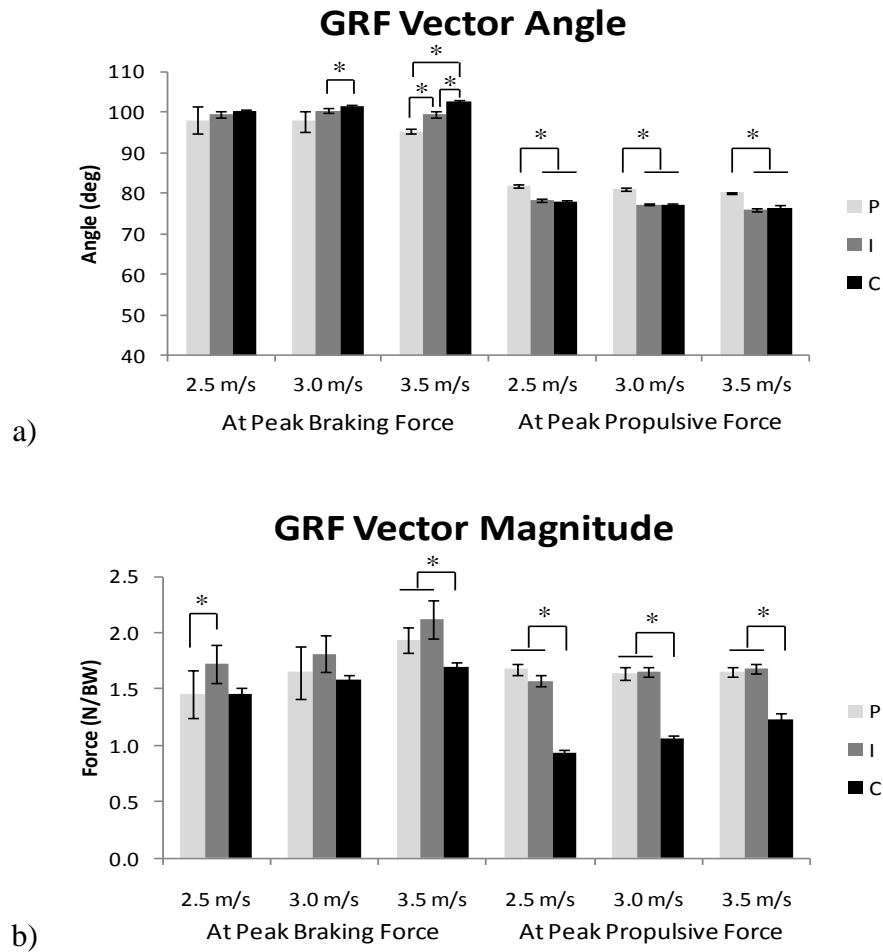
Figure 5.5. Sagittal plane ground reaction force (GRF) a) vector angles and b) vector magnitudes across velocities for the prosthetic (P), intact (I), and averaged control (C) limbs at the time of peak anteroposterior braking and propulsive force. Error bars represent ±1 standard error. * indicates significant differences between limbs.

exhibited a quadratic relationship with velocity. Control limb braking and propulsive vector magnitudes increased with velocity. Intact and prosthetic limb braking vector magnitudes increased with velocity but the propulsive vector magnitudes did not change with velocity. Group differences existed for the braking and propulsive vector angles and the propulsive vector magnitude ($p \leq 0.031$). Leg x group interactions

existed for propulsive vector angle and braking and propulsive vector magnitude (p≤0.029).

5.5 Discussion

5.5.1 Temporal-spatial parameters

Conflicting evidence exist on how ILEA modulate temporal-spatial parameters to increase running velocity. ILEA have been reported to increase running velocity by primarily increasing step frequency and maintaining similar step lengths (Enoka et al., 1982) or by primarily increasing stride length (Sanderson and Martin, 1996). However, the current data show that when running with RSPs, ILEA increased step and stride frequency along with step length to achieve greater velocities, which was the same strategy used by the current control group. Prosthetic limb step lengths, pushing off with the intact limb, were similar to those of able-bodied controls, but the intact limbs took shorter steps than both prosthetic and control limbs. To account for the shorter intact limb step lengths the ILEA group generated greater step and stride frequencies than the control group to maintain similar running velocities. Stride frequency, the inverse of cycle time, is a function of stance and swing time, and ILEA limbs had shorter stance times than control subjects while no differences existed between any limbs for swing time. Therefore reducing stance time appears to be an adaptation that ILEA running with RSPs use to increase velocity.

Gait cycle time, step time, swing time, and aerial time were not different within the ILEA limbs, so ILEA and able-bodied control subjects may control these parameters similarly to achieve the different tested velocities. Cycle time and step time decreased with increasing velocity while aerial time increased with velocity for

116

each limb; however, swing time did not change with velocity for either ILEA or control subjects. It appears that both groups of runners sought to maintain their limb swing times as running velocity increased. Aerial time (flight phase) increased with velocity, so stance time had to decrease in order to keep the swing times from toe-off to foot-strike the same. However, it is not clear from this relationship whether aerial time or stance time might be actively controlled and which one of these parameters is consequently adjusted to maintain swing time.

5.5.2 *Ground reaction force peaks and impulses.*

Consistent with previous literature (Grabowski et al., 2010; Nolan et al., 2003; Sanderson and Martin, 1996; Silverman et al., 2008), a majority of the GRF parameters in the current study increased in magnitude with velocity, but velocity did not significantly influence all GRF variables. Peak mediolateral GRFs did not significantly change with velocity for the ILEA group, although the prosthetic limb generated lower peak mediolateral forces than the intact limb. Generally, RSPs are designed to flex and provide support primarily in the sagittal plane. ILEA with transtibial amputations have different turning strategies than able-bodied subjects due to the lack of the biological ankle function in the prosthetic limb (Ventura et al., 2011). Additionally, ILEA must compensate for rotating forces acting on the prosthetic legs when running on a curved track (Lechler and Lilja, 2008). These observations along with the current data suggest that ILEA may adjust their gait to minimize the mediolateral forces generated by the prosthetic limbs, possibly to reduce the risk of slipping and falling. The greater variability observed in the intact limb peak mediolateral forces may indicate step by step adaptations that ILEA use to

adjust their gait to land on the prosthetic limb in a manner that keeps the mediolateral forces minimal on the RSP.

AP braking and propulsive impulses also did not significantly change with velocity for the prosthetic limb. These data show that the prosthetic limb is more invariant to velocity effects within the range of velocities tested. While previous studies demonstrated similar increases in GRF values with velocity for the prosthetic and intact limbs (Grabowski et al., 2010; Sanderson and Martin, 1996), the data from this study show the intact limb peak AP propulsive and vertical GRF values along with the AP braking impulse increased with velocity more than those generated by the prosthetic limb. The current data therefore suggest that ILEA rely more on the intact limb than the prosthetic limbs at greater running velocities. These data are consistent with previous studies that state RSPs impair force generation (Grabowski et al., 2010; Weyand et al., 2009). While this impairment may limit top running speeds (Grabowski et al., 2010), ILEA are able to compensate at submaximal velocities by relying more on the intact limb. However, the intact limb generated greater peak vertical GRFs than the control limbs, which could place ILEA at greater risk of injury. It has been suggested that chronic injuries associated with jogging are most likely to be related to the greater forces at mid- and late-stance rather than to those occurring at the time of impact (Winter, 1983b) because of the much greater loads at these time points.

Despite significantly lower peak AP propulsive GRFs in the prosthetic limb, no differences existed between the ILEA or control limbs for AP propulsive impulse. AP propulsive impulse has been used as a performance indicator for prosthetic feet

during running (Prince et al., 1992) where non-RSPs generated significantly lower propulsive impulses than the intact limb and control limbs indicating poor prosthetic push-off performance. An ILEA with bilateral amputations running with RSPs generated lower horizontal GRF impulses when compared to able-bodied subjects (Brüggemann et al., 2009; Weyand et al., 2009) also indicating poor relative push-off performance. In the current study, however, the RSPs generated similar propulsive impulses to the intact and control limbs despite having lower peak propulsive forces. The similar propulsive impulses were generated by the prosthetic limb by having a longer positive impulse period (see Figure 5.2). This increased time for generating a positive impulse appears to be a mechanism that ILEA with unilateral amputations running with RSPs utilize to maintain their running velocities. This mechanism has not been noted during running with non-RSPs and the different shape and rollover characteristics of non-RSPs may explain these differences. Previous research employing ILEA with unilateral amputations wearing RSPs has not reported AP impulses. Differences in these results compared to previously reported impulse data of an ILEA with bilateral amputations may highlight different running strategies employed by ILEA with unilateral and bilateral amputations.

The sagittal plane GRF vector analysis indicated that the prosthetic limb vector angles had smaller angles at peak braking and propulsion with a lower vector magnitude than the intact or control limbs. Overall, the GRF vector angles were smaller throughout stance phase for the prosthetic limb. This indicates a more upright posture throughout the prosthetic limb stance, which is consistent with previous observations (Sanderson and Martin, 1996) and can explain the lower AP braking and

propulsive peak GRFs for this limb. A more upright prosthetic limb posture would also allow the leg to be angled forward earlier in stance phase to generate a positive propulsive impulse. The intact limb also demonstrated smaller GRF vector angles at the time of the peak AP braking force than the control legs. This can be explained by the relatively shorter intact limb step lengths that result in a more upright intact leg position during the braking phase of stance.

This study has provided a detailed description of ILEA with unilateral amputations running at different velocities with RSPs; however, several limitations exist that must be taken into consideration when interpreting these data. RSP model was not controlled in this study and each subject ran in their own prescribed running prosthesis. This variable was not controlled to reduce variability due to using a new prosthetic design and to ensure proper alignment. Future studies are needed to examine whether differences exist when running with different RSP models and to compare running with RSPs directly to running with non-RSPs. An additional limitation is that subjects ran through a limited range of velocities, so the trends observed may not generalize to velocities outside of the tested range.

5.6 Conclusions

The study results indicate that ILEA running with RSPs demonstrate differences between their intact and prosthetic limbs in temporal-spatial and GRF parameters. ILEA demonstrated adaptive mechanisms within these variables that they used to increase running velocity. ILEA had faster step and stride frequencies than control subjects at each velocity and these faster frequencies were achieved by reducing stance times. Additionally, ILEA had lower peak AP propulsive GRFs with

the prosthetic limb but generated positive AP GRFs over a longer period of stance that allowed them to produce AP propulsive GRF impulses equivalent to the intact and control limbs. These data promote further study into the joint kinetics and limb energy flow to further elucidate compensatory control mechanisms that allow subjects with amputation to modulate their running velocity when using RSPs.

Chapter 6: Effects of Running-Specific Prosthesis Marker Placement on Joint Kinetics during Overground Running

6.1 Abstract

Motion analysis studies investigating individuals with lower extremity amputation (ILEA) using running-specific prostheses (RSPs) have estimated the prosthetic limb "ankle" joint to be either at the same relative position as the intact limb's ankle joint or the most acute point on the prosthesis curvature. RSP marker placements affect foot model definitions and could alter the lower extremity joint kinetic estimations. The aim of this study was to investigate the effect of RSP marker placement on the estimations of lower extremity joint moments during overground running. It was hypothesized that the number of markers and their placement on the keel of RSPs would not affect the residual limb joint moment estimations. Eight subjects with unilateral transtibial amputation wearing RSPs ran overground at 2.5, 3.0, and 3.5 m/s around a 100m track. Ten forceplates embedded in the track measured ground reaction force data and ten motion capture cameras collected marker positional data. Resultant joint moments in the residual limb "ankle," knee, and hip were calculated using inverse dynamics and were compared between four RSP foot models for each subject. The models included a 7-segment RSP, two 2-segment RSPs, and a single rigid RSP segment. No differences existed between models for the stance phase residual knee and hip joint moments, but the RSP "ankle" joint moment was sensitive to the model used. During swing phase, the models significantly differed in their calculation of peak knee flexion and hip extension moments, although the magnitude of the differences was small ($\leq$0.03 Nm/kg). These data suggest that marker placement on RSP keels has little effect on knee and hip

joint moments, especially during stance phase. "Ankle" moments, however, can differ

substantially based on the marker placement and should be interpreted with caution.

6.2 Introduction

During three-dimensional gait analyses, reflective markers are placed on anatomical landmarks to estimate the positions of joint centers and to define the body segment motions. The distal joint motion data along with ground reaction force data from a force platform can be used as inputs to inverse dynamics equations to estimate proximal joint kinetic values. Joint kinetic data can then be interpreted to provide insights into how individuals ambulate and control their movements. In locomotion studies using prostheses, markers defining the most distal joint axis, usually the ankle, are generally affixed to spots on the prosthetic foot that mimic the relative marker location on the intact foot and ankle complex (Buckley, 1999; Goujon et al., 2006; Sanderson and Martin, 1996; Selles et al., 2004; Silverman et al., 2008; Winter and Sienko, 1988). Prostheses are often modeled anthropometrically like an intact limb even though these devices may not have the same architecture or landmarks (Miller, 1987; Royer and Wasilewski, 2006; Su et al., 2007).

With the development of running-specific prostheses (RSPs), new prosthetic foot designs have emerged that no longer resemble the human foot. Many of the designs resemble a "C" or "J" shape at the distal end of the limb, which allows the prosthesis to flex and return more energy for propulsion during running, similar to a spring (Lechler, 2005; Nolan, 2008). Placing multiple markers to model RSPs as multisegmented objects during amputee locomotion studies provides a great challenge since definitive joint axes may not exist within the prosthetic foot design. Yet modeling RSPs as single rigid objects may not be appropriate since these devices can flex throughout their length. In the face of these challenges, many researchers
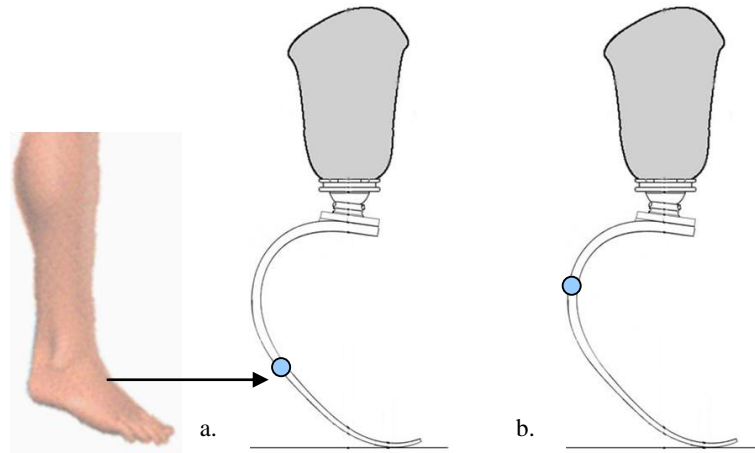
Figure 6.1. Literature has reported marker placement for running prostheses at (a) the height of the intact limb's lateral malleolus or (b) the point at which the radius of the prosthesis is most acute.

analyze these prostheses using similar biomechanical analysis methods as have been employed in prosthetic feet designed for walking and intact feet. Studies investigating running with RSPs have estimated the prosthetic limb "ankle" joint to be either at the same relative position as the intact limb's ankle joint (Figure 6.1a) or the most acute point on the prosthesis curvature (i.e., the greatest curvature; Figure 6.1b) (Buckley, 1999; Buckley, 2000; Burkett et al., 2003).

The inertial properties of RSPs used during inverse dynamics estimations have only been reported in one study to date (Brüggemann et al., 2009). Additionally, the various marker placements reported in the literature could affect the proximal joint kinetic estimations during running. Baum et al. (Baum et al., 2011) reported no differences in force or torque transfer through a variety of RSPs during an axial loading task. However, since running loads are applied to the lower extremities three-dimensionally, it is unknown whether those results generalize to actual running.

The aim of this study was to investigate the effect of RSP marker placement on the estimations of lower extremity joint kinetics during overground running. It was

hypothesized that the number of markers and their placement on the keel of RSPs would not affect the residual limb joint moment estimations.

6.3 Methods

6.3.1 Subjects

Eight male subjects with unilateral transtibial amputation (mean age = 32.0 ± 10.2 years, height = 1.80 ± 0.07 m, mass = 82.3 ± 13.0 kg) between 18 and 50 years of age volunteered to participate in the experiment. Prior to participating, all subjects gave informed written consent, which was approved by the University of Maryland Institutional Review Board.

6.3.2 Material Properties and Anthropometrics

The inertial properties of the prosthetic components and intact body segments were estimated for use with the inverse dynamics approach. Subject masses were measured using a force platform. Height and body weight of each subject were measured, and anthropometric measurements from marker positions were used to estimate the mass, center of mass, and moments of inertia of intact limb segments (Dempster, 1955; Hanavan, 1964). Since ILEA subjects were missing one foot and part of their shank, an adjusted body mass (ABM) (Smith, 2008) was used as an input to anthropometric regression equations that accounted for the missing body segments.

$$ABM = \frac{MBM - m_p - m_{res}}{1 - c} \qquad [1]$$

where *MBM* is measured body mass while wearing the prosthesis, m_p is the prosthesis mass including the socket, m_{res} is the estimated residual limb mass, and *c* (0.061) is the percent of ABM accounted for by the intact shank and foot (Dempster, 1955).

For subjects with amputation, the residual limb length and circumferences at the knee joint and distal end of the limb were measured using a measuring tape. The inertial properties of the residual limb were then estimated as a frustrum of a right circular cone (Hanavan, 1964; Mattes et al., 2000). The residual limb mass was estimated from the calculated geometric volume assuming a uniform 1.10 g/cm^3 tissue density (Mattes et al., 2000; Mungiole and Martin, 1990). The prosthetic socket and foot were treated as one unit and weighed with a laboratory scale. The RSP+socket unit's center of mass position was calculated using a reaction board method (Groves, 1950; Hay, 1985; McIntosh and Hayley, 1952; Payne and Blader, 1970), and the moment of inertia of the RSP+socket unit was calculated from the period of oscillation measured with a trifilar pendulum (Baum et al., 2012a; du Bois et al., 2008; Genta and Delprete, 1994). The inertial properties for the lower limb segment were then calculated from the combination of the residual limb and prosthetic components.

Figure 6.2 shows the marker placement guidelines used in this study. A total of eight markers were fixed on the prosthesis keels. Markers were placed on the most proximal ("head") and distal ("toe") points of each prosthesis keel along with on the point of most acute curvature. Markers were placed laterally and medially at the base of the most proximal linear segment of each prosthesis. Three additional markers were secured to the lateral keels by evenly distributing them between the most acute
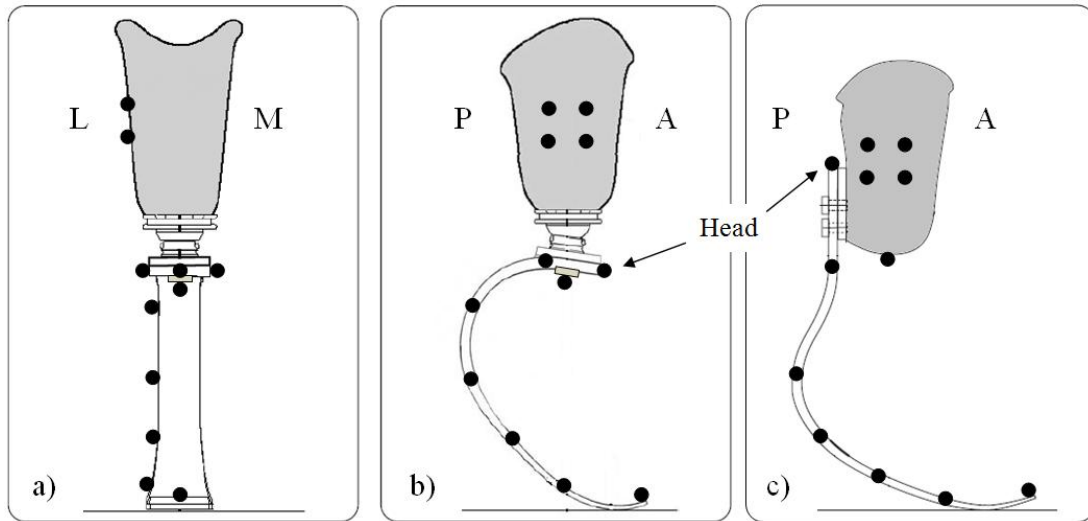
Figure 6.2. Marker placements on running-specific prostheses with views of the frontal plane (a) for all prostheses and sagittal planes for the (b) Flex-Run (shown) and Catapult and (c) Cheetah prostheses. L, M, P, and A refer to the lateral, medial, posterior, and anterior directions, respectively. The prosthesis "Head" markers are indicated for the different models.

point and the RSP toe. Prosthesis subsegments were considered rigid and defined from the marker positions on the keel. The subsegment inertial properties were estimated by using assumptions based on a trapezoidal cuboid as described by Baum et al. (Baum et al., 2011).

6.3.3 Experimental Procedures

Subjects ran overground around a 100m long track at three constant velocities (2.5 m/s, 3.0 m/s, and 3.5 m/s). Prior to beginning the experiment, retroreflective markers were placed bilaterally over the anterior and posterior iliac spines, heel, 3rd metatarsal head, 5th metatarsal head, and tip of the toe on the shoe. Marker clusters were placed bilaterally on the lateral thigh and shank segments. A static trial was collected prior to dynamic trials that included markers placed on the lateral and medial femoral condyles and the lateral and medial malleoli. On the amputated limb,
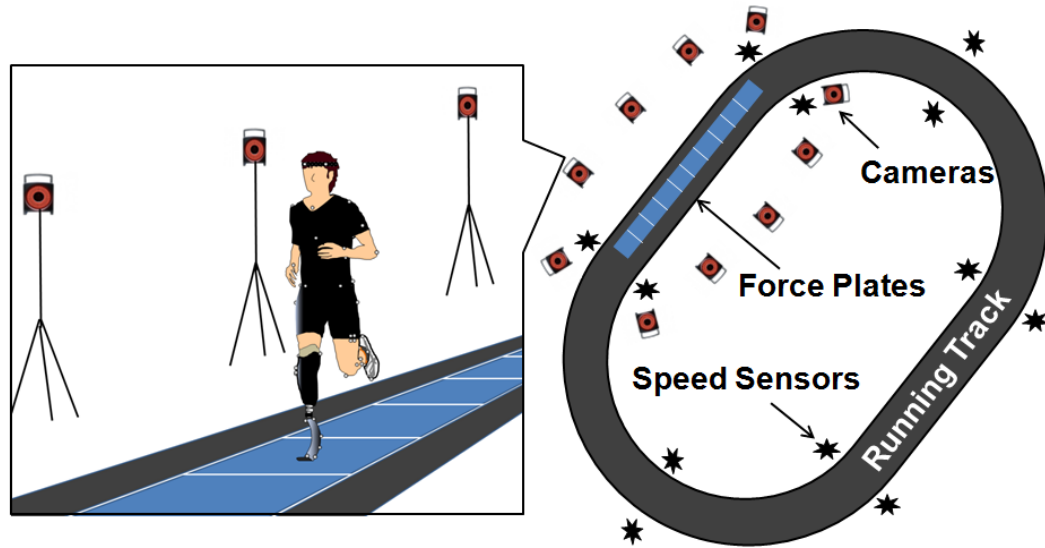
Figure 6.3. Schematic of testing setup. Subjects ran around a 100m track containing 10 force plates that captured ground reaction force data. Ten motion capture cameras captured 3D kinematic data and six sets of sensors around the track monitored running speed in real-time.

the shank cluster was placed laterally on the socket and a marker was placed at the distal tip of the socket to define the long axis of the residual shank segment. Additional markers were placed on the prosthetic keels as described earlier.

The testing setup (see Figure 6.3) included a 10-camera motion capture system (Vicon, Centennial, CO) that captured 3D positional data of the markers at 200 Hz for kinematic analysis, and ten 6-degree-of-freedom force platforms (Kistler, Amherst, NY) embedded in the track in series that collected ground reaction forces at 1000 Hz. Raw marker data were filtered using a 4th order, zero lag low pass Butterworth filter with a cutoff frequency of 6 Hz while raw force data were similarly filtered with a 30 Hz cutoff frequency. The kinematic and ground reaction force data were combined and inverse dynamics techniques were used to calculate joint moment data for each subject. Subjects completed at least five successful trials for each leg at each of the running velocities. A successful trial was defined as the subject running

within ±0.2 m/s of the target velocity within the track section containing the force platforms and stepping within the boundaries of the force platforms during the trial. Predetermined velocities were governed using concurrent biofeedback. Six sets of laser sensors were evenly distributed around the track such that when the subject runs past the sensors, the average velocity over the track section was instantaneously calculated. Verbal feedback was given to subjects during the trials to indicate whether or not they were running at the desired velocity. The order for running velocities was randomized. Subjects were allowed to rest for as long as needed between velocity conditions to reduce the effects of fatigue with a minimum rest of five minutes between conditions. Four RSP foot models were compared for each subject. Each model utilized different combinations of markers to determine the effects each marker set had on joint moment outputs (Figure 6.4). Model 1 used all RSP markers described in Figure 6.2 which resulted in a 7-segment RSP including the socket. The RSP "ankle" joint was considered to occur at the most acute point of RSP curvature. Model 2 used the socket, most acute point on the RSP curvature, and Toe marker to create a 3-segment model. The "ankle" joint was defined by the most acute marker, the distal segment was defined between the acute and Toe markers, and the proximal segment comprised of the keel and socket portion proximal to the acute marker. Model 3 was a 3-segment model defined similarly to Model 2, except the "ankle" joint and resultant segments were defined by the 3rd most distal marker on the RSP. This marker approximated the position of an intact limb's lateral malleolus. The final model, Model 4, considered the entire RSP+socket as one rigid body and therefore did not contain an "ankle" joint.
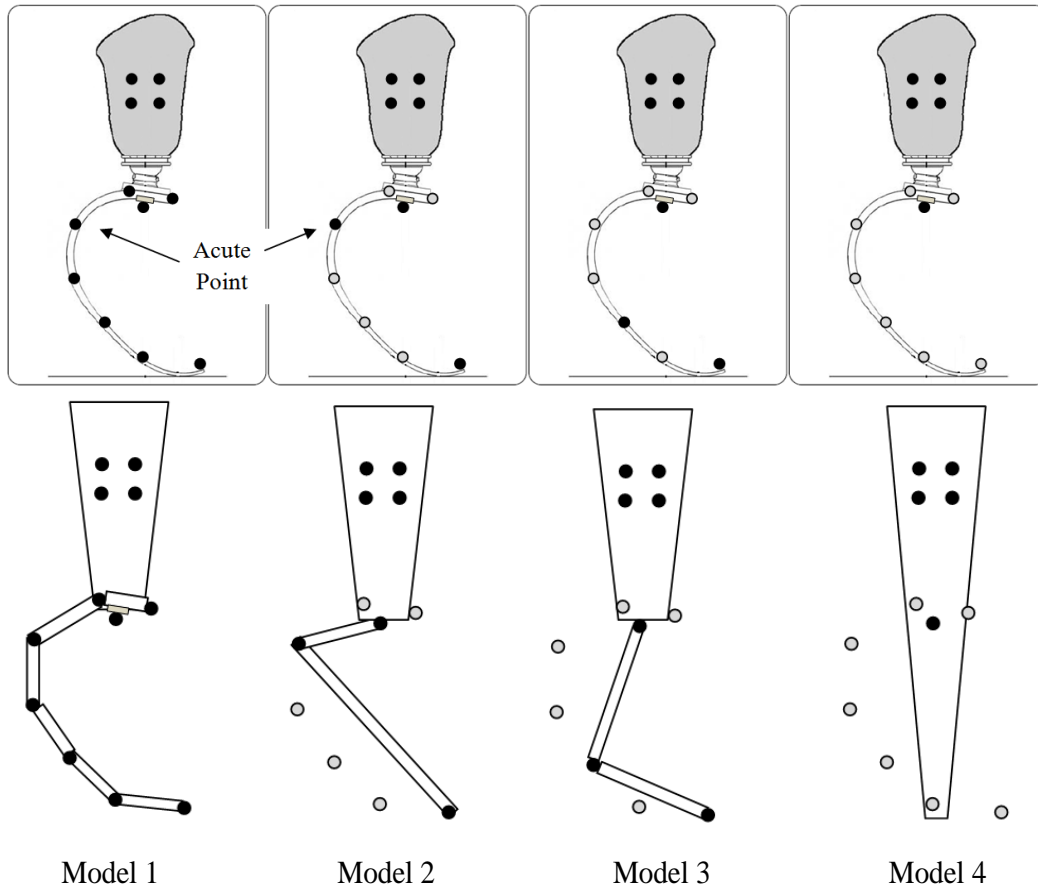
Figure 6.4. Markers used in the four model definitions. The upper panels show an exemplar RSP with the original marker placements where filled markers indicate those used in each model definition. The lower panel shows schematics of the resultant rigid body models. Model 1 used all markers to define a 7-segment model, Models 2 and 3 defined 3-segment models, and Model 4 defined a 1-segment model. The most acute point of the prosthesis curvature defining the ankle joint in Models 1 and 2 is identified. See text for additional details.

To assess how marker placement on the RSP affected the data, standard inverse dynamics calculations (Zatsiorsky, 2002) were used to estimate three dimensional lower extremity joint moments from the motion and ground reaction force data and were calculated using Visual3D (C-Motion, Germantown, MD) software using each model definition. The resultant RSP "ankle" joint peak moments were compared for Models 1-3, and the resultant residual limb knee and hip joint peak moments were compared across all Models.
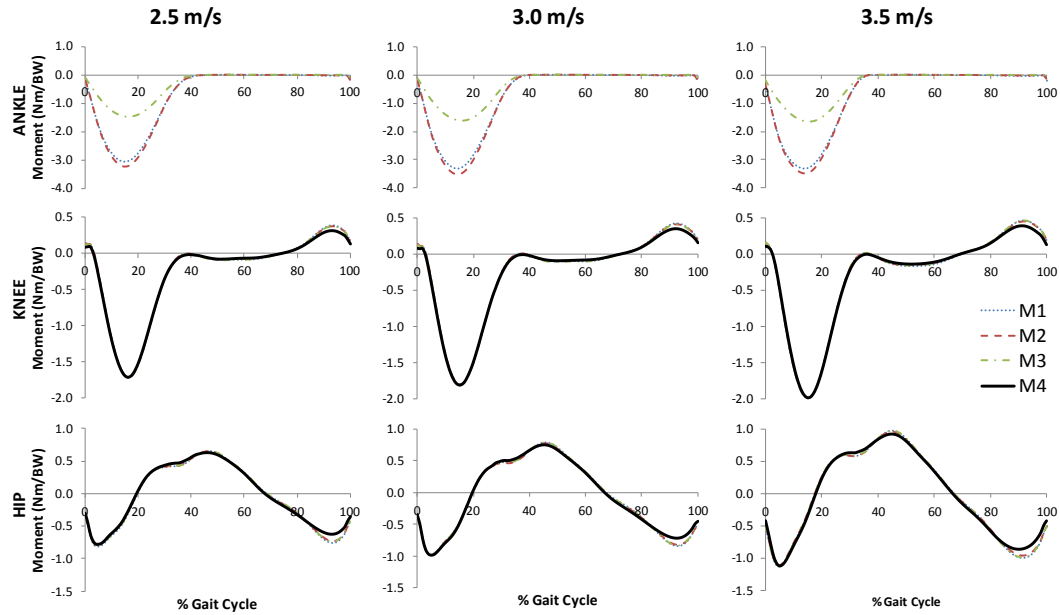
Figure 6.5. Resultant sagittal plane residual limb "ankle," knee, and hip joint moments across velocities normalized to body mass for each marker set model (M1-M4) throughout the gait cycle. The vertical line indicates toe-off. M1 used all RSP markers, M2 was a 2-segment model using the most acute marker, M3 was a 2-segment model using the 3rd most proximal marker, and M4 considered the RSP+socket as one rigid object. M4 did not contain an "ankle" so ankle moments could not be calculated.

6.3.4 Statistical Analysis

A two-factor repeated measures analysis of variance (ANOVA) was used to test for model (M1-M4) and running velocity (2.5, 3.0, and 3.5 m/s) main effects and their interactions for residual limb peak ankle, knee, and hip joint moments. Significance was set at $\alpha=0.05$.

6.4 Results

Figure 6.5 shows the resultant sagittal plane joint moment profiles across the gait cycle calculated by each of the four models. Figure 6.6 shows the ankle, knee, and hip peak stance phase extension moment values calculated by each model.

Ankle Stance Plantarflexion Moment

Knee Stance Extension Moment

Hip Stance Extension Moment
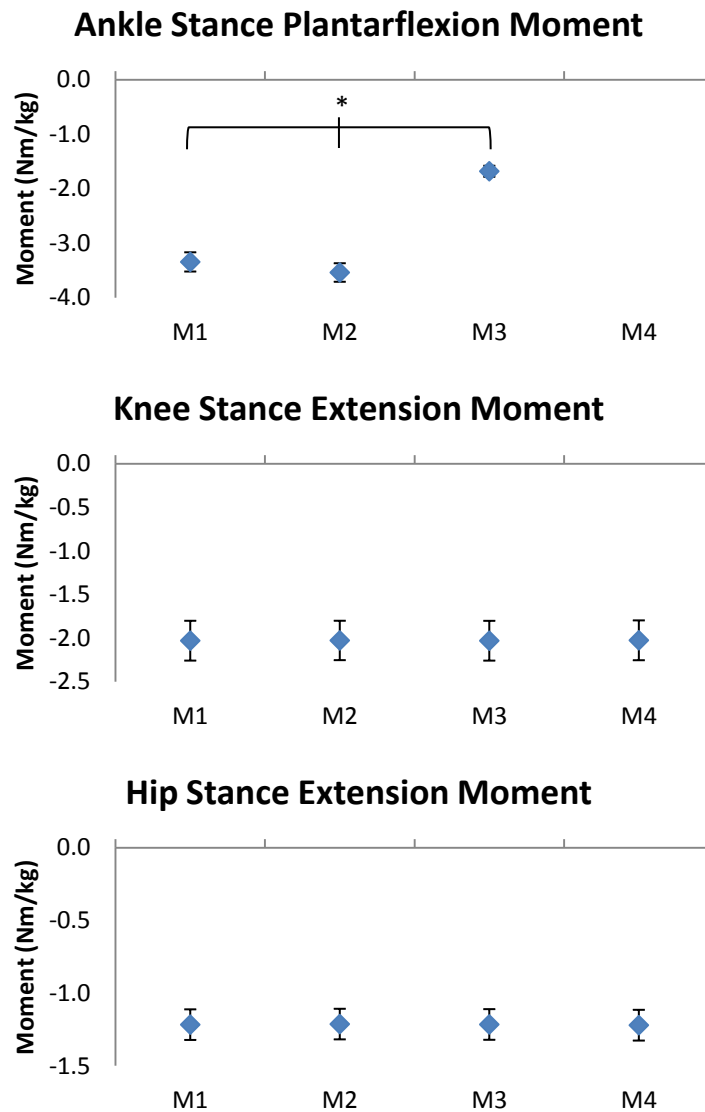
Figure 6.6. Peak stance phase ankle plantarflexion, knee extension, and hip extension moments for each of the marker set models (M1-M4) normalized to body mass when running at 3.5 m/s. Error bars represent ±1 standard error. The slower running velocities followed the same patterns. M4 did not contain an "ankle" joint definition. * indicates a statistically significant difference between models.

Significant velocity differences were observed for all parameters (p≤0.045) except for ankle stance peak plantarflexion moment (p=0.053). Model differences for peak stance phase ankle plantarflexion moments were evident between Models 1, 2, and 3 (p≤0.003). Model 3 underestimated peak plantarflexion by between 1.60-1.89 Nm/kg
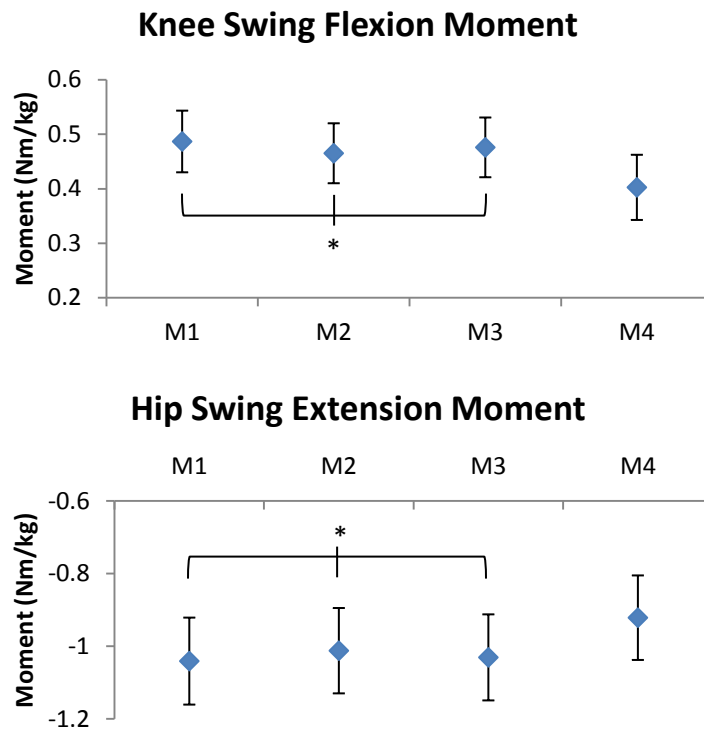
Figure 6.7. Peak swing phase knee flexion and hip extension moments for each of the marker set models (M1-M4) normalized to body mass when running at 3.5 m/s. Error bars represent ±1 standard error. The slower running velocities followed the same patterns. * indicates a statistically significant difference between the models.

compared to Models 1 and 2 across all velocities. Models 1 and 2 differed by ≤0.20 Nm/kg at any velocity. No differences were observed between any model for stance phase peak knee and hip extension moments. For peak swing phase knee flexion and hip extension moments, Models 1, 2, and 3 significantly differed from each other (p≤0.022, Figure 6.7), but no models differed from Model 4. Peak swing phase knee flexion moments differed by at most 0.08 Nm/kg between any model with a 0.02 Nm/kg maximal difference between Models 1-3. Peak swing phase hip extension moments differed by <0.12 Nm/kg for all models with a maximal difference of 0.03 Nm/kg between Models 1-3. No significant interactions were observed indicating that the model effects did not change as velocity increased.

Table 6.1. Average (± standard deviation) peak coronal and transverse plane joint moments in Nm/kg for each marker model (M1-M4). White areas indicate stance phase peaks while grey areas indicate swing phase peaks.

	M1		M2		M3		M4		Sig. Diff.
Ankle									
Varus	0.073	(0.03)	0.071	(0.02)	0.079	(0.03)	-	-	
Valgus	-0.086	(0.02)	-0.093	(0.03)	-0.117	(0.05)	-	-	
Internal	0.134	(0.04)	0.148	(0.04)	0.076	(0.01)	-	-	
External	-0.052	(0.02)	-0.052	(0.02)	-0.043	(0.02)	-	-	
Knee									
Varus	0.098	(0.04)	0.097	(0.04)	0.097	(0.04)	0.091	(0.05)	
Valgus	-0.436	(0.10)	-0.435	(0.10)	-0.436	(0.10)	-0.439	(0.10)	
Internal	0.258	(0.04)	0.257	(0.04)	0.257	(0.04)	0.258	(0.04)	
External	-0.061	(0.01)	-0.060	(0.01)	-0.058	(0.01)	-0.057	(0.01)	M1-M3
Varus	0.083	(0.02)	0.081	(0.02)	0.082	(0.02)	0.079	(0.02)	
Valgus	-0.084	(0.01)	-0.078	(0.01)	-0.082	(0.01)	-0.073	(0.01)	
Internal	0.071	(0.01)	0.069	(0.01)	0.069	(0.01)	0.064	(0.01)	M1-M3
External	-0.094	(0.01)	-0.091	(0.01)	-0.091	(0.01)	-0.082	(0.01)	
Hip									
Varus	0.014	(0.02)	0.014	(0.02)	0.014	(0.02)	0.019	(0.03)	
Valgus	-1.071	(0.10)	-1.069	(0.10)	-1.072	(0.10)	-1.075	(0.10)	
Internal	0.032	(0.03)	0.032	(0.03)	0.031	(0.03)	0.032	(0.03)	
External^v	-0.371	(0.05)	-0.371	(0.05)	-0.371	(0.05)	-0.373	(0.05)	
Varus^v	0.269	(0.03)	0.269	(0.03)	0.271	(0.03)	0.263	(0.02)	
Valgus^v	-0.245	(0.03)	-0.238	(0.02)	-0.239	(0.03)	-0.244	(0.03)	
Internal^v	0.146	(0.01)	0.144	(0.01)	0.145	(0.01)	0.152	(0.01)	
External	-0.110	(0.02)	-0.110	(0.02)	-0.111	(0.02)	-0.119	(0.02)	

Sig. Diff. = significant difference (p<0.05) between the indicated marker models
^{v} indicates significant velocity effect

Peak coronal and transverse plane joint moments for each of the marker models are shown in Table 6.1. No significant differences existed between any of the models for any peak varus or valgus moments during stance or swing phase. Models 1 and 3 significantly differed for stance phase peak knee external moments (p=0.001) and swing phase knee internal rotation moments (p=0.009). In both cases, these variables differed on average by only 0.003 Nm/kg. Velocity significantly affected several hip moment variables. The peak stance phase hip external rotation moments

(p=0.033) and peak swing phase hip varus (p=0.035), valgus (p=0.014), and internal rotation (p=0.001) moments increased in magnitude with velocity.

6.5 Discussion

Various methods of marker placement on RSPs are reported in ILEA running literature (Brüggemann et al., 2009; Buckley, 1999; Buckley, 2000; Burkett et al., 2003), but the effects of these placements and the subsequent modeling of the prosthetic foot segment on joint kinetic estimations were unknown to this point. The current data partially support and partially reject the hypothesis that the number of markers and their placement on the keel of RSPs do not significantly affect the residual limb joint moment estimations. With the exception of the peak knee external rotation moment, stance phase moments at the knee and hip joints were not affected by marker placement and modeling of the prosthetic foot. However, the RSP "ankle" joint plantarflexion moment estimations during running stance were sensitive to the marker placement and definition of the ankle joint in the prosthetic limb. During swing phase, the peak knee flexion, knee internal rotation, and hip extension moments were also sensitive to marker placement.

These data indicate that stance phase knee and hip kinetic data reported in prior research with ILEA using RSPs may be interpreted with greater confidence. Placing markers at the same relative position as the intact limb's ankle joint or the most acute point on the prosthesis curvature (Buckley, 1999; Buckley, 2000; Burkett et al., 2003) should yield similar results in resultant knee and hip joint kinetic values proximal to the prosthesis. The significantly different stance phase knee external rotation moments only differed by 0.003 Nm/kg between the models, which

extrapolates to only a 0.3 Nm difference for an individual with a mass of 100kg. When comparing between subjects this difference is smaller than the observed standard errors, which suggests that this difference may have limited functional significance. Bruggemann et al. (Brüggemann et al., 2009) asserted that marker placement on the RSP keel would affect the resultant ankle plantarflexion moment calculations. The current data support this as stance phase ankle plantarflexion moments were significantly affected by marker placement and modeling of the RSPs. Model 2, a 3-segment model defining the ankle joint at the most acute point of curvature on the prostheses, estimated the greatest peak ankle moment values. Model 3, a 3-segment model defining the ankle joint at the 3rd most proximal marker on the prostheses, estimated the lowest peak ankle moment values. Model 2 defined an ankle joint that had the greatest range of motion and angular acceleration between its proximal and distal segments and also had the greatest effective moment arm between the joint and the center of pressure. These factors induced a large extension moment during the stance phase. Model 3 defined an ankle joint that achieved low angular accelerations and a small effective moment arm between the joint and center of pressure. Model 1, the 7-segment model, defined the ankle joint at the same point as Model 2; however, the relative segment accelerations between the proximal and distal segments to the ankle joint were lower than those defined by Model 2 resulting in slightly lower ankle moment values.

While peak stance phase knee and hip joint moments were virtually unaffected by the marker models, peak swing phase knee and hip joint moments differed between the outputs for Models 1-3. These differences averaged less than

0.03 Nm/kg in magnitude for the sagittal plane moments and 0.003 Nm/kg in magnitude for the knee internal rotation moment, but statistical differences were achieved due to the consistent change between the models within subjects. The equations of motion during stance phase of running are primarily driven by the large ground reaction force components as opposed to the relatively smaller inertial characteristics of the RSP. During swing phase, however, no ground reaction forces exist, so the equations of motion are determined by the segment inertial properties and the limb accelerations. Accordingly, the RSP and body segment inertial properties have a much larger influence on the joint moment output during running swing phase. Since the residual limb segment definitions remained identical across trial conditions, inertial property errors due to segment simplifications in the model definitions caused the differences between the swing phase moment estimations. Model 4, the rigid RSP model, should have produced the most accurate swing phase knee and hip joint moment values in this study because the inertial properties of the RSP+socket unit were directly measured together. The RSP keels were not removed from the sockets to avoid realignment issues and damage to the prostheses. Consequently, the subsegment definitions in Models 1-3 involved a greater number of estimations of inertial properties that may have led to kinetic inaccuracies.

A limited number of markers were placed on the prosthesis during the running trials, so calculating the moment transfer through additional markers could alter the proximal joint moment results. However, Baum et al. (Baum et al., 2011) placed markers at 2cm intervals along the RSP keels to examine the effects of marker placement on kinetic estimations during an axial loading task. They reported that the

number of markers and their placement did not affect the force or torque transfer through RSPs. Together, both studies indicate that marker placement on RSPs and the number of markers used will not affect the results of the proximal joint kinetic data during ILEA running stance phase. This allows for valid comparisons between running studies for stance phase knee and hip joint kinetic data regardless of the marker set used. Care must be taken though when interpreting prosthetic "ankle" plantarflexion moments. These data are sensitive to the marker placement since the RSP subsegment moments of inertia and angular velocities depend on the joint definition. The ankle moment arm is also affected by the ankle joint definition, which can greatly influence the resultant moment estimation at this joint. The current data indicates that defining the RSP ankle using the intact ankle as a reference will underestimate the ankle moment by approximately 50% compared to the moment determined at the most acute point of RSP curvature. Interpretations of swing phase knee and hip moments are unlikely to change due to marker placement despite the significant differences observed between Models 1-3. The moment patterns did not change between models and the magnitude of differences between the peak values generated by Models 1-3 varied by less than 0.03 Nm/kg.

6.6 Conclusions

Based on the results of this study, marker placement on RSP keels has little effect on knee and hip joint moments, especially during stance phase. "Ankle" plantarflexion moments, however, can differ substantially based on the marker placement. For consistency and flexibility in modeling, it is recommended that markers are placed according to the prosthesis architecture rather than intact limb

architecture. This will allow markers to be placed on the same location of a particular prosthesis from subject to subject and will allow for the study of ILEA with bilateral amputations and comparison of these individuals with those with unilateral amputations. The statistical differences observed suggest that future ILEA running studies should clarify details on how prostheses are modeled to allow readers to appropriately interpret the biomechanical data and compare results between literature.

Chapter 7: Joint Moment Adaptations to Running Velocity in

Individuals with Unilateral Transtibial Amputation using

Running-Specific Prostheses

7.1 Abstract

Altered joint kinetics during running may be required to accommodate for physical deficiencies caused by lower extremity amputation. Neither these alterations nor the way individuals with lower extremity amputation (ILEA) modulate joint kinetics to achieve different running velocities using running-specific prostheses (RSPs) is currently understood. The aim of this study was to investigate lower extremity 3D joint moments during running with RSPs under different velocity constraints. ILEA with unilateral transtibial amputations and a control group ran overground at three constant velocities (2.5, 3.0, and 3.5 m/s). It was hypothesized that (1) ILEA would demonstrate lower peak joint moment magnitudes in the prosthetic limb than the intact and control limbs at each velocity, and (2) increased running velocity would be associated with similar increases in intact and prosthetic limb joint moments. Results showed that most peak joint moment parameters of the prosthetic limb were lower than peak moments of the intact limb, which were similar to control values. The prosthetic limb had a longer period of hip extension moment during stance than the intact or control limbs. The increases in the peak hip stance and knee swing flexion moments associated with velocity were greater in the intact limb than the prosthetic limb. In conclusion, ILEA relied on the intact limb more than the prosthetic limb to run at a particular velocity when wearing RSPs, but the intact joints were not overloaded relative to the control limbs. Prolonged stance phase hip extension moments in the prosthetic limb were also confirmed as an adaptive mechanism that ILEA subjects use when running with RSPs.

Individuals with lower extremity amputations (ILEA) must demonstrate different biomechanical strategies during running to compensate for physical deficiencies. Joint kinetics during running are adapted to account for the loss of major joints and musculature while also integrating the function of a mechanical prosthesis (Brouwer et al., 1989; Brüggemann et al., 2009; Buckley, 2000; Czerniecki and Gitter, 1992; Czerniecki et al., 1991; Enoka et al., 1982; Miller, 1987; Sanderson and Martin, 1996). A majority of the available running literature has been performed on subjects running with non-running-specific prostheses (non-RSPs), i.e. prostheses originally designed for walking. Several studies now exist that examine running mechanics with RSPs (Brüggemann et al., 2009; Buckley, 1999; Buckley, 2000; Grabowski et al., 2010; Weyand et al., 2009), but the subject populations are small and their focus tends toward maximal sprinting. Studies investigating running mechanics with RSPs at submaximal running velocities are limited to ground reaction force and metabolic data (Grabowski et al., 2010; Weyand et al., 2009), so joint kinetic information using these devices at submaximal running speeds is currently unknown.

Individuals with unilateral transtibial amputation running with non-RSPs demonstrate substantially different stance phase ankle, knee, and hip joint moments with lower peak values in the residual limb compared to the intact limb and able-bodied limbs (Brouwer et al., 1989; Czerniecki et al., 1991; Miller, 1987; Sanderson and Martin, 1996), which indicates altered muscular force generation strategies. Only two studies are currently available that report stance phase joint moment data for

ILEA running with RSPs (Brüggemann et al., 2009; Buckley, 2000). These studies provide information on a total of three subjects while sprinting. It is established that sprinting and submaximal running mechanics differ in able-bodied runners (Novacheck, 1998b), and indeed, the moment profiles reported in these studies differ from those reported for ILEA wearing non-RSPs. However, it is not clear whether these differences are due to the task (sprinting vs submaximal running), prosthetic components (RSPs vs non-RSPs), or both.

RSPs may provide improved running function compared to non-RSPs; however, these devices are still passive and most likely necessitate altered joint control strategies during stance compared to running with intact limbs. Furthermore, due to their reduced mass compared with the intact limbs they replace, RSPs may induce different swing phase joint moment control strategies. The literature indicates that many gaps exist in our knowledge of ILEA running mechanics and their lower extremity joint kinetic adaptations. Joint moments at submaximal running velocities, swing phase mechanics, and how ILEA adapt their joint mechanics to achieve different running velocities are not understood when subjects wear RSPs.

Increased velocities increase ground reaction forces during ILEA running (Baum et al., 2012b; Grabowski et al., 2010; Sanderson and Martin, 1996), and peak sagittal plane joint moments also increase similarly between limbs in ILEA running with non-RSPs (Sanderson and Martin, 1996). ILEA with unilateral amputations have an inherent structural and functional asymmetry where the joint moments in all planes may differ between the limbs. Differences between the intact and prosthetic limb sagittal plane peak joint moments are prevalent during ILEA running with non-RSPs

(Brouwer et al., 1989; Miller, 1987; Sanderson and Martin, 1996) and RSPs (Buckley, 2000); however, no reports of coronal or transverse plane joint moments exist in the ILEA running literature. A complete description of the 3D joint moment profiles would provide greater insights into how ILEA run and compensate for replacing an active limb with a passive prosthetic device.

The aim of this study was to investigate lower extremity joint moments in ILEA when running with RSPs under different velocity constraints. It was hypothesized that (1) ILEA would demonstrate lower peak joint moment magnitudes in the prosthetic limb than the intact and control limbs throughout stance and swing phase at each velocity, and (2) increased running velocity would be associated with similar increases in intact and prosthetic limb peak joint moments.

7.3 Methods

7.3.1 Subjects

Eight male subjects with unilateral transtibial amputation (mean age = 32.0 ± 10.2 years, height = 1.80 ± 0.07 m, mass = 82.3 ± 13.0 kg; see Table 5.1) and eight healthy male control subjects (mean age = 29.0 ± 6.9 years, height = 1.84 ± 0.05 m, mass = 79.3 ± 7.9 kg) between 18 and 50 years of age volunteered to participate in the experiment. To maintain a uniform study population only ILEA with unilateral transtibial amputations were recruited. ILEA ran in their own prescribed RSPs to reduce variability due to using a new prosthetic design and to ensure proper alignment. ILEA had at least 3 months of running experience (range: 3-256 months) and the causes of amputation were either congenital (1) or trauma (7). Prior to participating, all subjects gave informed written consent, which was approved by the

University of Maryland Institutional Review Board. Subjects with amputation were excluded if they had comorbidities on the intact limb that would affect gait.

7.3.2 Material Properties and Anthropometrics

Inertial properties of the prosthetic components and intact body segments were estimated for use with the inverse dynamics approach. Subject masses were measured using a force platform. Height and body weight of each subject were measured, and anthropometric measurements from marker positions were used to estimate the mass, center of mass, and moments of inertia of intact limb segments (Dempster, 1955; Hanavan, 1964). Since ILEA subjects were missing one foot and part of their shank, an adjusted body mass (ABM) (Smith, 2008) was used as an input to anthropometric regression equations that accounted for the missing body segments.

$$ABM = \frac{MBM - m_p - m_{res}}{1 - c} \qquad [1]$$

where *MBM* is measured body mass while wearing the prosthesis, m_p is the prosthesis mass including the socket, m_{res} is the estimated residual limb mass, and *c* (0.061) is the percent of ABM accounted for by the intact shank and foot (Dempster, 1955).

For subjects with amputation, the residual limb length and circumferences at the knee joint and distal end of the limb were measured using a measuring tape. Residual limb inertial properties were then estimated as a frustrum of a right circular cone (Hanavan, 1964; Mattes et al., 2000). Residual limb mass was estimated from the calculated geometric volume assuming a uniform 1.10 g/cm^3 tissue density (Mattes et al., 2000; Mungiole and Martin, 1990). The prosthetic socket and RSP

147

were treated as one unit and weighed with a laboratory scale. The socket+RSP unit's center of mass position was calculated using a reaction board method (Groves, 1950; Hay, 1985; McIntosh and Hayley, 1952; Payne and Blader, 1970), and the moment of inertia of the socket+RSP unit was calculated from the period of oscillation measured with a trifilar pendulum (Baum et al., 2012a; du Bois et al., 2008; Genta and Delprete, 1994). Inertial properties for the lower limb segment were then calculated from the combination of the residual limb and prosthetic components. The RSP keels were not able to be disconnected from the sockets for each subject, so inertial properties for each prosthetic keel were estimated using data reported by Baum et al. (Baum et al., 2012a) for the RSP model and stiffness category that most closely matched those used by the subjects. The inertial properties of the socket were then estimated by subtracting the inertial properties of the RSP keel from the total socket+RSP segment using the parallel axis theorem. Subsegments within the RSP keels were defined via reflective marker placements and the inertial properties of each subsegment were estimated by assuming each segment as a rigid trapezoidal cuboid (Baum et al., 2011). All segments used a coordinate system that defined the x-axis as anteroposterior, y-axis as mediolateral, and z-axis as superior/inferior.

7.3.3 Experimental Procedures

Subjects ran overground around a 100m long track at three constant velocities (2.5 m/s, 3.0 m/s, and 3.5 m/s). Prior to beginning the experiment, retroreflective markers were placed bilaterally over the anterior and posterior iliac spines, heel, 3rd metatarsal head, 5th metatarsal head, and tip of the toe on the shoe. Marker clusters were placed bilaterally on the lateral thigh and shank segments. A static trial was
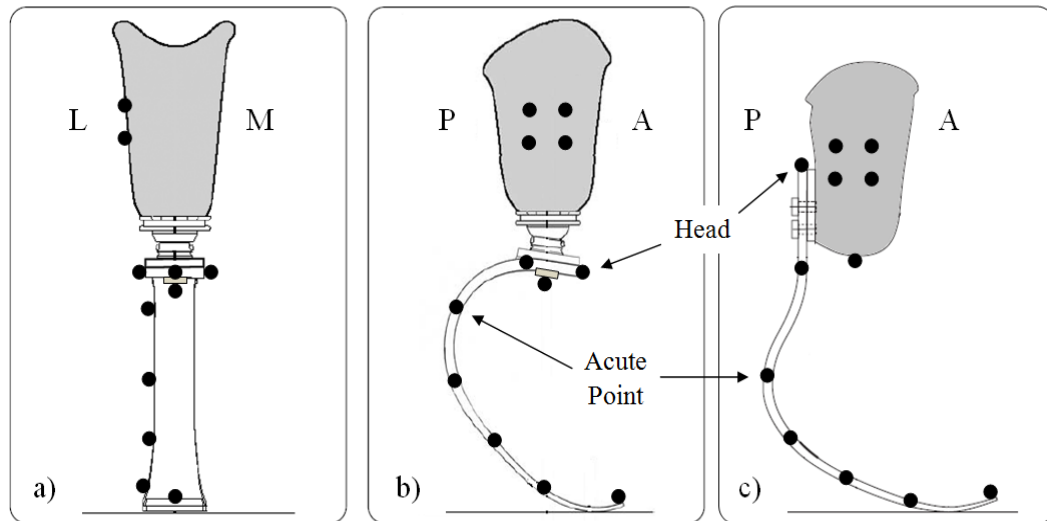
Figure 7.1. Marker placements on running-specific prostheses with views of (a) the frontal plane for all prostheses and sagittal planes for the (b) Flex-Run (shown) and Catapult and (c) Cheetah prostheses. L, M, P, and A refer to the lateral, medial, posterior, and anterior directions, respectively. The prosthesis "Head" and most acute point markers are indicated for the different models.

collected that included markers placed on the lateral and medial femoral condyles and the lateral and medial malleoli. On the amputated limb, the shank cluster was placed laterally on the socket and a marker was placed at the distal tip of the socket to define the long axis of the residual shank segment. Eight additional markers were placed on the prosthesis keel including the most proximal end ("Head"), the most distal end ("Toe"), bilaterally at the end of the linear segment distal to the Head marker, laterally on the most acute point of the prosthesis curvature and three markers evenly spaced between the acute and Toe markers. See Figure 7.1 for a schematic of these marker placements. The marker on the most acute point of the prosthesis defined the prosthetic limb "ankle" joint.

The testing setup (see Figure 7.2) included a 10-camera motion capture system (Vicon, Centennial, CO) that captured 3D positional data of the markers at 200 Hz for kinematic analysis, and ten 6 degree-of-freedom force platforms (Kistler,
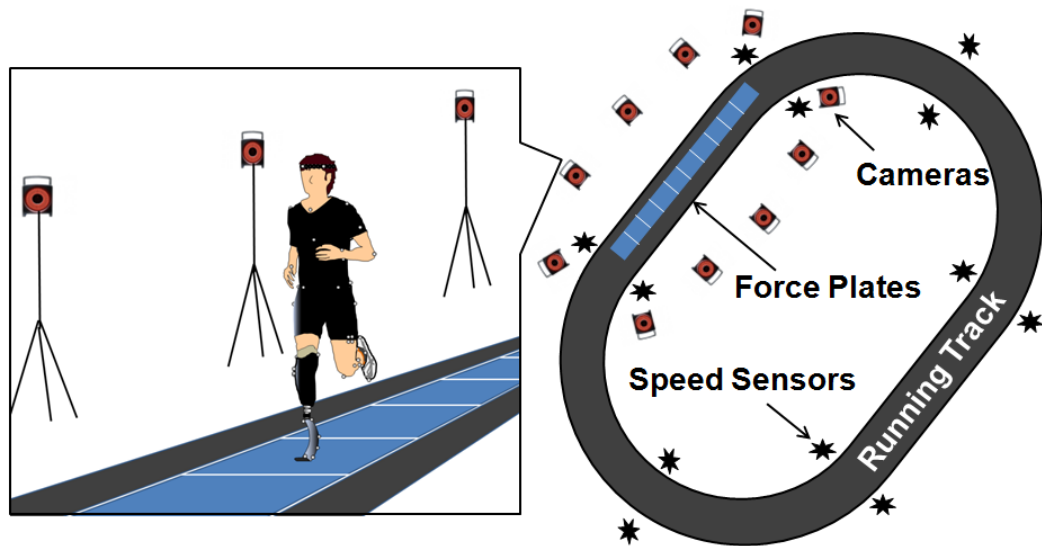
Figure 7.2. Schematic of testing setup. Subjects ran around a 100m track containing 10 force plates that captured ground reaction force data. Ten motion capture cameras captured 3D kinematic data and six sets of sensors around the track monitored running speed in real-time.

Amherst, NY) embedded in the track in series that collected ground reaction forces at 1000 Hz. Raw marker data were filtered using a 4th order, zero lag low pass Butterworth filter with a cutoff frequency of 6 Hz while raw force data were similarly filtered with a 30 Hz cutoff frequency. Kinematic and ground reaction force data were combined and inverse dynamics techniques were used to calculate joint moment data. Subjects completed at least five successful trials for each leg at each running velocity. A successful trial was defined as the subject running within ±0.2 m/s of the target velocity within and stepping within the boundaries of the force platforms during the trial. Predetermined velocities were governed using concurrent biofeedback. Six sets of laser sensors were evenly distributed around the track such that when the subject ran past the sensors, the average velocity over the track section was instantaneously calculated. Verbal feedback was given to subjects during the trials to indicate whether or not they were running at the desired velocity. The order for running velocities was

randomized. Subjects were allowed to rest for as long as needed between velocity conditions to reduce the effects of fatigue with a minimum rest of five minutes between conditions.

Standard inverse dynamics calculations (Zatsiorsky, 2002) were used to estimate lower extremity joint moments from the motion and ground reaction force data and were calculated using Visual3D (C-Motion, Germantown, MD) software. The outcome variables were compared between the intact and residual limbs of ILEA subjects and between the ILEA and Control groups at each running velocity.

7.3.4 Statistical Analysis

This research was designed to determine the influence of group, leg, and running velocity on peak ankle, knee, and hip joint moments. Statistical comparisons were performed in SPSS 19.0 (SPSS Inc.). A 2x2x3 three factor repeated measures analysis of variance (ANOVA) was used to identify statistical differences between the dependent variables using Group (ILEA and Control), Leg (prosthetic/intact and left/right), and Velocity (2.5 m/s, 3.0 m/s, 3.5 m/s) as independent variables (IVs). Group was treated as a between-subjects variable while Leg and Velocity were treated as within-subjects variables. When significant differences were identified from the full factorial model, two-way ANOVAs and pair-wise comparisons with Bonferroni adjustments for multiple comparisons were used when appropriate to determine which conditions were significantly different from each other. Significance for all statistical tests were set at $\alpha = 0.05$.

Table 7.1. Subject residual limb length and prosthesis inertial properties. The prostheses could not be disconnected from the sockets so all measured inertial properties were taken for the prosthesis and socket combined unit.

ILEA Subject	RSP model	Amputated Limb	Residual Limb Length (m)	RSP mass (kg)	CM_x (m)	CM_y (m)	CM_z (m)	I_{xx} (kg·m²)	I_{yy} (kg·m²)	I_{zz} (kg·m²)
1	Flex-Run	Right	0.12	1.478	-0.050	-0.0003	0.056	0.0356	0.0377	0.0041
2	Flex-Run	Left	0.14	1.328	-0.042	0.0004	0.082	0.0302	0.0317	0.0037
3	Flex-Run	Left	0.21	1.315	-0.044	0.0036	0.016	0.0310	0.0330	0.0038
4	Cheetah	Left	0.24	1.439	0.060	-0.0093	-0.086	0.0369	0.0404	0.0065
5	Cheetah	Right	0.20	1.892	0.044	-0.0045	-0.088	0.0858	0.0892	0.0104
6	Flex-Run	Left	0.21	1.770	-0.044	0.0057	0.070	0.0579	0.0598	0.0284
7	Catapult	Left	0.24	1.341	-0.036	-0.0025	0.028	0.0264	0.0284	0.0042
8	Catapult	Right	0.18	1.802	-0.032	0.0050	0.095	0.0775	0.0799	0.0067

ILEA = Individual with lower extremity amputation
RSP = Running-specific prosthesis
CM_x, CM_y, CM_z= Center of mass position of the RSP+socket along the x,y, and z axes with respect to the most proximal end of the prosthesis keel
I_{xx}, I_{yy}, I_{zz} = Principal axis moments of inertia about the center of mass of the RSP+socket

7.4 Results

Inertial properties measured for each ILEA subject are presented in Table 7.1. No differences were observed between the left and right control limbs for any variable. Consequently, the data were averaged to generate a representative control limb for clearer presentation in the tables and figures. However, all statistical outcomes were based on the balanced statistical design that included both control limbs. Figures 7.3-7.5 shows the joint moment profiles for the ankle, knee, and hip normalized to the gait cycle for each of the three running velocities, and Figure 7.6 shows the sagittal joint angle profiles for these joints.

7.4.1 Ankle Moments

Ankle moment profiles are presented in Figure 7.3 with peak values presented in Figure 7.7. Peak ankle plantarflexion moments were significantly affected by speed (p<0.001). Each leg increased peak plantarflexion moment with velocity (p≤0.003). No other significant main effects or interaction effects existed for this variable. Peak ankle stance varus moments had significant leg (p<0.001) main effects and leg x group (p<0.001) interaction effects. The prosthetic limb had significantly lower peak varus moments than the intact and control limbs (p<0.001), and the interaction effect was due to the ILEA limbs having greater differences than the control limbs. No significant differences existed for peak ankle internal/external rotation moments.

7.4.2 Knee Moments

Knee moment profiles are presented in Figure 7.4 with peak values presented in Figure 7.8. Significant leg and speed main effects were present for the stance phase
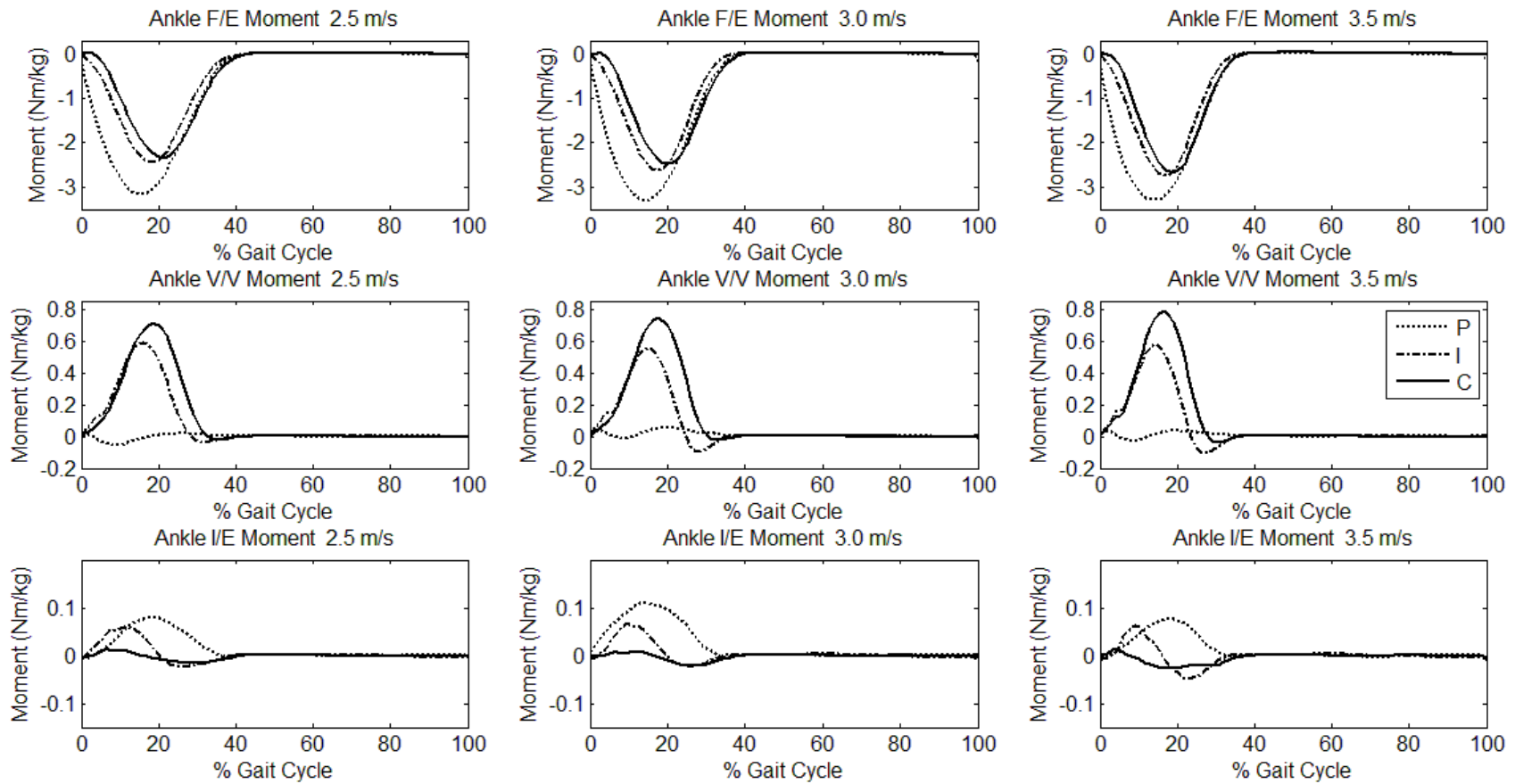
Figure 7.3. Average internal ankle joint moments normalized to body mass and the gait cycle for the prosthetic (P), intact (I) and combined control (C) limbs across running velocities for each plane of motion. F/E, V/V, and I/E represent dorsi/plantarflexion, varus/valgus, and internal/external rotational moments, respectively. Positive values indicate dorsiflexion, varus, and internal rotation moments.
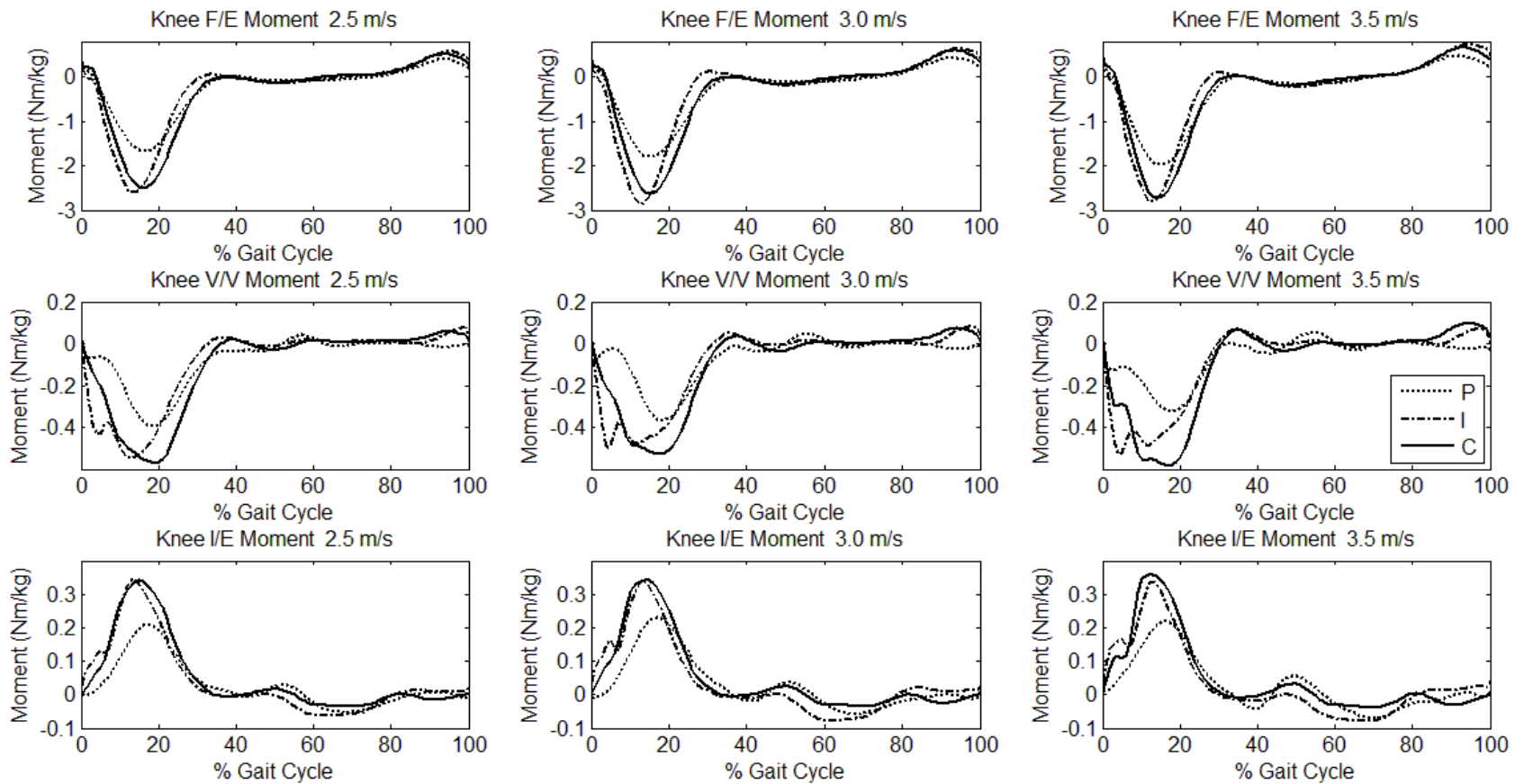
Figure 7.4. Average internal knee joint moments normalized to body mass and the gait cycle for the prosthetic (P), intact (I) and combined control (C) limbs across running velocities for each plane of motion. F/E, V/V, and I/E represent flexion/extension, varus/valgus, and internal/external rotational moments, respectively. Positive values indicate flexion, varus, and internal rotation moments.
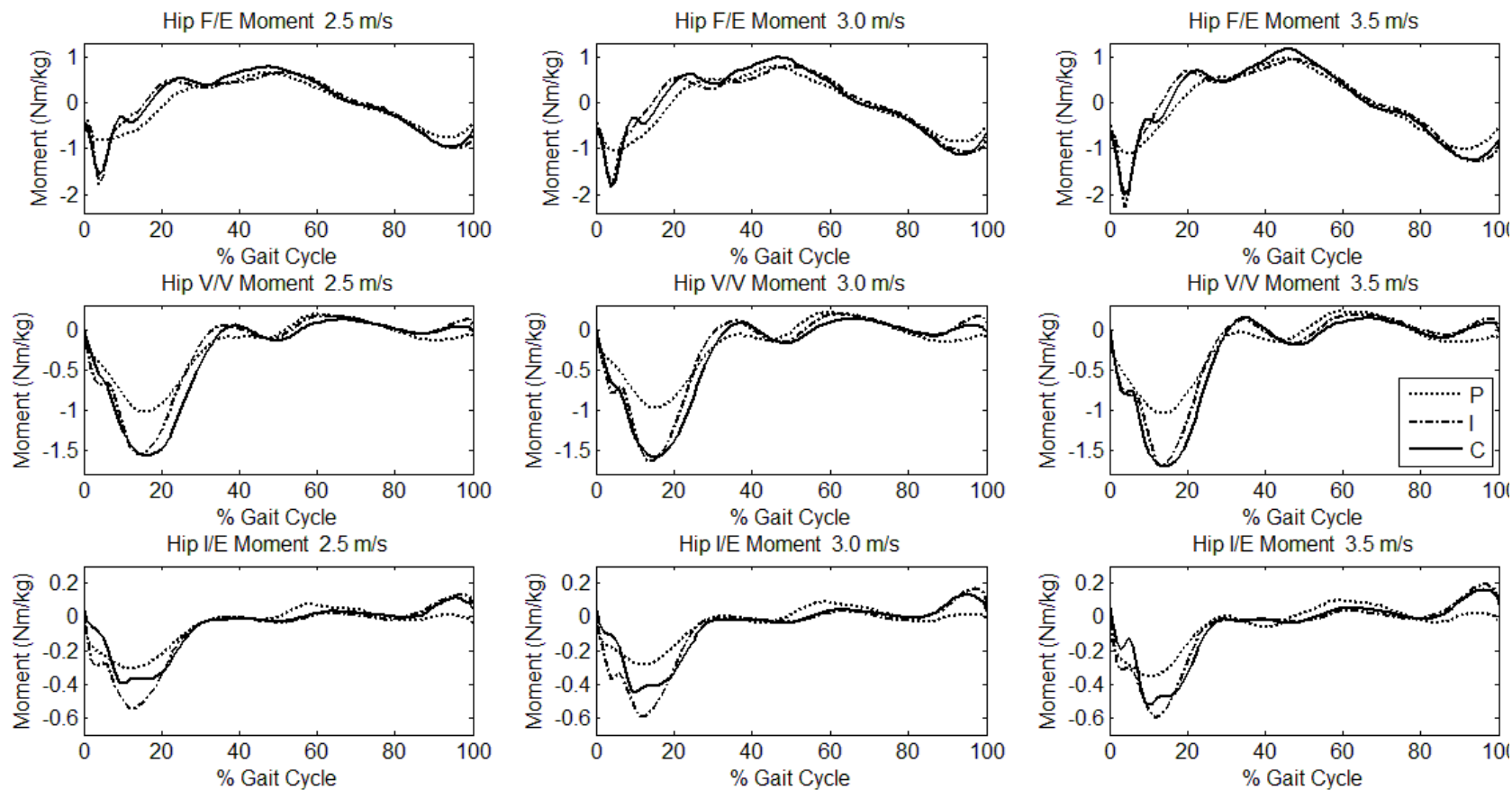
Figure 7.5. Average internal hip joint moments normalized to body mass and the gait cycle for the prosthetic (P), intact (I) and combined control (C) limbs across running velocities for each plane of motion. F/E, V/V, and I/E represent flexion/extension, varus/valgus, and internal/external rotational moments, respectively. Positive values indicate flexion, varus, and internal rotation moments.
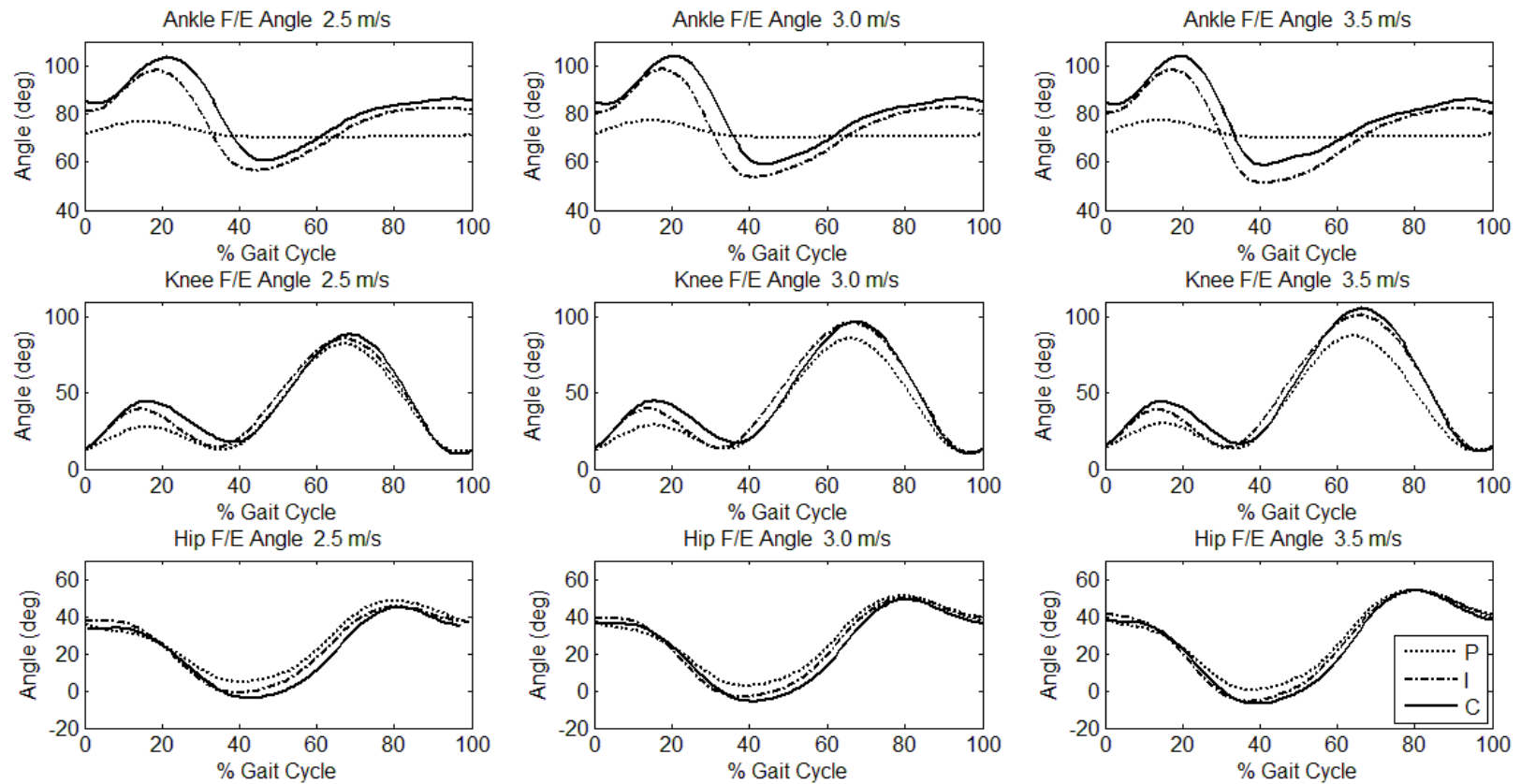
Figure 7.6. Average sagittal plane ankle, knee, and hip angles for the prosthetic (P), intact (I) and combined control (C) limbs across running velocities normalized to the gait cycle for each plane of motion. F/E represents flexion/extension for the knee and hip joints and dorsi/plantarflexion for the ankle joints, respectively. Positive values indicate dorsiflexion and flexion. Ankle angles are absolute angles between the foot and shank segments for the intact and control limbs and between the keel segments adjacent to the most acute marker on the prosthesis for the prosthetic limb. Anatomical neutral for the intact and control limb ankles is considered 90 degrees.
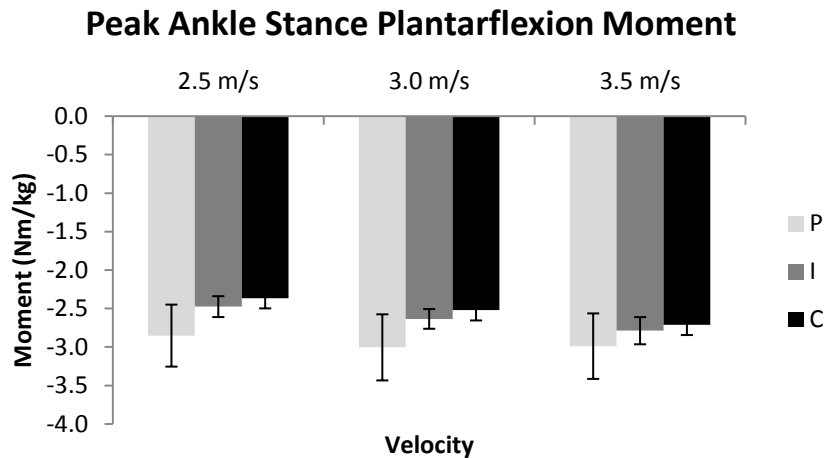
Figure 7.7. Peak ankle plantarflexion moments normalized to body mass for the prosthetic (P), intact (I), and averaged control (C) limbs across the tested velocities. Error bars represent ±1 standard error. No differences were observed between limbs at any velocity. Significant velocity effects were observed at each limb (p<0.05).

peak knee extension and swing phase peak knee flexion moments (p≤0.007). Leg differences were apparent for both variables with the prosthetic limb knee having significantly lower stance peak knee extension and swing peak knee flexion moments than the intact limb and the control limbs (p≤0.017). No differences existed between the control limbs or the intact and control limbs for these parameters. The prosthetic and intact limb peak stance extension moments increased with velocity (p<0.003), but the control limbs did not (p≥0.071). All limbs peak swing flexion moments increased with velocity (p≤0.001). A significant leg x group interaction existed for both of these variables (p≤0.003) where the differences between the ILEA group limbs were greater than the differences between the control group limbs. A significant leg x speed interaction existed for peak knee flexion moment during swing phase (p=0.001). This interaction was due to a leg x speed interaction for the ILEA group
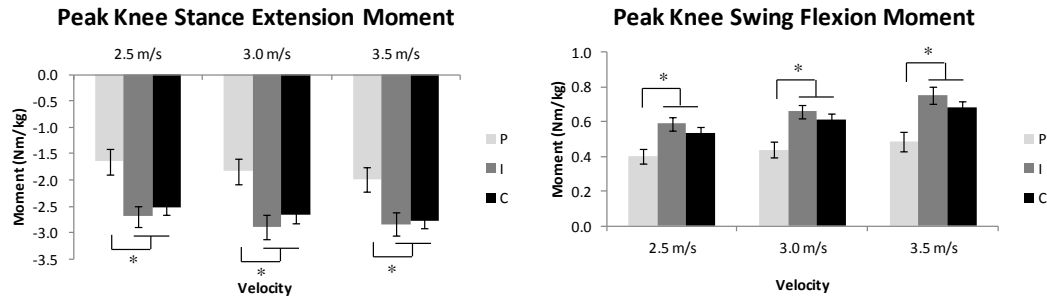
Figure 7.8. Peak knee stance extension and swing flexion moments for the prosthetic (P), intact (I), and averaged control (C) limbs normalized to body mass across the tested velocities. Error bars represent ±1 standard error. * indicates significant differences (p<0.05) between limbs. Significant velocity effects were observed for the prosthetic and intact limbs for peak stance extension moments and at each limb for swing flexion moments.

where the intact knee increased its peak swing flexion at a greater rate than the prosthetic limb knee with increasing velocity.

Peak knee valgus moments had a significant velocity main effect (p=0.01) where the intact limb valgus moment increased with velocity. Peak knee internal rotation moments had a significant leg main effect (p=0.042) where the prosthetic limb had lower peak internal rotation moments than the intact limb.

7.4.3 Hip Moments

Hip moment profiles are presented in Figure 7.5 with peak values presented in Figure 7.9-7.10. Significant leg main effects were evident for the peak hip stance and swing extension moments (p≤0.004). The prosthetic limb hip had significantly lower peak stance extension moment values than the intact limb (p<0.001) and the control limbs (p<0.001) at all velocities. The prosthetic limb had significantly lower peak swing extension moments than the intact limb at each velocity (p<0.001) and was significantly lower than the control limb at 3.0 m/s (p=0.017) but did not reach
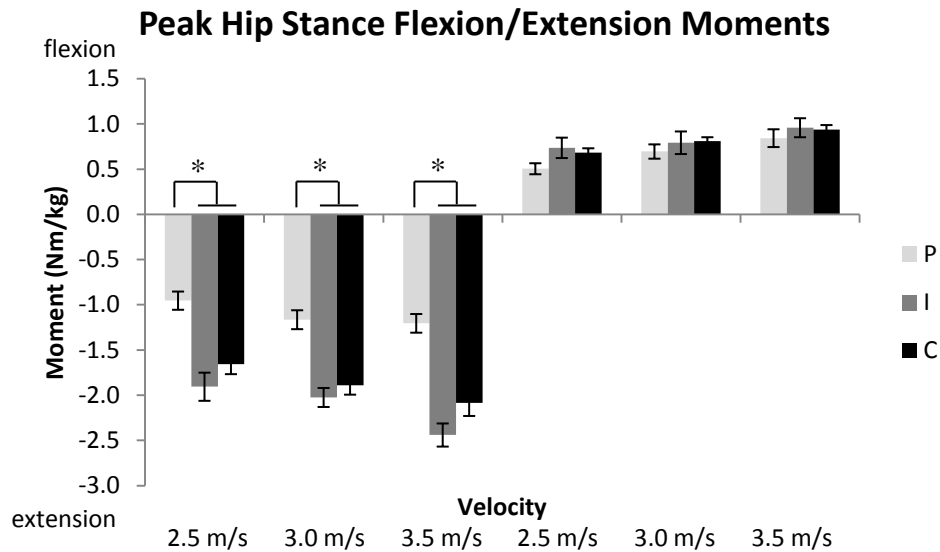
Figure 7.9. Peak hip stance flexion and extension moments for the prosthetic (P), intact (I), and averaged control (C) limbs normalized to body mass across the tested velocities. Error bars represent ±1 standard error. * indicates significant differences (p<0.05) between limbs. No differences were observed between any limbs for peak stance flexion moments. Significant velocity effects were observed at each limb for both variables.

statistical significance at 2.5 m/s (p=0.053) or 3.5 m/s (p=0.053) All four limbs had significant velocity effects for the peak stance and swing flexion and extension moments (p≤0.008) where the peak moment magnitudes increased with velocity. Significant group differences (p=0.026) existed for peak hip swing flexion moments where the control group had greater peak hip moments than the ILEA group. Significant leg x group interactions (p<0.001) were evident for the hip peak stance and swing extension moments. This indicated the ILEA group had greater differences between the limbs than the control group. A significant leg x speed interaction existed for peak hip stance flexion moment (p=0.05) where the intact limb peak hip stance flexion moment increased with magnitude at a greater rate with velocity than did the peak prosthetic limb stance flexion moment.

160
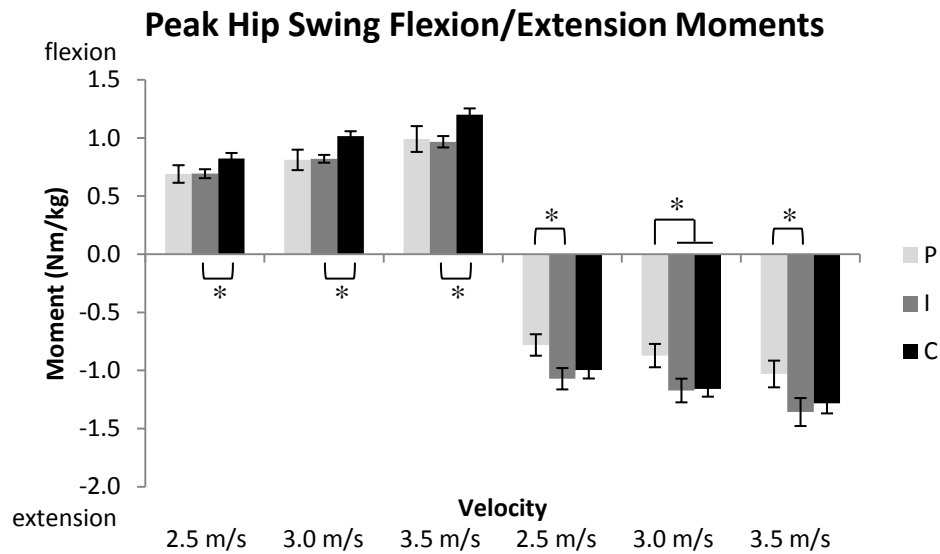
Figure 7.10. Peak hip swing flexion and extension moments for the prosthetic (P), intact (I), and averaged control (C) limbs normalized to body mass across the tested velocities. Error bars represent ±1 standard error. * indicates significant differences (p<0.05) between limbs. Significant velocity effects were observed at each limb for both variables.

Peak stance phase hip valgus and external rotation moments had significant speed and leg main effects (p≤0.001) and a significant leg x group interaction effects (p≤0.004). The control limb peak valgus and external rotation moments both increased with velocity (p≤0.018), while the intact limb peak valgus moment and prosthetic limb peak external rotation moment increased with velocity (p≤0.02). The prosthetic limb had significantly lower peak valgus and external rotation moments than the intact and control limbs (p≤0.036). The intact limb had greater peak external rotation moments than the control limbs (p=0.029). The leg x group interaction effects were caused by greater differences between the ILEA limbs than the control limbs for both of these parameters.

7.5 Discussion

This study provides the first report of 3D lower extremity joint moments throughout the entire gait cycle for ILEA running with RSPs. The first hypothesis predicted that ILEA would demonstrate lower joint moment magnitudes in the prosthetic limb than the intact and control limbs throughout stance and swing phase at each velocity. This hypothesis was accepted for most peak moment variables but rejected for the peak ankle stance plantarflexion, ankle internal rotation moment, hip stance flexion, and hip swing flexion moments. Overall, these data support that the intact limb is loaded to a greater extent than the prosthetic limb when subjects run with RSPs. The "ankle" plantarflexion moments calculated in the RSP are suggested to be sensitive to marker placement (Brüggemann et al., 2009) and are not directly comparable to the intact limb ankle moments due to vastly different architecture and mechanical moment arms. The lower extremity extension moments that provide both resistance to limb collapse and propulsive power generation along with the coronal and transverse plane moments were lower in the prosthetic limb compared to both the intact and control limbs. Lower prosthetic limb stance knee extension moments are consistent with previous running studies of ILEA wearing non-RSPs (Brouwer et al., 1989; Czerniecki et al., 1991; Miller, 1987; Sanderson and Martin, 1996) and of a single subject sprinting with bilateral RSPs (Brüggemann et al., 2009). Lower prosthetic limb stance hip extension moments are consistent with the bilateral sprinter (compared to control subjects) (Brüggemann et al., 2009). However, Buckley (Buckley, 2000) reported that two ILEA sprinters with unilateral amputations wearing two RSP models each showed different relative peak prosthetic and intact limb hip

extension moments depending on the RSP. Out of the eight subjects in the current study, three different RSP models were tested. Each subject only wore one RSP model, but the subjects generated similar sagittal plane joint moment patterns to each other with consistent patterns of greater knee and hip stance extension moments in the intact limb. Buckley's two subjects also performed maximal sprints using spiked shoes and RSPs fitted with spike plates that could alter running mechanics.

Sanderson & Martin (Sanderson and Martin, 1996) reported that ILEAs running with non-RSPs demonstrated longer duration stance phase hip extension moments on the prosthetic limb as an adaptive mechanism. Buckley's (Buckley, 2000) subjects also demonstrated this adaptation when sprinting with RSPs. The results of the current study with subjects running with RSPs at submaximal velocities support those findings although the discrepancy between the prosthetic and intact limb extensor period decreased with increasing velocity as a percentage of the gait cycle. The prosthetic limb hip generated an extensor moment for the first 23% of the gait cycle (62% of stance phase) when running at 2.5 m/s and for 19% of the gait cycle (59% of stance) when running at 3.5 m/s compared to 17% (46% of stance) and 15% (45% of stance) of the gait cycle, respectively for the intact limb. This equated to the prosthetic limb generating a hip extension moment for approximately 15% more of the stance phase than the intact limb. These discrepancies were less than the approximately 25% of stance phase longer prosthetic limb hip extension period reported by Sanderson & Martin. RSPs may provide improved propulsion compared to non-RSPs which would help explain these differences. However, RSPs are still unable to replace the function of an intact limb, and the prolonged hip extension

moment will increase the prosthetic limb hip's angular impulse that assists with maintaining upright posture (Sanderson and Martin, 1996) and generating propulsion.

The sagittal plane joint angles indicated reduced ranges of motion for the residual knee and hip joints throughout the gait cycle with a more upright posture. The reduced knee flexion loading responses during stance phase would minimize the muscular demand from the knee and hip joints to control knee flexion and prevent knee collapse during weight acceptance. This may be an attempt by the ILEA group to either minimize the joint loading on or ease the control demands of the prosthetic limb. Additionally, prosthetic limb knee extensor strength may be reduced as a consequence of the amputation (Sanderson and Martin, 1996), which might cause ILEA to adapt their running style to minimize the residual knee joint loading. No differences in peak moment values were identified between the intact and control limbs during stance phase suggesting that the joint loading on the intact limb is not greater than normal. These data also indicate that the intact limb behaves very similarly to able-bodied limbs with respect to the sagittal plane joint moment profiles.

The coronal plane peak knee and hip moments were similar between the intact and control limbs; however, the rate of knee valgus moment generation during weight acceptance appeared to be greater in the intact limbs. Elevated rates of knee valgus moment generation have been identified as a risk factor for osteoarthritis during ILEA walking (Lloyd et al., 2010), but these rates have not been identified during ILEA running. Typically, high transverse and frontal plane knee moments have been implicated as risks for injury during able-bodied running (Scott and Winter, 1990; Stefanyshyn et al., 2001). These risk factors could be related to the high rates of

injury observed in ILEA competitive athletes (Nyland et al., 2000). These observations could also impact ILEA running around a track where they must compensate for the greater rotating forces acting on the prosthetic limb during the track bend (Lechler and Lilja, 2008). Rather than or in addition to large peak frontal plane moments, the rate of moment generation could be a factor that would increase the risk of injury during running. However, a more detailed analysis is warranted to further examine this observation. The intact limb hip external rotation moments were greater than the control limbs, which may imply that these subjects are at greater risk of injury when running. While not significantly different due to high variability, the data suggest increased ankle joint internal rotation moments in the ILEA group compared to the control subjects. The different timing of the peak values, with the intact limb peak moment occurring later in stance phase, could also be an indicator of future orthopaedic issues, but more specific investigation into these variables is needed to confirm this.

ILEA running with RSPs have significantly lower terminal swing phase knee flexion moments in the prosthetic limb knee than the intact and control limbs. These reduced knee flexion moments are most likely due to the reduced mass and inertia of the prosthetic shank/foot complex when wearing RSPs. Less demand is placed on the knee flexor musculature to slow down the knee extension as the knee joint approaches full extension. Hip extension moments at terminal swing were also lower in the prosthetic limb as compared to the intact limb. Again, this may reflect the lower muscular demand to slow down the thigh due to the lower overall mass of the lower extremity on the amputated limb. The intact limb hip peak swing flexion

moments were lower than the control group peaks which may be linked to the shorter step lengths in this limb compared to the control group at each running velocity (Baum et al., 2012b). Generating a shorter step length would lower the peak demand for the hip flexion moment for each stride as the hip would not need to flex as much. Electromyography and power analyses would provide valuable information on the muscle firing patterns and mechanical energy flow during ILEA running and further elucidate altered control strategies.

The second hypothesis that increased running velocity would be associated with similar increases in peak joint moments of the intact and prosthetic limbs was accepted for most parameters but rejected for peak hip stance flexion and knee swing moments. No leg x speed interactions existed for the knee and hip stance extension moments, which indicates that the ILEA subjects did not increase their reliance on the intact limb at faster running velocities. It therefore appears that the intact and residual limb joints increase their moment magnitudes with velocity in a similar manner when supporting body weight or generating propulsion. However, the increase in peak hip stance flexion moment associated with running velocity was greater in the intact limb than the prosthetic limb. This was influenced by the greater intact limb hip joint accelerations at faster running velocities. Running velocity also had a greater effect on the intact limb knee swing flexion moment than the prosthetic limb. These results are in contrast with the only previous ILEA running study to report swing phase joint moments. Sanderson & Martin showed similar swing phase knee moment profiles between the intact, residual, and able-bodied limbs (Sanderson and Martin, 1996). However, in that study ILEAs wore non-RSPs that had masses and inertial properties

much closer to those of the intact limbs they replace, so the prosthetic and intact limb knee joint musculature would have similar mechanical demands to slow knee extension at terminal swing. The RSPs worn by the current study subjects have lower masses than the intact limb and the prostheses worn by subjects in Sanderson & Martin's study. Therefore an increasingly greater knee flexor demand was induced in the intact limb compared to the prosthetic limb in order to slow the shank extension as limb swing speeds increased.

7.6 Conclusions

The intact limb knee and hip joints generated greater peak moments than the prosthetic limb in all three planes of motion suggesting a greater reliance on the intact limb during running at a particular velocity. However, with the exception of hip internal rotation moments, the intact limb generated similar peak moment values to the control limbs, which indicates that the intact limb is not overloaded when ILEA run with RSPs. Only the hip peak stance flexion moment and knee swing flexion moment increases associated with velocity were greater in the intact limb than the prosthetic limb, which is most likely a result of the greater joint accelerations and inertial properties in the intact limb requiring a greater muscular demand at faster running velocities. Previously identified prolonged stance phase hip extension moments in the prosthetic limb (Sanderson and Martin, 1996) were confirmed in this study, supporting this observation as an adaptive mechanism that allow ILEA to run with passive prosthetic devices at the same velocities as able-bodied individuals. Increased peak hip internal rotation moments and knee valgus moment rates of loading in the intact limb were identified as possible risk factors for injury. Study of

the joint power, joint work, and segmental energy flow will further elucidate compensatory control mechanisms that allow subjects with amputation to modulate their running velocity when using RSPs.

Chapter 8: Mechanical Energy Adaptations to Running Velocity

in Individuals with Amputation using Running-Specific

Prostheses

8.1 Abstract

Altered mechanical energetics during running may be necessary to accommodate for physical deficiencies caused by lower extremity amputation. The mechanical energy adaptations required to change running velocities are not well understood in individuals with lower extremity amputations (ILEA) wearing running-specific prostheses (RSPs). The purpose of this study was to investigate lower extremity joint powers and mechanical work when running with a passive RSP at different running velocities. ILEA with unilateral transtibial amputations and a control group ran overground at three constant velocities (2.5, 3.0, and 3.5 m/s). It was hypothesized that (1) ILEA would exhibit lower mechanical energy in the prosthetic limb than the intact and control limbs at each velocity, and (2) increased running velocity would be associated with similar increases in mechanical energy of the intact and prosthetic limbs. Results indicated ILEA generated lower prosthetic limb "ankle" and knee work compared to the intact and control limbs. ILEA adapted by generating more work at the prosthetic limb hip compared to the intact and control limbs. The prosthetic limb also generated lower swing phase knee eccentric and hip concentric flexion energies that were attributed to the lower inertial properties of the lower extremity with the RSP. To change running velocity, able-bodied runners increased their ankle concentric work. ILEA increased the intact limb ankle work to increase velocity but also adapted to the lack of prosthetic ankle energy changes by increasing their prosthetic limb knee and hip concentric energy. These data highlight deficiencies in the prosthetic limb "ankle" and knee total work during running and

indicate that ILEA wearing RSPs use altered mechanical energy strategies compared

with able-bodied runners to increase running velocity.

8.2 Introduction

One goal of lower extremity prosthetic components is to replace the function of amputated limbs. However, these devices do not provide similar sensory function and the mechanical function of prostheses has yet to match that of the intact limb. Consequently, individuals with lower extremity amputations (ILEA) must alter their biomechanical strategies to compensate for these deficiencies. Joint control must also be adapted to account for the loss of major joints and musculature while also integrating the function of a passive mechanical prosthesis. The introduction of running-specific prostheses (RSPs) and the recent running performances by an ILEA with bilateral amputations has fueled a debate on whether or not these devices may actually provide a performance advantage over intact limbs and able-bodied runners (Buckley et al., 2010; Kram et al., 2010; Weyand and Bundle, 2010a; Weyand and Bundle, 2010b; Weyand and Bundle, 2010c). While improved performance would be an obvious advantage for elite runners, it could also provide greater access to running for ILEA who wish to simply maintain an active lifestyle (Kegel et al., 1978). Unfortunately, limited information exists relative to running with RSPs at submaximal velocities and the adaptations that ILEA make to run at various velocities. Examining the mechanical energy profiles will provide insights into the muscular adaptations that ILEA make when running. These insights can then lead to targeted improvements in rehabilitation and running training for this group of individuals.

Individuals with transtibial amputation have demonstrated significant differences in joint power and mechanical work generation as compared to healthy

individuals when running with both non-RSPs (Czerniecki and Gitter, 1992; Czerniecki et al., 1996; Czerniecki et al., 1991) (prostheses originally designed for walking) and RSPs (Brüggemann et al., 2009; Buckley, 2000). The ankle joint is the primary energy generator during able-bodied running (Heiderscheit et al., 2011; Novacheck, 1998b; Winter, 1983b); however, after amputation, prostheses are generally shown to be incapable of matching this energy production. When running with non-RSPs, the prosthetic limb absorbs and generates less energy during stance phase than normal and performs considerably less total work (Czerniecki and Gitter, 1992; Czerniecki et al., 1991). Only two studies to date have reported joint power data of ILEA running while wearing RSPs, but these studies dramatically differ in their results. Both studies examined ILEA sprinting, and Buckley (Buckley, 2000) reported much lower peak "ankle" powers in the prosthetic limb of two sprinters with unilateral amputations compared to their intact limb. Bruggemann et al. (Brüggemann et al., 2009) reported greater peak "ankle" powers in the prosthetic limbs of one sprinter with bilateral amputations compared to an able-bodied control group. These differences could be due to differences in runners with unilateral versus bilateral amputations or from individual differences between the three subjects.

Czerniecki et al. (Czerniecki and Gitter, 1992) identified that the major compensatory patterns allowing ILEA with transtibial amputation to run with non-RSPs included an increase in stance phase hip muscle work on the prosthetic limb and increased hip and knee muscle work on the intact limb during swing phase. Buckley's (Buckley, 2000) data supported these conclusions for one subject; however, his second subject generated greater eccentric and concentric work in the residual knee as

an adaptive mechanism. Conversely, Bruggemann et al. (Brüggemann et al., 2009) reported lower mechanical work at the knee joints during stance with lower energy loss in prosthetic ankle joint than control subjects. It is unknown whether these compensations are due to individual adaptations or if a larger subject population might identify a more consistent trend for mechanical energy adaptive mechanisms when ILEA run with RSPs. Furthermore, the data from subjects wearing RSPs are only reported for the running stance phase. RSPs have reduced masses compared with both the intact limbs they replace and prostheses designed for walking. Therefore, RSPs may induce different joint power and mechanical work compensations while running, especially during swing phase. None of the studies examined how mechanical energy changes when running at different velocities. In able-bodied runners, mechanical energy at each joint increases with velocity (Novacheck, 1998b), and lower extremity joint moments increase with velocity when ILEA wear non-RSPs (Sanderson and Martin, 1996). It is reasonable to expect that the total mechanical energy, i.e. the summation of the joint mechanical energies, of ILEA wearing RSPs would increase with running velocity, but examining the joint mechanical energy at each velocity would indicate how the individual joints contribute to total energy increases.

The purpose of this study was to investigate lower extremity joint power and mechanical work adaptations when running with a passive RSP at different running velocities. The residual and intact limb joint (ankle, knee, and hip) powers and mechanical work and those of healthy control subjects were compared across a range of velocities to identify adaptations in energy generation and absorption needed to

adapt to the passive RSP. It was hypothesized that (1) ILEA would exhibit lower mechanical energy in the prosthetic limb than the intact and control limbs at each velocity, and (2) increased running velocity would be associated with similar increases in mechanical energy of the intact and prosthetic limbs.

8.3 Methods

8.3.1 Subjects

Eight male subjects with unilateral transtibial amputation (mean age = 32.0 ± 10.2 years, height = 1.80 ± 0.07 m, mass = 82.3 ± 13.0 kg; see Table 5.1) and eight healthy male control subjects (mean age = 29.0 ± 6.9 years, height = 1.84 ± 0.05 m, mass = 79.3 ± 7.9 kg) between 18 and 50 years of age volunteered to participate in the experiment. To maintain a uniform study population and reduce the potential data variability due to bilateral amputations and/or different design and function of prosthetic knee components, only ILEA with unilateral transtibial amputations were recruited. ILEA ran in their own prescribed RSPs to reduce variability due to using a new prosthetic design and to ensure proper alignment. ILEA had at least 3 months of running experience (range: 3-256 months) and the causes of amputation were either congenital (1) or trauma (7). Prior to participating, all subjects gave informed written consent, which was approved by the University of Maryland Institutional Review Board. Subjects with amputation were excluded if they had comorbidities on the intact limb that would affect gait.

The inertial properties of the prosthetic components and intact body segments were estimated for use with the inverse dynamics approach. Subject masses were measured using a force platform. Height and body weight of each subject were measured, and anthropometric measurements from marker positions were used to estimate the mass, center of mass, and moments of inertia of intact limb segments (Dempster, 1955; Hanavan, 1964). Since ILEA subjects were missing one foot and part of their shank, an adjusted body mass (Smith, 2008) was used as an input to anthropometric regression equations that accounted for the missing body segments.

For subjects with amputation, the residual limb length and circumferences at the knee joint and distal end of the limb were measured using a measuring tape. The inertial properties of the residual limb were then estimated as a frustrum of a right circular cone (Hanavan, 1964; Mattes et al., 2000). The residual limb mass was estimated from the calculated geometric volume assuming a uniform 1.10 g/cm^3 tissue density (Mattes et al., 2000; Mungiole and Martin, 1990). The prosthetic socket and RSP were treated as one unit and weighed with a laboratory scale. The socket+RSP unit's center of mass position was calculated using a reaction board method (Hay, 1985), and the moment of inertia of the socket+RSP unit was calculated from the period of oscillation measured with a trifilar pendulum (Baum et al., 2012a; du Bois et al., 2008; Genta and Delprete, 1994). The inertial properties for the lower limb segment were then calculated from the combination of the residual limb and prosthetic components. The RSP keels were not able to be disconnected from the sockets for each subject, so inertial properties for each prosthetic keel were

estimated using data reported by Baum et al. (Baum et al., 2012a) for the RSP model and stiffness category that most closely matched those used by the subjects. The inertial properties of the socket were then estimated by subtracting the inertial properties of the RSP keel from the total socket+RSP segment using the parallel axis theorem. Subsegments within the RSP keels were defined via reflective marker placements and the inertial properties of each subsegment were estimated by assuming each segment as rigid trapezoidal cuboids (Baum et al., 2011).

8.3.3 Experimental Procedures

Subjects ran overground around a 100m long track at three constant velocities (2.5 m/s, 3.0 m/s, and 3.5 m/s). Prior to beginning the experiment, retroreflective markers were placed bilaterally over the anterior and posterior iliac spines, heel, 3rd metatarsal head, 5th metatarsal head, and tip of the toe on the shoe. Marker clusters were placed bilaterally on the lateral thigh and shank segments. A static trial was collected prior to dynamic trials that included markers placed on the lateral and medial femoral condyles and the lateral and medial malleoli. On the amputated limb, the shank cluster was placed laterally on the socket and a marker was placed at the distal tip of the socket to define the long axis of the residual shank segment. Eight additional markers were placed on the prosthesis keel including the most proximal end ("Head"), the most distal end ("Toe"), bilaterally at the end of the linear segment distal to the Head marker, laterally on the most acute point of the prosthesis curvature and three markers evenly spaced between the acute and Toe markers. The marker on the most acute point of the prosthesis defined the prosthetic limb "ankle" joint. The testing setup (see Figure 8.1) included a 10-camera motion capture system (Vicon,
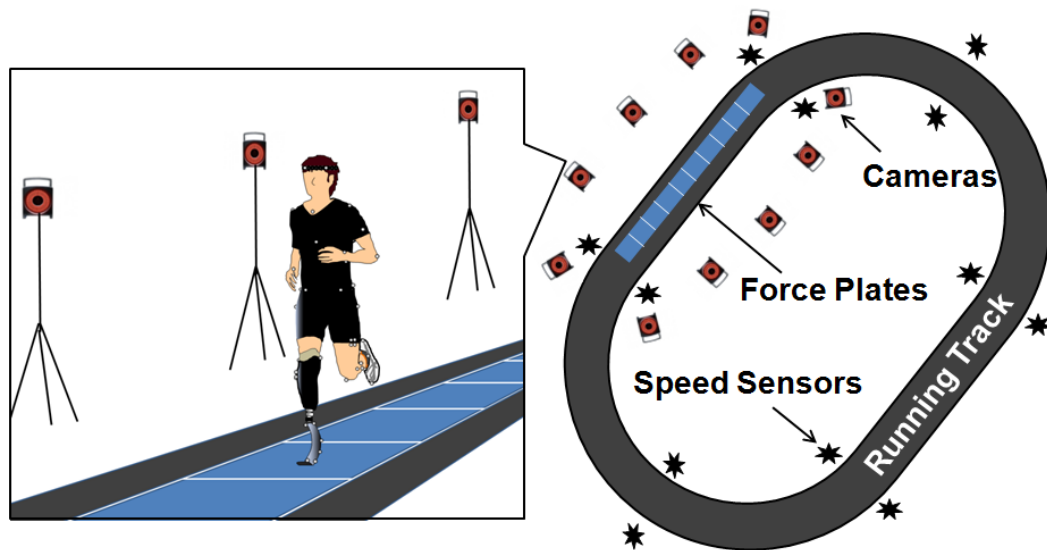
Figure 8.1. Schematic of testing setup. Subjects ran around a 100m track containing 10 force plates that captured ground reaction force data. Ten motion capture cameras captured 3D kinematic data and six sets of sensors around the track monitored running speed in real-time.

Centennial, CO) that captured 3D positional data of the markers at 200 Hz for kinematic analysis, and ten 6 degree-of-freedom force platforms (Kistler, Amherst, NY) embedded in the track in series that collected ground reaction forces at 1000 Hz. Raw marker data were filtered using a 4th order, zero lag low pass Butterworth filter with a cutoff frequency of 6 Hz while raw force data were similarly filtered with a 30 Hz cutoff frequency. The kinematic and ground reaction force data were combined and standard inverse dynamics techniques (Zatsiorsky, 2002) were used to calculate joint moment data for each subject. Subjects completed at least five successful trials for each leg at each of three running velocities. A successful trial was defined as the subject running within ±0.2 m/s of the prescribed velocity within the track section containing the force platforms and stepping within the boundaries of the force platforms during the trial. Predetermined velocities were governed using concurrent biofeedback. Six sets of laser sensors were evenly distributed around the track such

that when the subject runs past the sensors, the average velocity over the track section was instantaneously calculated. Verbal feedback was given to subjects during the trials to indicate whether or not they were running at the desired velocity. The order for prescribed running velocities was randomized. Subjects were allowed to rest for as long as needed between velocity conditions to reduce the effects of fatigue with a minimum rest of five minutes between conditions.

The outcome variables were compared between the intact and residual limbs of ILEA subjects and between the ILEA and Control groups at each running velocity. Muscle power at a particular joint is the product of the net muscular moment and angular velocity about the joint (Winter, 2005) and was calculated using Equation 1 through Visual3D (C-Motion, Germantown, MD) software:

$$P_j = M_j \omega_j \qquad \qquad [1]$$

where P_j is the muscle power at the joint, j, M_j is the net muscle moment about the joint (in Nm), and ω_j is the joint angular velocity (in rad/s). Muscle power is the time rate that the muscles about a joint perform mechanical work. Mechanical work done by the muscles about each joint was calculated by integrating the muscle power curves for the joints using Equation 2:

$$W_j = \int P_j \, dt \qquad \qquad [2]$$

where W_j is the mechanical work performed by the muscles about a joint, j, and P_j is the instantaneous muscle power at that joint.

Joint power curves yield periods of energy absorption (negative power) and generation (positive power). The time integral of the negative and positive power periods for each joint yields the eccentric and concentric work, respectively, for that joint. Total stance and swing phase eccentric and concentric work for each joint was defined as the sum of the respective eccentric and concentric joint work periods throughout the stance and swing phases, respectively. Total eccentric and concentric work at each joint was calculated by summing the stance and swing phase total eccentric and concentric work. Total work at each joint was then calculated by summing the absolute values of the total eccentric and concentric joint work. Total work of the lower extremity was calculated by summing the total work from each joint.

8.3.4 Statistical Analysis

This research was designed to determine the influence of group, leg, and running velocity on lower extremity mechanical energy. Statistical comparisons were performed in SPSS 19.0 (SPSS Inc.). A 2x2x3 three factor repeated measures analysis of variance (ANOVA) was used to identify statistical differences between the dependent variables using Group (ILEA and Control), Leg (prosthetic/intact and left/right), and Velocity (2.5 m/s, 3.0 m/s, 3.5 m/s) as independent variables (IVs). Group was treated as a between-subjects variable while Leg and Velocity were treated as within-subjects variables. When significant differences were identified from the full factorial model, two-way ANOVAs and pair-wise comparisons with

Bonferroni adjustments for multiple comparisons were used when appropriate to determine which conditions were significantly different from each other. Significance for all statistical tests were set at $\alpha = 0.05$.

8.4 Results

No differences existed between the left and right control limbs for any variable, so these data were averaged to generate a representative control limb for clearer presentation in the tables and figures. However, all statistical outcomes were based on the balanced statistical design that included both control limbs. Figure 8.2 shows the joint power profiles for the ankle, knee, and hip normalized to body weight and to the gait cycle for each of the three running velocities. Peak joint power data are presented in Table 8.1.

8.4.1 Ankle Powers

The ankle joint produced negligible mechanical energy during the swing phase, so these data were not presented. Significant velocity effects were present ($p<0.001$) where each limb increased peak power with velocity ($p\leq0.028$ for all). Ankle work increased with velocity for all limbs except for the prosthetic "ankle". Significant leg x group interactions existed for all ankle mechanical energy variables ($p<0.001$) where the ILEA group limbs had greater differences than the control group limbs. Significant velocity x group ($p=0.002$) and velocity x leg ($p=0.006$) interactions existed for peak ankle power generation. The control group peak ankle power generation increased at a greater rate than the ILEA group. The intact and
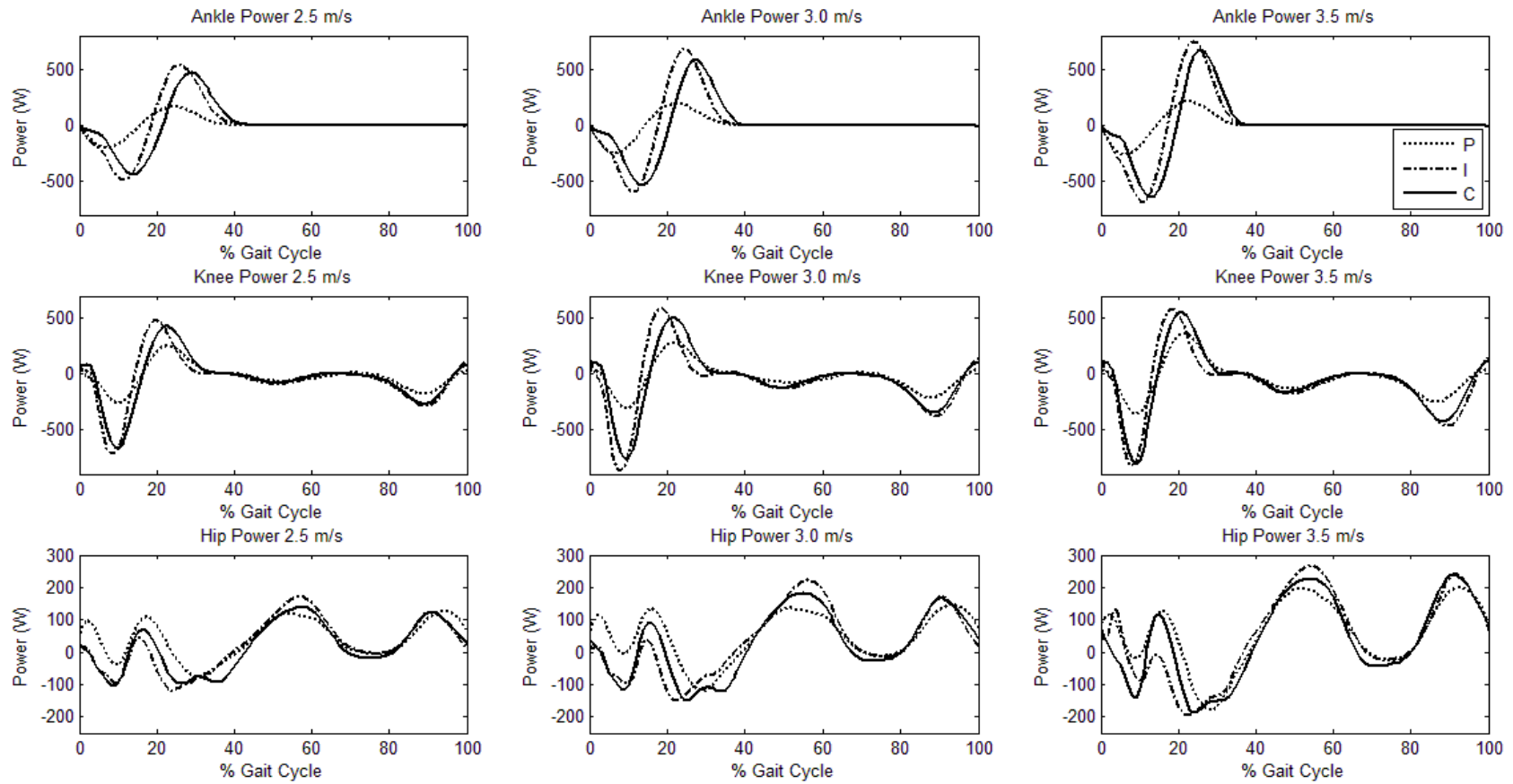
Figure 8.2. Average ankle, knee, and hip powers for the prosthetic (P), intact (I) and combined control (C) limbs across running velocities normalized to body mass and to the gait cycle. Positive values indicate power generation and negative values indicate power absorption.

Table 8.1. Average (standard deviation) lower extremity peak power values, in Watts, for the prosthetic, (P), intact (I), and control (C) limbs across each of the tested velocities. White areas indicate stance phase powers and grey areas indicate swing phase powers.

	2.5 m/s			3.0 m/s			3.5 m/s		
	P	I	C	P	I	C	P	I	C
Ankle Abs[v]	-198* (95)	-530 (111)	-445 (101)	-258* (152)	-646 (114)	-555 (129)	-261* (126)	-781 (243)	-671 (125)
Ankle Gen[v]	184* (83)	608 (133)	492 (102)	220* (115)	726 (123)	609 (122)	238* (111)	828 (155)	722 (127)
Knee Abs[v]	-264* (163)	-765 (234)	-680 (142)	-314* (191)	-902 (329)	-773 (167)	-367* (222)	-855 (350)	-824 (146)
Knee Gen[v]	264* (165)	537 (230)	447 (113)	317* (173)	621 (275)	517 (145)	395* (229)	637 (239)	574 (136)
Knee Abs[v]	-198* (56)	-301 (129)	-278 (48)	-240* (66)	-391 (153)	-354 (58)	-292* (83)	-490 (180)	-437 (65)
Hip Abs[v]	-106[i] (68)	-213[c] (79)	-152 (37)	-144[i] (69)	-221 (118)	-196 (62)	-190 (136)	-259 (122)	-235 (71)
Hip Gen[v]	176 (95)	120 (71)	80 (44)	213 (99)	138 (118)	115 (45)	224 (102)	209 (192)	155 (54)
Hip Abs[v]	-35 (27)	-34 (35)	-47 (25)	-37 (25)	-42 (32)	-39 (22)	-48 (19)	-44 (21)	-53 (19)
Hip Gen[v]	161 (59)	197[c] (53)	157 (21)	183[i] (54)	256 (61)	212 (48)	251[i] (66)	320 (63)	278 (37)

Abs = power absorption

Gen = power generation

v = significant (p<0.05) velocity effect

* = prosthetic limb significantly differs from intact and control limbs

i = significant difference between prosthetic and intact limb

c = significant difference between intact and control limb

183

control limbs each increased peak power generation at a greater rate with velocity than the prosthetic limb.

8.4.2 Knee Powers

Significant velocity effects were present (p<0.001) where each limb increased peak power absorption and generation with velocity (p≤0.022 for all). Significant leg x group interactions existed for all three peak knee power variables (p≤0.007) where the ILEA group limbs had greater differences than the control group limbs. Significant velocity x leg interactions existed for peak knee power absorption in stance (p=0.042) and swing (p=0.001), but not for stance generation (p=0.120). During swing phase, the intact and control limbs both increased peak knee power absorption with velocity at a greater rate than the prosthetic limb knee. The intact limb knee power stance absorption had a quadratic relationship with velocity (peak at 3.0 m/s) while the prosthetic and control limb knee absorption peaks increased with velocity.

8.4.3 Hip Powers

Significant velocity effects were present (p≤0.015). Peak hip stance power absorption and generation increased with velocity for the prosthetic (p≤0.033) and control limbs (p≤0.012) but not the intact limb. Peak hip swing power absorption increased with velocity for all limbs (p≤0.001) but peak swing power generation only increased with velocity for the control limbs (p=0.006). Significant leg x group interactions existed for peak hip stance absorption (p=0.0227) and swing generation
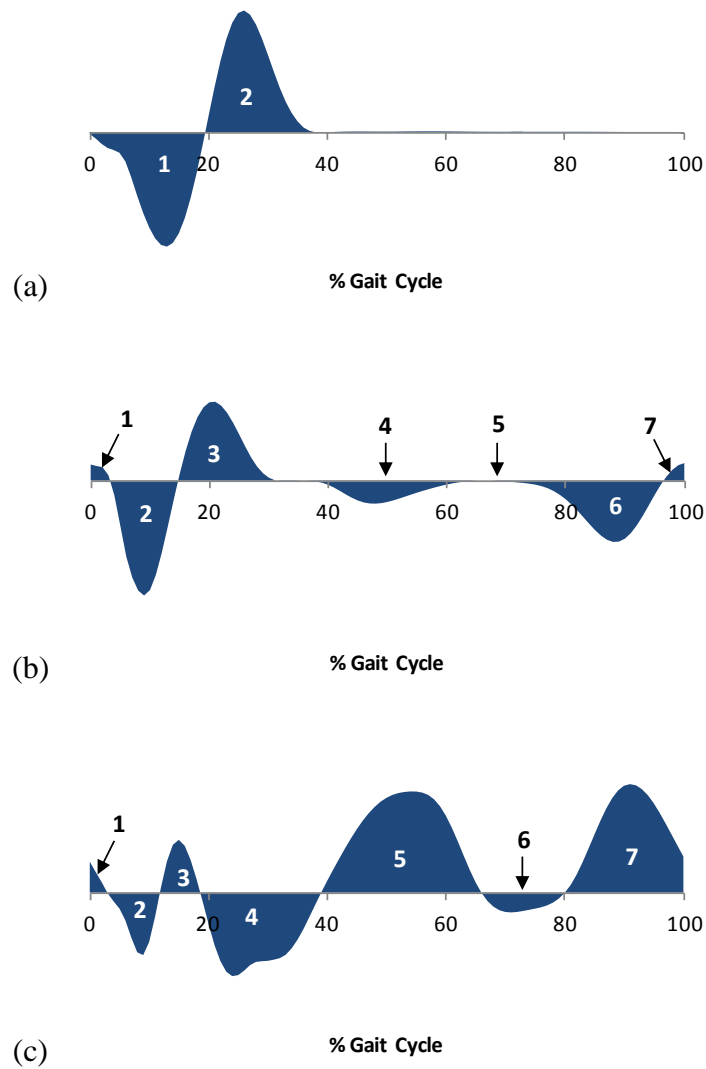
Figure 8.3. Periods of joint mechanical work for the (a) hip, (b) knee, and (c) ankle.

(p=0.04) where the ILEA group limbs had greater differences than the control group limbs. No other significant interactions existed for hip power variables.

8.4.4 Joint Work

Figure 8.3 highlights the periods of joint work with respect to the power curves and Table 8.2 presents the stance and swing phase joint work performed by

Table 8.2. Average (standard deviation) lower extremity joint mechanical work, in J, for the prosthetic (P), intact (I), and control (C) limbs across each of the tested velocities. White areas indicate stance work periods and grey areas indicate swing phase work periods.

	Period	2.5 m/s P		2.5 m/s I		2.5 m/s C		3.0 m/s P		3.0 m/s I		3.0 m/s C		3.5 m/s P		3.5 m/s I		3.5 m/s C	
Ankle Work																			
Ecc p-flexor[v]	A1	-14.4*	(6.8)	-39.3	(11.5)	-37.5	(9.8)	-16.6*	(9.0)	-43.2	(10.6)	-42.5	(11.1)	-16.2*	(8.4)	-48.1	(15.6)	-47.6	(11.2)
Con p-flexor[v]	A2	16.1*	(7.3)	46.9	(10.4)	41.6	(5.9)	17.8*	(8.9)	49.8	(8.5)	44.8	(7.0)	17.8*	(8.3)	52.2	(9.7)	47.5	(8.1)
Knee Work																			
Con flexor	K1	0.8	(0.5)	1.7	(2.4)	2.7	(1.0)	1.1	(0.8)	2.0	(2.4)	2.9	(1.1)	0.9	(0.7)	2.4	(2.6)	2.7	(1.5)
Ecc extensor	K2	-15.5*	(9.7)	-39.9	(16.7)	-40.7	(8.1)	-17.6*	(11.7)	-43.5	(19.0)	-42.2	(9.1)	-19.0*	(11.9)	-38.5	(19.8)	-42.0	(8.5)
Con extensor	K3	19.9	(12.0)	33.5	(17.5)	33.4	(7.6)	21.7	(12.5)	35.5	(17.3)	35.9	(8.9)	25.1	(15.5)	34.3	(14.8)	37.0	(8.6)
Ecc extensor[v]	K4	-8.0	(3.5)	-9.2	(3.0)	-7.0	(2.2)	-10.1	(5.0)	-12.1	(5.1)	-10.7	(4.0)	-11.9	(8.0)	-16.4	(7.5)	-15.2	(7.0)
Con extensor	K5	0.7	(0.6)	0.2	(0.2)	0.3	(0.2)	0.9	(0.9)	0.4	(0.5)	0.2	(0.1)	0.7	(1.0)	0.4	(0.4)	0.2	(0.2)
Ecc flexor[v]	K6	-16.2*	(5.1)	-26.4	(9.7)	-26.0	(3.8)	-18.9*	(6.5)	-34.4	(11.4)	-33.0	(5.1)	-26.0*	(7.4)	-41.3	(11.7)	-38.8	(4.1)
Con flexor[v]	K7	0.7*	(0.6)	2.2	(1.4)	1.8	(1.2)	1.0*	(0.8)	2.8	(1.8)	2.3	(1.3)	1.1[i]	(0.9)	2.6	(2.1)	2.4	(1.6)
Hip Work																			
Con extensor[v]	H1	2.3*	(1.7)	1.9[c]	(2.9)	0.4	(0.2)	1.8*	(1.0)	4.1[c]	(4.6)	0.8	(0.6)	2.1[i]	(1.2)	5.4[c]	(8.3)	1.5	(1.4)
Ecc extensor	H2	-3.7[i]	(2.7)	-6.9	(3.1)	-5.4	(2.7)	-3.8[i]	(2.2)	-6.7	(4.8)	-5.7	(2.8)	-4.0	(2.9)	-5.0	(3.4)	-6.2	(3.3)
Con extensor	H3	9.9	(7.0)	5.0	(3.2)	3.8	(2.6)	13.4	(8.5)	3.7	(4.3)	4.5	(2.9)	12.4	(7.3)	5.7	(5.4)	5.3	(3.6)
Ecc flexor[v]	H4	-7.4	(7.5)	-13.5	(10.1)	-13.6	(6.3)	-11.0	(8.7)	-15.5	(12.3)	-17.0	(7.6)	-15.1	(14.7)	-22.5	(11.8)	-19.4	(6.8)
Con flexor[v]	H5	17.1[i]	(6.0)	22.2	(6.2)	18.0	(3.5)	20.6[i]	(6.1)	28.1	(7.4)	24.1	(5.5)	26.9[i]	(7.9)	34.0	(6.6)	29.6	(5.3)
Ecc extensor[v]	H6	-1.2	(1.2)	-1.2	(1.1)	-1.5	(0.8)	-1.4	(1.5)	-1.3	(1.0)	-2.1	(0.9)	-2.4	(1.4)	-1.9	(1.0)	-3.6	(1.7)
Con extensor[v]	H7	12.2	(4.7)	11.8	(6.3)	11.5	(1.8)	14.4	(5.4)	14.4	(9.0)	15.7	(3.9)	19.0	(6.7)	20.6	(9.7)	23.0	(3.4)

Ecc = eccentric work; Con = concentric work; p-flexor = plantarflexor

v = significant (p<0.05) velocity effect

* = prosthetic limb significantly different from intact and control limbs

i = prosthetic limb significantly different from intact limb

c = intact limb significantly different from control limbs
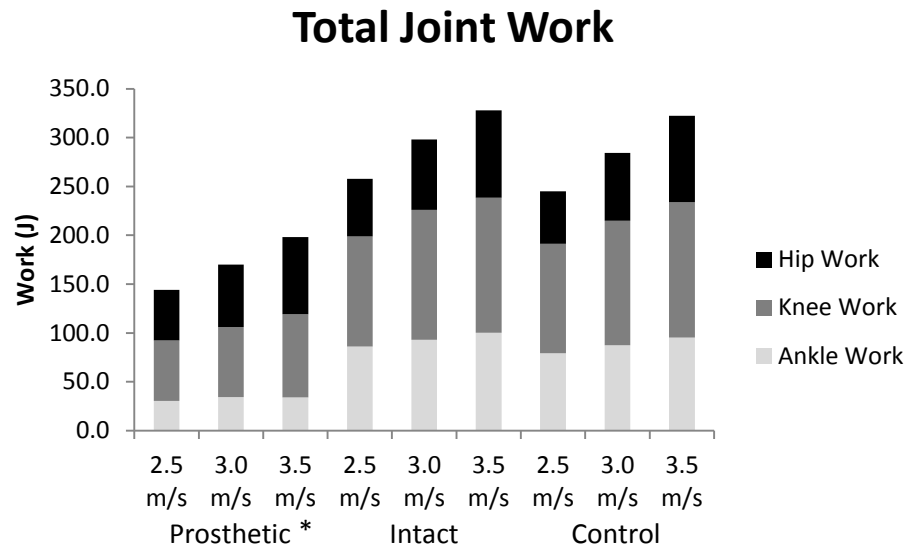
Total Joint Work

Figure 8.4. Total joint work throughout the gait cycle with each joint's contribution for the prosthetic, intact, and averaged control limbs across the tested velocities. * indicates the prosthetic limb significantly differed (p<0.05) from the intact and control limbs at all velocities. Significant velocity effects existed for each limb.

each limb across velocities. Total joint work throughout the gait cycle and total stance and swing phase work are shown in Figures 8.4-8.5. Stance and swing phase eccentric and concentric mechanical energy for each limb across velocities are shown in Figures 8.6-8.7. The control group showed significant velocity effects for ankle concentric work (p≤0.048) but neither total knee nor hip concentric energy changed with velocity. ILEA intact limb joints also increased ankle concentric work (p=0.025) but did not change knee and hip concentric work with velocity increases. The prosthetic ankle concentric work did not change (p=0.152), but the knee (p=0.042) and hip (p=0.015) concentric work increased with velocity. All limbs increased their total joint stance work with velocity (p≤0.013 for all).

Total Stance and Swing Phase Work
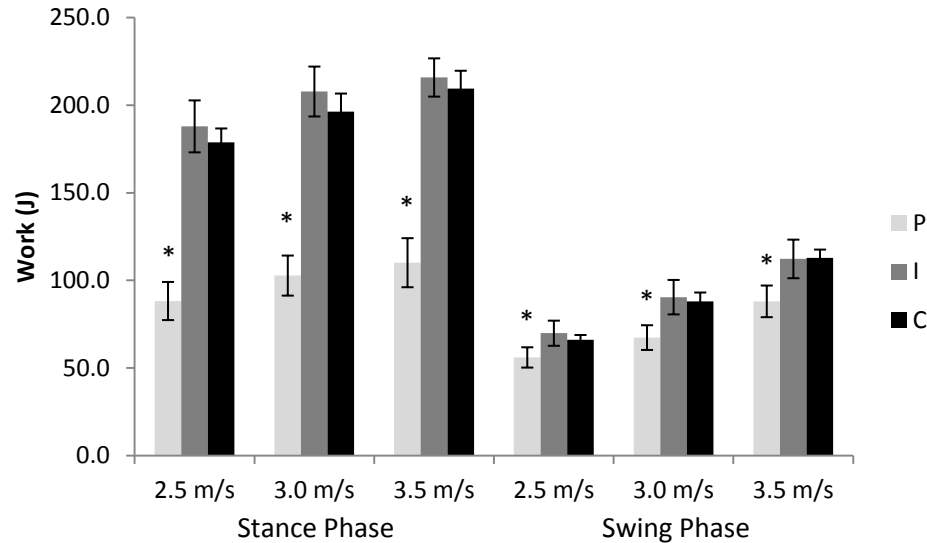
Figure 8.5. Total joint work during running stance and swing phase for the prosthetic (P), intact (I), and averaged control (C) limbs across the tested velocities. Error bars represent ±1 standard error. * indicates the prosthetic limb significantly differed (p<0.05) from the intact and control limbs. Significant velocity effects existed for each limb.

During swing phase, all limbs increased knee eccentric and hip concentric energy with velocity (p<0.001 for all). Knee concentric energy during swing increased with velocity only for the intact limb (p=0.001), and swing hip eccentric energy increased with velocity for all limbs (p≤0.020) except for the intact limb (p=0.374).

8.5 Discussion

The joint power and mechanical energy data from the control subjects in this study correspond well with those previously reported during able-bodied running (Czerniecki and Gitter, 1992; Novacheck, 1998b; Winter, 1983b) indicating that the control data validly represent able-bodied running energies. The ankle generates the
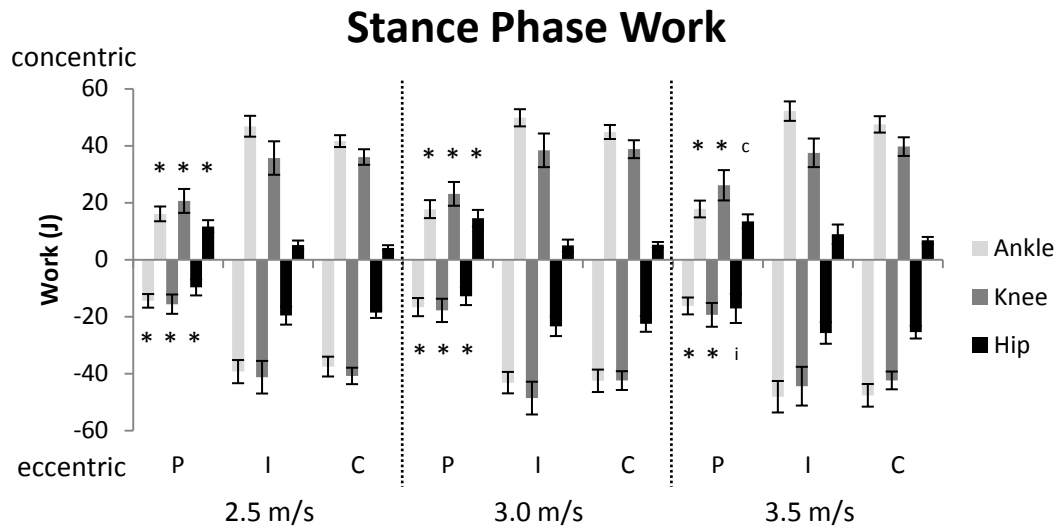
Figure 8.6. Stance phase total concentric (positive) and eccentric (negative) work at each joint for the prosthetic (P), intact (I), and averaged control (C) limbs across the tested velocities. Error bars represent ±1 standard error. * indicates the prosthetic limb significantly differed ($p<0.05$) from the intact and control limbs at the specific velocity. c and i indicate that the prosthetic limb differed only from the control or intact limbs, respectively.

greatest amount of stance phase energy followed by the knee joint musculature. The hip joint generates minimal energy during running stance. The ankle and knee joints share the primary energy absorbing duties during stance while the hip joint absorbs a moderate amount. During swing phase, the ankle joint energy is negligible. The knee musculature performs large amounts of eccentric work to slow shank extension and resist knee hyperextension in the latter half of swing. The hip joint musculature performs large amounts of concentric work first to pull the thigh forward in early swing phase and then to extend the hip joint in the second half of swing.

Mechanical energy changes of ILEA running with RSPs has received little attention (Brüggemann et al., 2009; Buckley, 2000) and no studies to date have examined how joint mechanical energy changes with velocity when using RSPs. The ILEA group running with RSPs demonstrated several differences from the able-

189
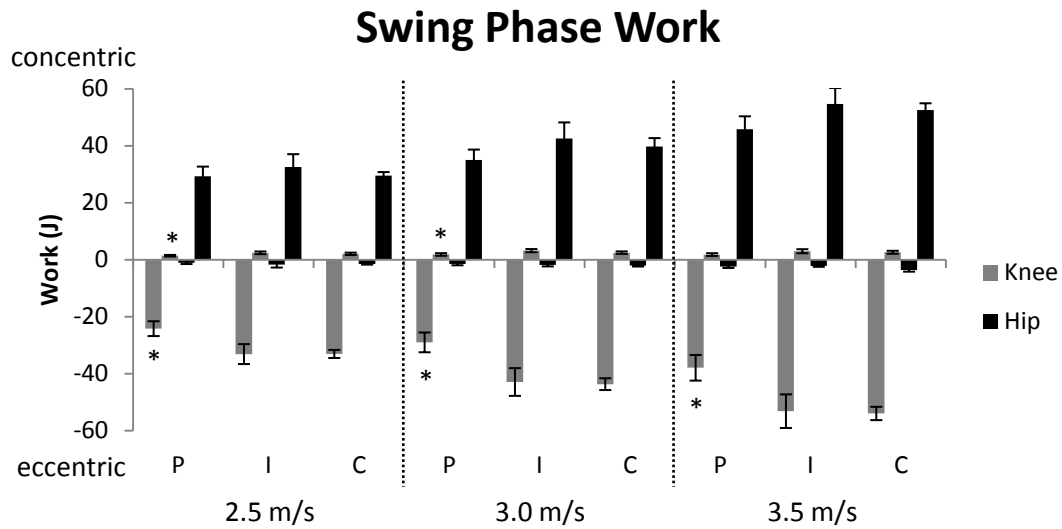
Figure 8.7. Swing phase total concentric (positive) and eccentric (negative) work at the knee and hip joints for the prosthetic (P), intact (I), and averaged control (C) limbs across the tested velocities. Error bars represent ±1 standard error. * indicates the prosthetic limb significantly differed (p<0.05) from the intact and control limbs at the specific velocity. Significant velocity effects existed for knee eccentric work at each limb, for knee concentric work in the intact limb, for hip eccentric work in the prosthetic and control limbs, and for hip concentric work at each limb.

bodied mechanical energy profiles and they also demonstrated mechanical energy differences between the prosthetic and intact limbs. The first hypothesis that ILEA would exhibit lower mechanical energy in the prosthetic limb than the intact and control limbs at each velocity was partially supported and partially rejected. Total work performed by the prosthetic limb (144-198 J at 2.5-3.5 m/s) was nearly half of the total work of the intact limb (257-328 J) and control limbs (245-322 J); this was a function of lower ankle and knee work in the prosthetic limb. However, the prosthetic limb hip joint generated similar amounts of total energy to the intact limb hip. The intact limb total work was similar to the control limbs and the prosthetic limb showed the same work reductions relative to the able-bodied limbs. Examining the concentric and eccentric work profiles of each joint identifies where the reduction in total work

190

occurs. The reduction in total work by the prosthetic limb was due to reductions in the prosthetic limb ankle and knee concentric and eccentric work. The lower prosthetic ankle eccentric and concentric work highlights the limitations of the passive prosthesis in contributing to energy used during running. Similar data were previously reported for two ILEA with unilateral amputations sprinting with RSPs (Buckley, 2000), but an ILEA with bilateral amputations sprinting with RSPs was shown to absorb and generate greater amounts of "ankle" work than able-bodied runners (Brüggemann et al., 2009). Given the dramatic difference between the bilateral RSP data and the consistent results from this study and two other ILEA with unilateral amputations running with RSPs, this could indicate that ILEA with bilateral amputations have significantly different lower extremity mechanical energy profiles. It is also possible that this ILEA with bilateral amputations has learned to apply greater loads to the RSPs out of necessity and subsequently the RSPs return greater amounts of energy.

Lower prosthetic limb knee eccentric and concentric work suggests either greater muscular co-contractions that reduce the net work performed, or that ILEA adapt their running style to use the knee joint more passively (Czerniecki and Gitter, 1992). The prosthetic limb generated greater concentric hip work compared to the intact and control limbs that is consistent with the prolonged hip extension moments observed in ILEA running with RSPs (Buckley, 2000). This has previously been identified as an adaptive mechanism employed by ILEA with unilateral amputations to compensate for the lower energy generated by the prosthetic limb ankle and knee joints (Buckley, 2000; Czerniecki and Gitter, 1992; Czerniecki et al., 1991), and it

appears to be an adaptation that occurs regardless of the type of prosthesis used when running.

The reduction of total work in the prosthetic limb was also influenced by reductions in the swing phase knee and hip work. The swing phase knee eccentric work and hip concentric flexion work were both significantly reduced in the prosthetic limb. This knee eccentric work is produced when the hamstring musculature is activated to slow the knee extension at the end of swing phase. This prepares the limb for footstrike and prevents the knee from hyperextending. The hip concentric flexion work pulls the thigh and lower leg forward in the first half of swing. The reduced inertial properties of the prosthetic lower limb lowers the muscular energetic needs to accelerate the lower extremity during initial swing and decelerate the shank segment at terminal swing. No prior studies of ILEA running with RSPs investigated swing phase dynamics, but runners wearing non-RSPs absorb similar amounts of energy at the knee and hip during swing to able-bodied runners (Czerniecki and Gitter, 1992). The foot+shank segments of non-RSPs have inertial properties greater than those when wearing RSPs and closer to those of intact limbs leading to greater eccentric energy demands than when wearing RSPs. The concentric knee work during swing phase was also reduced in the prosthetic limb compared to both the intact and control limb knees. The knee joint generates minimal concentric energy during swing, but this relative reduction in prosthetic limb knee energy also supports that ILEA may use this knee joint more passively when running.

The second hypothesis that increased running velocity would be associated with similar increases in mechanical energy of the intact and prosthetic limbs was

partially accepted and partially rejected. These results also underscore different strategies used by ILEA and able-bodied subjects to increase running velocity. Velocity effects were evident for a majority of the mechanical energy parameters, but they were not always consistent between the limbs. The control group increased their running velocity by increasing ankle concentric work but the total knee and hip concentric energy did not change with velocity. This highlights the dependence on the ankle joint musculature when running and modulating speed. However, after losing this musculature, ILEA must rely on a passive device and their remaining musculature to change velocity. ILEA intact limb joints followed a similar pattern to the control subjects with increased ankle concentric work and no change in knee and hip concentric work with velocity increases. However, the prosthetic limb produced opposite responses. The prosthetic ankle concentric work did not change, but the knee and hip concentric work increased with velocity. All limbs increased their total joint work with velocity, so ILEA runners must increase the prosthetic limb concentric work with velocity by modulating the only joints they can voluntarily control.

8.6 Conclusions

ILEA running with RSPs generated reduced stance phase work in the prosthetic limb that resulted from reduced work at the "ankle" and knee compared to the intact and control limbs. To overcome these reduced energies, ILEA generated more work at the prosthetic limb hip as compared to the intact and control limbs. The prosthetic limb also generated lower swing phase knee eccentric and hip concentric flexion energies that were attributed to the lower inertial properties of the lower extremity with the RSP. To change running velocity, able-bodied runners increased

their ankle concentric work. ILEA increased the intact limb ankle work to increase velocity but also adapted to the lack of prosthetic ankle energy increases by increasing their prosthetic limb knee and hip concentric energy. These adaptations show that the prosthetic limb hip muscles do more work and that ILEA who run may benefit from prosthetic limb hip muscle strengthening. This supports suggestions that ILEA running rehabilitation and training methods should focus on these muscle groups when learning to run with RSPs (Czerniecki and Gitter, 1992; Nolan, 2012).

Chapter 9: Conclusions

The purpose of this dissertation was to characterize changes in kinetics and mechanical energy across a range of running velocities in ILEA wearing running-specific prostheses (RSPs). This was investigated using a series of six experiments, each with a specific aim to complement the overarching objective. Experiments 1 and 2 investigated technical developments for measurement methods and anthropometric properties relevant to studying RSP biomechanics. Experiment 1 described in Chapter 3, examined the effects of marker placement on force and torque estimation proximal to the RSP. Experiment 2 described in Chapter 4, verified the accuracy of a trifilar pendulum method for measuring RSP moments of inertia and presented anthropometric properties for four common RSP designs. The technical developments were successful in providing guidelines and error values for modeling RSPs during biomechanical studies of ILEA running.

Experiments 3-6 described in Chapters 5-8 investigated overground running kinetics and mechanical energy in ILEA wearing RSPs. The series of experiments presented in this dissertation suggest that RSPs did not perform equivalently to intact limbs during running tasks, and as a result, ILEA runners had to adapt their lower extremity kinetic profiles to maintain a particular velocity and to increase velocity. The prosthetic limb typically generated lower peak kinetic parameters and 50% lower total mechanical work than the intact and control limbs, indicating a greater reliance on the intact limb. To counter the prosthetic limb deficiencies, ILEA increased stride frequencies compared to control subjects. Additionally, the prosthetic limb demonstrated prolonged periods of anterior ground reaction force to increase

propulsive impulse and prolonged hip stance phase extension moments that generated increased hip concentric work. ILEA using RSPs increased running velocity by increasing step lengths and reducing stance times. Furthermore, the intact limb increased ankle concentric work and the prosthetic limb increased knee and hip concentric work to increase velocity while able-bodied subjects primarily increased ankle concentric work with velocity.

This dissertation proposed four existing problems within the ILEA running literature, two technical and anthropometric problems and two problems related to running kinetics and energetics. The presented series of experiments successfully addressed each of these issues. Although the problems are not completely solved, the dissertation has improved our understanding of ILEA running kinetics and lessened the severity of each problem. Prior to this dissertation, no validated models existed for ILEA running with RSPs and marker placements placed on RSPs to define the foot models were arbitrary. Chapters 3 and 6 indicated that marker placement and subsequent modelling of the RSPs has little effect on joint kinetic estimations proximal to the prosthesis, but kinetic estimations within the prosthesis architecture were sensitive to marker placement. Limitations in knowledge of RSP inertial properties have also been addressed with this dissertation. Inertial properties of a variety of RSPs were presented along with a method for accurately measuring RSP moments of inertia.

With these improvements to our technical and anthropometric knowledge, problems related to running kinetics and energetics could then be addressed. This dissertation provided the most complete description of ILEA running kinetics and

energetics to date. It has greatly improved our understanding of how ILEA run with RSPs and identified numerous adaptations that ILEA make to ground reaction forces, joint moments, joint power, and mechanical work. This research has also identified numerous topics where additional research is necessary to continue our understanding of ILEA running.

The hypotheses from the running experiments and whether the hypotheses were accepted or rejected are presented according to the experiment number:

Hypothesis 3.1: ILEA running with RSPs would exhibit altered temporal-spatial and GRF profiles compared to a control group running at matched velocities.

Accepted: Multiple differences between ILEA and control subject temporal-spatial and GRF parameters were identified. The intact limbs took shorter steps than both prosthetic and control limbs, ILEA limbs had shorter stance times than control subjects, intact limbs generated significantly greater peak vertical GRFs than both the control and prosthetic limbs, and the prosthetic limb generated lower peak AP propulsive GRFs than the intact and control limbs.

Hypothesis 3.2: ILEA will exhibit greater loading on and propulsion generated by the intact limb compared to the prosthetic limb as indicated by GRF parameters, but differences between limbs would not increase with velocity.

Partially Accepted, Partially Rejected: Greater loading was observed in the intact limb as compared to the prosthetic limb; however, the peak propulsive and vertical GRF variables along with braking impulse all increased at a greater rate with velocity for the intact limb.

Hypothesis 3.3: ILEA will increase running velocity by increasing step frequency and reducing the related temporal parameters.

Accepted: ILEA increased step frequency with velocity. This was primarily achieved by reducing step time as swing time did not change across velocities. Step lengths also increased with velocity indicating that ILEA modulate both step frequency and step length to run faster.

Hypothesis 4.1: The number of markers and their placement on the keel of RSPs would not affect the residual limb joint moment estimations.

Parially Accepted, Partially Rejected: Prosthetic limb stance phase peak knee and hip joint moments did not change due to marker placement or the number of markers placed on the RSP keel. Ankle moments were sensitive to marker placement and the determination of the "ankle" joint location. During swing phase, the peak knee flexion and hip extension moments were also statistically sensitive to marker placement, but the magnitude of the marker model differences was small (≤ 0.03 Nm/kg).

Hypothesis 5.1: ILEA would demonstrate lower peak joint moment magnitudes in the prosthetic limb than the intact and control limbs throughout stance and swing phase at each velocity.

Partially Accepted, Partially Rejected: A majority of lower extremity peak moment variables were significantly lower in the prosthetic limb compared to both the intact and control limbs. However, peak ankle stance plantarflexion, ankle internal rotation

moment, hip stance flexion, and hip swing flexion moments did not support the hypothesis as no difference existed between the limbs.

Hypothesis 5.2:   Increased running velocity would be associated with similar increases in intact and prosthetic limb peak joint moments.

Partially Accepted, Partially Rejected: Intact limb peak hip stance and knee swing flexion moments increased at a greater rate with velocity than they did for the prosthetic limb. No other peak joint moment parameters displayed this relationship.

Hypothesis 6.1: ILEA would exhibit lower mechanical energy in the prosthetic limb than the intact and control limbs at each velocity.

Partially Accepted, Partially Rejected: Total work performed by the prosthetic limb was nearly half of the total work of the intact and control limbs due to lower prosthetic limb "ankle" and knee work. However, the prosthetic limb hip joint generated similar amounts of total energy to the intact and control limbs. The prosthetic limb generated greater concentric hip work compared to the intact and control limbs.

Hypothesis 6.2:   Increased running velocity would be associated with similar increases in mechanical energy of the intact and prosthetic limbs.

Partially Accepted, Partially Rejected: Both limbs demonstrated increases in total joint work with velocity. The control subjects increased running velocity by increasing ankle concentric work while knee and hip energy did not change. ILEA subjects increased the intact limb ankle concentric work in addition to the prosthetic

limb knee and hip concentric work. The intact limb knee and hip work did not change with velocity, nor did the prosthetic limb ankle work.

9.1 Summary of Conclusions

1. The number of markers and their placement on RSP keels does not affect proximal joint kinetic estimations during axial loading.

2. Using a reaction board and trifilar pendulum will allow for reasonably accurate estimations of RSP inertial properties. Errors due to misaligning the RSP's center of mass with the pendulum's axis of rotation by less than 8 cm will result in errors less than those currently accepted for intact limb inertial estimations.

3. ILEA adapt their temporal-spatial and ground reaction force parameters differently than control subjects in order to modulate running velocity. ILEA run with faster step frequencies achieved by reducing stance times. ILEA also generate lower peak AP propulsive GRFs with their prosthetic limb, but they generate positive AP GRFs over a longer period of stance. This allows ILEA to produce AP propulsive impulses equivalent to the intact and control limbs.

4. The number of markers and their placement on RSP keels does not greatly affect proximal joint kinetic estimations during overground running; however, the choice of location for the "ankle" joint does affect the ankle joint kinetic estimations.

5. ILEA intact limbs generate greater knee and hip peak moments than the prosthetic limb suggesting a greater reliance on the intact limb when running. The intact limb did not generate greater moments than the control subjects suggesting the intact limb is not overloaded when running with RSPs. The prosthetic limb demonstrated a

prolonged stance phase hip extension moment that appears to be an adaptive mechanism compensating for reduced RSP function. Increased intact limb hip internal rotation moments and knee valgus moment rates of loading were identified as possible injury risk factors.

6. The prosthetic limb generates reduced stance phase work compared to the intact limb and control limbs. This was due to reduced "ankle" and knee work. ILEA compensated for these reductions by generating more work at the prosthetic limb hip compared to both the intact hip and control hips. ILEA increased running velocity by increasing the intact limb ankle concentric work along with the prosthetic limb knee and hip concentric work. Control subjects increased running velocity by increasing ankle concentric work.

Based on this research, able-bodied runners and ILEA running with RSPs most likely use similar joint control strategies; however, ILEA must retune the control paradigms to adjust to the use of a passive prosthesis, as has been previously suggested (Sanderson and Martin, 1996). Joint moment and power patterns remained similar between the intact and residual joints, and the magnitudes of these variables generally increased with velocity. A majority of the kinetic variables examined in this dissertation demonstrated that while the intact and residual limb joint kinetics differed from each other at a particular velocity, the changes in these variables with velocity were similar. This suggests that joint control had to be retuned to adapt to the different limb properties and function of the prosthesis; however, once retuned, the

control signal could be scaled similarly to achieve a new velocity. Much more work is needed to determine whether this rationale is feasible.

From a performance perspective, RSPs appear to be mechanically disadvantageous on the whole when compared to intact limbs. The prostheses and residual limbs generally produced less mechanical work and power, lower peak moments, and lower ground reaction forces than the intact and control limbs. However, lower mechanical work and energy generation in the prosthetic limb could be perceived as an advantage since less work is done to run at the same velocity. This may also equate to lower metabolic energy needed to run at the same velocity, but more research is needed to confirm this. One advantage that had been previously discussed is that ILEA could achieve unnaturally fast swing times with RSPs; however, at the submaximal velocities tested here, no difference was observed between ILEA and able-bodied limb swing times. Consequently, no such advantage was apparent. ILEA with bilateral amputations could achieve an advantage with RSPs over able-bodied runners by artificially heightening both limbs and therefore be able to unnaturally increase their stride lengths. However, ILEA with unilateral amputations would induce dramatic limb length discrepancy by running with longer RSPs. This would most likely cause asymmetrical running mechanics that would be quite disadvantageous. At the current state of RSP design, I believe that the mechanical disadvantages of running with RSPs outweigh the potential advantages for running performance.

The biomechanical analyses in this dissertation also identify opportunities to improve RSP design to take advantage of areas that could surpass intact limb

function. For example current RSP designs allowed ILEA to generate similar propulsive impulses to the intact and able-bodied limbs despite reductions in peak anterior ground reaction forces. Optimizing RSP design to promote rollover generating a propulsive impulse earlier in the gait cycle could allow for prosthetic limb propulsive impulses to exceed intact limb propulsion. At the same time, this would reduce the braking impulse on the prosthetic limb. As a result, ILEA would slow down less and accelerate more during each step on the prosthetic limb.

As technology improves along with our understanding of biomechanical integration between prostheses and the intact body, it is my hope that prosthesis function will eventually surpass intact limb function. Running with RSPs appears to provide several advantages over running with non-RSPs such as improved propulsive impulses and kinetic asymmetries of lesser magnitudes indicating RSPs perform more similarly to an intact limb than do non-RSPs. Additionally, since non-RSPs are usually designed for walking, the lower stiffness characteristics could cause the non-RSP to "bottom out" during running loads which may increase risk of damage to the prosthesis and increase risk of injury to the runner. It is therefore recommended that, when possible, ILEA use dedicated running prostheses for running activities, whether for recreational exercise or for sport. Unfortunately, lack of insurance coverage and the general cost of RSPs make these prostheses cost prohibitive for many ILEA who may wish to run. Additional research and political support are needed to provide greater access to these and other devices that can improve function, health, and quality of life for individuals with amputation.

9.2 Future Directions

The results from this dissertation have identified a number of kinetic adaptations that ILEA make when running with RSPs. These results can be used to guide additional studies targeted at improving rehabilitation methods and prosthetic designs including investigating injury risks and running performance. The following experiments are suggested as continuations of this dissertation research:

1. Investigating the effects of increasing hip strength on ILEA running performance.

2. Investigating loading rates as injury risk factors in ILEA using RSPs: Ground reaction force, sagittal plane moment, and frontal/coronal plane moment loading rates.

3. Prospective investigations into the mechanisms of running injuries in ILEA.

4. Energy flow analysis in ILEA running with RSPs to identify potential energy transfer mechanisms used as compensatory strategies.

5. Does RSP design influence running biomechanics? Investigating ILEA running biomechanics with different RSP designs.

6. Investigating the effects of RSP alignment on running kinetics to maximize performance and/or to minimize injury risks and joint loading.

9.3 Lessons Learned

A dissertation is a journey full of obstacles and eye opening experiences. I have learned an enormous amount from this research experience and throughout my formal studies in completing the Ph.D. degree. I am convinced that good research requires a team effort to not only reduce the burden of one person trying to accomplish everything, but also to view and solve problems from different points of view. Multiple minds working together creates an atmosphere that enhances analyses and interpretations.

All research endeavors have challenges to overcome, some that are anticipated and others unanticipated. These challenges are not always resolved as quickly as one would like. This series of experiments was not exempt from issues as challenges arose with prosthesis procurement, programming complex analyses, recruiting subjects, and sharing data collection equipment and space. Each problem resulted in unanticipated delays and some creative adaptations. Procuring RSPs for material testing analyses was the first major issue since some of the prosthetic companies were unable to initially sell prostheses to non-prosthetists. These issues were overcome by discussing the research with the companies and developing a research-specific purchase code within the company's ordering system. The complex programming for the material testing analysis in Chapter 3 required many months of development and validation. Examining inverse dynamics results from every possible combination of markers placed on a prosthesis would have taken over one year for each prosthesis, which was impractical. Therefore a solution had to be identified that reduced the number of marker combinations used without affecting the breadth of the study.

Determining an inclusion threshold of marker and prosthesis motion solved this problem so markers under the threshold were considered as part of a greater rigid segment. This reduced the number of included markers in the overall analysis so it could be completed more efficiently without affecting the overall applicability of the data.

Subject recruitment with small populations can be a difficult undertaking, and recruiting subjects with lower extremity amputations who run with RSPs proved to be a much more challenging task than originally anticipated. After distributing flyers and uncountable emails and phone calls to clinics, clinicians, and specialty running and sports groups, I learned that no recruitment method produces results better than meeting with people in person. While several subjects were recruited using the original methods, but taking time to meet with clinicians and clinic staff in their offices generated the most effective subject recruitment results. In the future, whenever possible I aim to go directly to the source of potential subject pools personally and early in the recruitment stage so this issue can be minimized.

An additional major challenge was the sharing of motion capture equipment and data collection space with other lab groups and campus groups. Not having sole access to either equipment or space produced inevitable delays, but also strengthened my organizational skills. I gained a greater appreciation for working under constraints and learned to become as efficient as possible with collecting data.

Some key concepts of my professional development that have been reinforced throughout this learning process include surround yourself with good people when possible, communicate, do not get discouraged when challenges arise, and plan as

best as possible but be ready to adapt. Also, balancing my personal life with work life has become a key element in maintaining my overall happiness and health. Finally, I continue to realize that the more I learn, the less I know. This will continue to motivate me to ask questions and search for answers.

Bibliography

Alexander, R. M. (1992). The Human Machine. New York: Columbia University Press.

Andriacchi, T. P., Koo, S. and Scanlan, S. F. (2009). Gait mechanics influence healthy cartilage morphology and osteoarthritis of the knee. *Journal of Bone and Joint Surgery, American Volume* **91 Suppl 1**, 95-101.

Andriacchi, T. P. and Mündermann, A. (2006). The role of ambulatory mechanics in the initiation and progression of knee osteoarthritis. *Current Opinions in Rheumatology* **18**, 514-8.

Barr, A. E., Siegel, K. L., Danoff, J. V., McGarvey, C. L., Tomasko, A., Sable, I. and Stanhope, S. J. (1992). Biomechanical comparison of the energy-storing capabilities of SACH and Carbon Copy II prosthetic feet during the stance phase of gait in a person with below-knee amputation. *Physical Therapy* **72**, 344-54.

Baum, B. S., Borjian, R., Linberg, A., Koh, K. and Shim, J. K. (2011). Optimization and validation of a biomechanical model for running-specific prostheses. In *15th Annual Meeting of the Gait and Clinical Movement Analysis Society*. Bethesda, MD.

Baum, B. S., Schultz, M. P., Tian, A., Hobara, H., Kwon, H. J. and Shim, J. K. (2012a). Determining the inertial properties of running-specific prostheses. In *Annual Meeting of the American Society of Biomechanics*. Gainesville, FL.

Baum, B. S., Tian, A., Schultz, M. P., Hobara, H., Linberg, A., Wolf, E. J. and Shim, J. K. (2012b). Ground reaction force and temporal-spatial adaptations to running velocity when wearing running-specific prostheses. In *Annual Meeting of the American Society of Biomechanics*. Gainesville, FL.

Belli, A., Kyrolainen, H. and Komi, P. V. (2002). Moment and power of lower limb joints in running. *International Journal of Sports Medicine* **23**, 136-141.

Beyaert, C., Grumillier, C., Martinet, N., Paysant, J. and André, J. M. (2008). Compensatory mechanism involving the knee joint of the intact limb during gait in unilateral below-knee amputees. *Gait & Posture* **28**, 278-84.

Bezodis, I. N., Kerwin, D. G. and Salo, A. I. T. (2008). Lower limb mechanics during the support phase of maximum-velocity spring running. *Medicine and Science in Sports and Exercise* **40**, 707-715.

Brouwer, B. J., Allard, P. and Labelle, H. (1989). Running patterns of juveniles wearing SACH and single-axis foot components. *Archives of Physical Medicine and Rehabilitation* **70**, 128-34.

Brown, M. B., Millard-Stafford, M. L. and Allison, A. R. (2009). Running-specific prostheses permit energy cost similar to nonamputees. *Medicine and Science in Sports and Exercise* **41**, 1080-7.

Brüggemann, G.-P., Arampatzis, A., Emrich, F. and Potthast, W. (2009). Biomechanics of double transtibial amputee sprinting using dedicated sprinting prostheses. *Sports Technology* **1**, 220-227.

Buckley, J. (1999). Sprint kinematics of athletes with lower-limb amputations. *Archives of Physical Medicine and Rehabilitation* **80**, 501-508.

Buckley, J. G. (2000). Biomechanical adaptations of transtibial amputee sprinting in athletes using dedicated prostheses. *Clinical Biomechanics* **15**, 352-358.

Buckley, J. G., Juniper, M. P., Cavagna, G. A., Zelik, K. E., Adamczyk, P. G. and Morin, J.-B. (2010). Comments on Point:Counterpoint: Artificial limbs do/do not make artificially fast running speeds possible. *Journal of Applied Physiology* **108**, 1016-1018.

Burkett, B., Smeathers, J. and Barker, T. (2001). Optimising the trans-femoral prosthetic alignment for running, by lowering the knee joint. *Prosthetics and Orthotics International* **25**, 210-219.

Burkett, B., Smeathers, J. and Barker, T. (2003). Walking and running inter-limb asymmetry for Paralympic trans-femoral amputees, a biomechanical analysis. *Prosthetics and Orthotics International* **27**, 36-47.

Bussmann, J. B., Grootscholten, E. A. and Stam, H. J. (2004). Daily physical activity and heart rate response in people with a unilateral transtibial amputation for vascular disease. *Archives in Physical Medicine and Rehabilitation* **85**, 240-4.

Chandler, R. F., Clauser, C. E., McConville, J. T., Reynolds, H. M. and Young, J. W. (1975). Investigation of the inertial properties of the human body. Ohio: Aerospace Medical Research Laboratories, Wright-Patterson Air Force Base.

Charteris, J. (1999). Effects of velocity on upper to lower extremity muscular work and power output ratios of intercollegiate athletes. *British Journal of Sports Medicine* **33**, 250-4.

Chaudhari, A. M., Briant, P. L., Bevill, S. L., Koo, S. and Andriacchi, T. P. (2008). Knee kinematics, cartilage morphology, and osteoarthritis after ACL injury. *Medicine and Science in Sports and Exercise* **40**, 215-22.

Clauser, C. E., McConville, J. T. and Young, J. W. (1969). Weight, volume and center of mass of segments of the human body. Ohio: Wright-Patterson Air Force Base.

Collins, J. J. and Whittle, M. W. (1989). Influence of gait parameters on the loading of the lower limb. *Journal of Biomedical Engineering* **11**, 409-12.

Czerniecki, J. M. and Gitter, A. (1992). Insights into amputee running. A muscle work analysis. *American Journal of Physical Medicine & Rehabilitation* **71**, 209-18.

Czerniecki, J. M., Gitter, A. J. and Beck, J. C. (1996). Energy transfer mechanisms as a compensatory strategy in below knee amputee runners. *Journal of Biomechanics* **29**, 717-722.

Czerniecki, J. M., Gitter, A. J. and Munro, C. (1991). Joint moment and muscle power output characteristics of below knee amputees during running: the influence of energy storing prosthetic feet. *Journal of Biomechanics* **24**, 63-75.

de Leva, P. (1996). Adjustments to Zatsiorsky-Seluyanov's segment inertia parameters. *Journal of Biomechanics* **29**, 1223-1230.

Dempster, W. T. (1955). Space requirements of the seated operator. Ohio: Wright-Patterson Air Force Base.

DiAngelo, D. J., Winter, D. A., Ghista, D. N. and Newcombe, W. R. (1989). Performance assessment of the Terry Fox jogging prosthesis for above-knee amputees. *Journal of Biomechanics* **22**, 543-58.

Dillman, C. J. (1975). Kinematic analyses of running. *Exercise and Sport Sciences Reviews* **3**, 193-218.

Donker, S. F. and Beek, P. J. (2002). Interlimb coordination in prosthetic walking: effects of asymmetry and walking velocity. *Acta Psychologica* **110**, 265-88.

du Bois, J. L., Lieven, N. a. J. and Adhikari, S. (2008). Error Analysis in Trifilar Inertia Measurements. *Experimental Mechanics* **49**, 533-540.

Dyer, B., Noroozi, S. and Redwood, S. (2010). The design of lower-limb sports prostheses: fair inclusion in disability sport. *Disability & Society* **25**, 593-602.

Edelstein, J. E. (1988). Prosthetic feet. State of the Art. *Physical Therapy* **68**, 1874-81.

Ehde, D. M., Smith, D. G., Czerniecki, J. M., Campbell, K. M., Malchow, D. M. and Robinson, L. R. (2001). Back pain as a secondary disability in persons with lower limb amputations. *Archives of Physical Medicine and Rehabilitation* **82**, 731-4.

Enoka, R. M., Miller, D. I. and Burgess, E. M. (1982). Below-knee amputee running gait. *American Journal of Physical Medicine* **61**, 66-84.

Feinglass, J., Brown, J. L., LoSasso, A., Sohn, M. W., Manheim, L. M., Shah, S. J. and Pearce, W. H. (1999). Rates of lower-extremity amputation and arterial

reconstruction in the United States, 1979 to 1996. *American Journal of Public Health* **89**, 1222-7.

Ferris, D. P., Louie, M. and Farley, C. T. (1998). Running in the real world : adjusting leg stiffness for different surfaces. *Proceedings, Biological Sciences / the Royal Society* **265**, 989-994.

Fey, N. P., Klute, G. K. and Neptune, R. R. (2011). The influence of energy storage and return foot stiffness on walking mechanics and muscle activity in below-knee amputees. *Clinical Biomechanics* **26**, 1025-32.

Friel, K. (2005). Componentry for lower extremity prostheses. *Journal of the American Academy of Orthopaedic Surgery* **13**, 326-35.

Gailey, R. (2003). Optimizing prosthetic running performance of the transtibial amputee. In *AOPA Annual Meeting*.

Genta, G. and Delprete, C. (1994). Some considerations on the experimental determination of moments of inertia. *Meccanica* **29**, 125-141.

Gitter, A., Czerniecki, J. M. and DeGroot, D. M. (1991). Biomechanical analysis of the influence of prosthetic feet on below-knee amputee walking. *American Journal of Physical Medicine and Rehabilitation* **70**, 142-8.

Goldberg, E. J., Requejo, P. S. and Fowler, E. G. (2008). The effect of direct measurement versus cadaver estimates of anthropometry in the calculation of joint moments during above-knee prosthetic gait in pediatrics. *Journal of Biomechanics* **41**, 695-700.

Gottschall, J. S. and Kram, R. (2005). Ground reaction forces during downhill and uphill running. *Journal of Biomechanics* **38**, 445-52.

Goujon, H., Bonnet, X., Sautreuil, P., Maurisset, M., Darmon, L., Fode, P. and Lavaste, F. (2006). A functional evaluation of prosthetic foot kinematics during lower-limb amputee gait. *Prosthetics and Orthotics International* **30**, 213-223.

Grabowski, A. M., McGowan, C. P., McDermott, W. J., Beale, M. T., Kram, R. and Herr, H. M. (2010). Running-specific prostheses limit ground-force during sprinting. *Biology Letters* **6**, 201-4.

Graham, L. E., Datta, D., Heller, B., Howitt, J. and Pros, D. (2007). A comparative study of conventional and energy-storing prosthetic feet in high-functioning transfemoral amputees. *Archives of Physical Medicine and Rehabilitation* **88**, 801-6.

Groves, W. H. (1950). Mechanical analysis of diving. *Research Quarterly* **21**, 132-144.

Grumillier, C., Martinet, N., Paysant, J., André, J. M. and Beyaert, C. (2008). Compensatory mechanism involving the hip joint of the intact limb during gait in unilateral trans-tibial amputees. *Journal of Biomechanics* **41**, 2926-31.

Hafner, B. J., Sanders, J. E., Czerniecki, J. M. and Fergason, J. (2002). Transtibial energy-storage-and-return prosthetic devices: a review of energy concepts and a proposed nomenclature. *Journal of Rehabilitation Research and Development* **39**, 1-11.

Han, T. R., Chung, S. G. and Shin, H. I. (2003). Gait patterns of transtibial amputee patients walking indoors barefoot. *American Journal of Physical Medicine and Rehabilitation* **82**, 96-100.

Hanavan, E. P. (1964). A mathematical model of the human body. AMRL-TR-64-102., pp. 1-149.

Hansen, A. H., Childress, D. S., Miff, S. C., Gard, S. a. and Mesplay, K. P. (2004). The human ankle during walking: implications for design of biomimetic ankle prostheses. *Journal of Biomechanics* **37**, 1467-74.

Hay, J. G. (1985). The Biomechanics of Sports Techniques. Englewood Cliffs, New Jersey: Prentice-Hall.

Hay, J. G. (1993). The Biomechanics of Sports Techniques. Englewood Cliffs, N.J.: Prentice-Hall.

Heiderscheit, B. C., Chumanov, E. S., Michalski, M. P., Wille, C. M. and Ryan, M. B. (2011). Effects of step rate manipulation on joint mechanics during running. *Medicine and Science in Sports and Exercise* **43**, 296-302.

Hillery, S. C., Wallace, E. S., McIhagger, R. and Watson, P. (1997). The effect of changing the inertia of a trans-tibial dynamic elastic response prosthesis on the kinematics and ground reaction force patterns. *Prosthetics and Orthotics International* **21**, 114-123.

Hobara, H., Tominaga, S., Umezawa, S., Iwashita, K., Okino, A., Saito, T., Usui, F. and Ogata, T. (In Press). Leg stiffness and sprint ability in amputee sprinters. *Prosthetics and Orthotics International*.

Hreljac, A. (2004). Impact and overuse injuries in runners. *Medicine and Science in Sports and Exercise* **36**, 845-9.

Hreljac, A. (2005). Etiology, prevention, and early intervention of overuse injuries in runners: a biomechanical perspective. *Physical Medicine and Rehabilitation Clinics of North America* **16**, 651-67, vi.

Hreljac, A., Marshall, R. N. and Hume, P. A. (2000). Evaluation of lower extremity overuse injury potential in runners. *Medicine and Science in Sports and Exercise* **32**, 1635-41.

Hsu, M. J., Nielsen, D. H., Yack, H. J. and Shurr, D. G. (1999). Physiological measurements of walking and running in people with transtibial amputations with 3 different prostheses. *The Journal of Orthopaedic and Sports Physical Therapy* **29**, 526-33.

Hunter, J. P., Marshall, R. N. and McNair, P. J. (2004). Interaction of step length and step rate during sprint running. *Medicine and Science in Sports and Exercise* **36**, 261-71.

Isakov, E., Burger, H., Krajnik, J., Gregoric, M. and Marincek, C. (1996). Influence of speed on gait parameters and on symmetry in trans-tibial amputees. *Prosthetics and Orthotics International* **20**, 153-158.

Jacobs, R., Bobbert, M. F. and van Ingen Schenau, G. J. (1993). Function of mono- and biarticular muscles in running. *Medicine and Science in Sports and Exercise* **25**, 1163-73.

Jacobs, R., Bobbert, M. F. and van Ingen Schenau, G. J. (1996). Mechanical output from individual muscles during explosive leg extensions: the role of biarticular muscles. *Journal of Biomechanics* **29**, 513-23.

Jacobs, S. J. and Berson, B. L. (1986). Injuries to runners: a study of entrants to a 10,000 meter race. *American Journal of Sports Medicine* **14**, 151-5.

Johnson, M. D. and Buckley, J. G. (2001). Muscle power patterns in the mid-acceleration phase of sprinting. *Journal of Sports Sciences* **19**, 263-272.

Kavanagh, T. (1983). Exercise and the heart. *Annals of the Academy of Medicine Singapore* **12**, 331-7.

Kegel, B. (1985). Physical fitness. Sports and recreation for those with lower limb amputation or impairment. *Journal of Rehabilitation Research and Development. Clinical S*, 1-125.

Kegel, B., Carpenter, M. L. and Burgess, E. M. (1978). Functional capabilities of lower extremity amputees. *Archives of Physical Medicine and Rehabilitation* **59**, 109-20.

Keller, T. S., Weisberger, A. M., Ray, J. L., Hasan, S. S., Shiavi, R. G. and Spengler, D. M. (1996). Relationship between vertical ground reaction force and speed during walking, slow jogging, and running. *Clinical Biomechanics* **11**, 253-259.

Kingma, I., Toussaint, H. M., De Looze, M. P. and Van Dieen, J. H. (1996). Segment inertial parameter evaluation in two anthropometric models by application of a dynamic linked segment model. *Journal of Biomechanics* **29**, 693-704.

Kivi, D. M. R., Maraj, B. K. V. and Gervais, P. (2002). A kinematic analysis of high-speed treadmill sprinting over a range of velocities. *Medicine and Science in Sports and Exercise* **34**, 662-662.

Klute, G. K., Berge, J. S. and Segal, A. D. (2004). Heel-region properties of prosthetic feet and shoes. *Journal of Rehabilitation Research and Development* **41**, 535-46.

Kram, R., Grabowski, A. M., McGowan, C. P., Brown, M. B. and Herr, H. M. (2010). Counterpoint: Artificial legs do not make artificially fast running speeds possible. *Journal of Applied Physiology* **108**, 1012-4; discussion 1014; author reply 1020.

Kulkarni, J., Gaine, W. J., Buckley, J. G., Rankine, J. J. and Adams, J. (2005). Chronic low back pain in traumatic lower limb amputees. *Clinical Rehabilitation* **19**, 81-6.

Laferrier, J. Z. and Gailey, R. (2010). Advances in Lower-limb Prosthetic Technology. *Physical Medicine and Rehabilitation Clinics of North America* **21**, 87-110.

Lechler, K. (2005). Lower-limb prosthetics − Design improvements of a prosthetic spring foot. In *American Academy of Orthotics and Prosthetics*.

Lechler, K. and Lilja, M. (2008). Lower extremity leg amputation: an advantage in running? *Sports Technology* **1**, 229-234.

Lee, S. S. M. and Piazza, S. J. (2009). Built for speed: musculoskeletal structure and sprinting ability. *The Journal of Experimental Biology* **212**, 3700-7.

Lehmann, J. F., Price, R., Okumura, R., Questad, K., de Lateur, B. J. and Négretot, A. (1998). Mass and mass distribution of below-knee prostheses: effect on gait efficacy and self-selected walking speed. *Archives of Physical Medicine and Rehabilitation* **79**, 162-8.

Lloyd, C. H., Stanhope, S. J., Davis, I. S. and Royer, T. D. (2010). Strength asymmetry and osteoarthritis risk factors in unilateral trans-tibial, amputee gait. *Gait & Posture* **32**, 296-300.

Lysholm, J. and Wiklander, J. (1987). Injuries in runners. *American Journal of Sports Medicine* **15**, 168-71.

Macera, C. A., Pate, R. R., Powell, K. E., Jackson, K. L., Kendrick, J. S. and Craven, T. E. (1989). Predicting lower-extremity injuries among habitual runners. *Archives of Internal Medicine* **149**, 2565-8.

Mann, R. A. and Hagy, J. (1980). Biomechanics of walking, running, and sprinting. *American Journal of Sports Medicine* **8**, 345-50.

Marti, B., Vader, J. P., Minder, C. E. and Abelin, T. (1988). On the epidemiology of running injuries. The 1984 Bern Grand-Prix study. *American Journal of Sports Medicine* **16**, 285-94.

Martin, P. E., Mungiole, M., Marzke, M. W. and Longhill, J. M. (1989). The use of magnetic resonance imaging for measuring segment inertial properties. *Journal of Biomechanics* **22**, 367-76.

Mattes, S. J., Martin, P. E. and Royer, T. D. (2000). Walking symmetry and energy cost in persons with unilateral transtibial amputations: Matching prosthetic and intact limb inertial properties. *Archives of Physical Medicine and Rehabilitation* **81**, 561-568.

Mayfield, J. A., Reiber, G. E., Maynard, C., Czerniecki, J. M., Caps, M. T. and Sangeorzan, B. J. (2000). Trends in lower limb amputation in the Veterans Health Administration, 1989-1998. *Journal of Rehabilitation Research and Development* **37**, 23-30.

McIntosh, P. C. and Hayley, H. W. B. (1952). An investigation into the running long jump. *Journal of Physical Education* **44**, 105-108.

Mensch, G. and Ellis, P. E. (1986). Running patterns of transfemoral amputees: a clinical analysis. *Prosthetics and Orthotics International* **10**, 129-34.

Messier, S. P., Davis, S. E., Curl, W. W., Lowery, R. B. and Pack, R. J. (1991). Etiologic factors associated with patellofemoral pain in runners. *Medicine and Science in Sports and Exercise* **23**, 1008-15.

Michaud, S. B., Gard, S. A. and Childress, D. S. (2000). A preliminary investigation of pelvic obliquity patterns during gait in persons with transtibial and transfemoral amputation. *Journal of Rehabilitation Research and Development* **37**, 1-10.

Miller, D. I. (1987). Resultant lower extremity joint moments in below-knee amputees during running stance. *Journal of Biomechanics* **20**, 529-41.

Milner, C. E., Ferber, R., Pollard, C. D., Hamill, J. and Davis, I. S. (2006). Biomechanical factors associated with tibial stress fracture in female runners. *Medicine and Science in Sports and Exercise* **38**, 323-8.

Mokha, M. and Conrey, R. (2007). Proshtetic devices and performance enhancement. *Athletic Therapy Today* **12**, 44-45.

Mungiole, M. and Martin, P. E. (1990). Estimating segment inertial properties: comparison of magnetic resonance imaging with existing methods. *Journal of Biomechanics* **23**, 1039-46.

Munro, C. F., Miller, D. I. and Fuglevand, A. J. (1987). Ground reaction forces in running: a reexamination. *Journal of Biomechanics* **20**, 147-55.

Naschitz, J. E. and Lenger, R. (2008). Why traumatic leg amputees are at increased risk for cardiovascular diseases. *QJM* **101**, 251-9.

Nielsen, D., Shurr, D., Golden, J. and Meier, K. (1989). Comparison of energy cost and gait efficiency during ambulation in below-knee amputees using different prosthetic feet--a preliminary report. *Journal of Prosthetics and Orthotics* **1**, 24-31.

Nigg, B. M., Denoth, J. and Neukomm, P. A. (1981). Quantifying the load on the human body: problems and some possible solutions. In *Biomechanics VII-B*, (ed. f. K. Morecki A, Kedzior K, et al.), pp. 88-99. Baltimore, MD: University Park.

Nilsson, J. and Thorstensson, A. (1989). Ground reaction forces at different speeds of human walking and running. *Acta Physiologica Scandinavica* **136**, 217-27.

Nolan, L. (2008). Carbon fibre prostheses and running in amputees: A review. *Foot and Ankle Surgery* **14**, 125-129.

Nolan, L. (2012). A training programme to improve hip strength in persons with lower limb amputation. *Journal of Rehabilitation Medicine* **44**, 241-8.

Nolan, L. and Lees, A. (2000a). The functional demands on the intact limb during walking for active trans-femoral and trans-tibial amputees. *Prosthetics and Orthotics International* **24**, 117-125.

Nolan, L. and Lees, A. (2000b). Touch-down and take-off characteristics of the long jump performance of world level above- and below-knee amputee athletes. *Ergonomics* **43**, 1637-50.

Nolan, L. and Lees, A. (2007). The influence of lower limb amputation level on the approach in the amputee long jump. *Journal of Sports Sciences* **25**, 393-401.

Nolan, L., Patritti, B. and Simpson, K. (2006). A biomechanical analysis of the long-jump technique of elite female amputee athletes. *Medicine and Science in Sports and Exercise* **38**, 1829-1835.

Nolan, L. and Patritti, B. L. (2008). The take-off phase in transtibial amputee high jump. *Prosthetics and Orthotics International* **32**, 160-71.

Nolan, L., Wit, A., Dudziñski, K., Lees, A., Lake, M. and Wychowañski, M. (2003). Adjustments in gait symmetry with walking speed in trans-femoral and trans-tibial amputees. *Gait & Posture* **17**, 142-51.

Norvell, D. C., Czerniecki, J. M., Reiber, G. E., Maynard, C., Pecoraro, J. A. and Weiss, N. S. (2005). The prevalence of knee pain and symptomatic knee osteoarthritis among veteran traumatic amputees and nonamputees. *Archives of Physical Medicine and Rehabilitation* **86**, 487-93.

Novacheck, T. F. (1995). Walking, running, and sprinting: a three-dimensional analysis of kinematics and kinetics. *Instructional Course Lecture* **44**, 497-506.

Novacheck, T. F. (1998a). Running injuries: a biomechanical approach. *Instructional Course Lecture* **47**, 397-406.

Novacheck, T. F. (1998b). The biomechanics of running. *Gait & Posture* **7**, 77-95.

Nyland, J., Snouse, S. L., Anderson, M., Kelly, T. and Sterling, J. C. (2000). Soft tissue injuries to USA paralympians at the 1996 summer games. *Archives of Physical Medicine and Rehabilitation* **81**, 368-73.

Ounpuu, S. (1994). The biomechanics of walking and running. *Clinical Sports Medicine* **13**, 843-63.

Pailler, D., Sautreuil, P., Piera, J.-B., Genty, M. and Goujon, H. (2004). Evolution in prostheses for sprinters with lower-limb amputation. *Annales de Réadaptation et de Médecine Physique* **47**, 374-81.

Payne, A. H. and Blader, F. (1970). A preliminary investigation into the mechanics of the sprint start. *Bulletin of Physical Education* **8**.

Perry, J. (2011). Below-the-knee compared with above-the-knee amputation. *Journal of the American Veterinary Medical Association* **239**, 297-298.

Poirier, P. and Després, J. P. (2001). Exercise in weight management of obesity. *Cardiology Clinics* **19**, 459-70.

Postema, K., Hermens, H., de Vries, J., Koopman, H. and Eisma, W. (1997). Energy storage and release of prosthetic feet, Part 1: biomechanical analysis related to user benefits. *Prosthetics and Orthotics International* **21**, 17-27.

Powers, C. M., Rao, S. and Perry, J. (1998). Knee kinetics in trans-tibial amputee gait. *Gait & Posture* **8**, 1-7.

Powers, C. M., Torburn, L., Perry, J. and Ayyappa, E. (1994). Influence of prosthetic foot design on sound limb loading in adults with unilateral below-knee amputations. *Archives of Physical Medicine and Rehabilitation* **75**, 825-9.

Prilutsky, B. I. and Zatsiorsky, V. M. (1994). Tendon action of two-joint muscles: transfer of mechanical energy between joints during jumping, landing, and running. *Journal of Biomechanics* **27**, 25-34.

Prince, F., Allard, P., Therrien, R. G. and McFadyen, B. J. (1992). Running gait impulse asymmetries in below-knee amputees. *Prosthetics and Orthotics International* **16**, 19-24.

Prinsen, E. C., Nederhand, M. J. and Rietman, J. S. (2011). Adaptation strategies of the lower extremities of patients with a transtibial or transfemoral amputation during level walking: a systematic review. *Archives of Physical Medicine and Rehabilitation* **92**, 1311-25.

Rabuffeti, M., Recalcati, M. and Ferrarin, M. (2005). Trans-femoral amputee gait: socket-pelvis constraints and compensation strategies. *Prosthetics and Orthotics International* **29**, 183-192.

Rao, G., Amarantini, D., Berton, E. and Favier, D. (2006). Influence of body segments' parameters estimation models on inverse dynamics solutions during gait. *Journal of Biomechanics* **39**, 1531-1536.

Richards, J. G. (1999). The measurement of human motion: A comparison of commercially available systems. *Human Movement Science* **18**, 589-602.

Riemer, R., Hsiao-Wecksler, E. T. and Zhang, X. (2008). Uncertainties in inverse dynamics solutions: a comprehensive analysis and an application to gait. *Gait & Posture* **27**, 578-88.

Robertson, D. G. and Winter, D. A. (1980). Mechanical energy generation, absorption and transfer amongst segments during walking. *Journal of Biomechanics* **13**, 845-54.

Royer, T. D. and Wasilewski, C. A. (2006). Hip and knee frontal plane moments in persons with unilateral, trans-tibial amputation. *Gait & Posture* **23**, 303-6.

Rusaw, D. and Ramstrand, N. (2010). Sagittal plane position of the functional joint centre of prosthetic foot/ankle mechanisms. *Clinical Biomechanics* **25**, 713-20.

Salo, A. I., Bezodis, I. N., Batterham, A. M. and Kerwin, D. G. (2011). Elite sprinting: are athletes individually step-frequency or step-length reliant? *Medicine and Science in Sports and Exercise* **43**, 1055-62.

Sanderson, D. and Martin, P. (1996). Joint kinetics in unilateral below-knee amputee patients during running. *Archives of Physical Medicine and Rehabilitation* **77**, 1279.

Saris, W. H., Blair, S. N., van Baak, M. A., Eaton, S. B., Davies, P. S., Di Pietro, L., Fogelholm, M., Rissanen, A., Schoeller, D., Swinburn, B. et al. (2003). How

much physical activity is enough to prevent unhealthy weight gain? Outcome of the IASO 1st Stock Conference and consensus statement. *Obesity Reviews* **4**, 101-14.

Scott, S. H. and Winter, D. A. (1990). Internal forces of chronic running injury sites. *Medicine and Science in Sports and Exercise* **22**, 357-69.

Segal, A. D., Orendurff, M. S., Klute, G. K., McDowell, M. L., Pecoraro, J. A., Shofer, J. and Czerniecki, J. M. (2006). Kinematic and kinetic comparisons of transfemoral amputee gait using C-Leg and Mauch SNS prosthetic knees. *Journal of Rehabilitation Research and Development* **43**, 857-70.

Selles, R. W., Bussmann, J. B., Klip, L. M., Speet, B., Van Soest, A. J. and Stam, H. J. (2004). Adaptations to mass perturbations in transtibial amputees: Kinetic or kinematic invariance? *Archives of Physical Medicine and Rehabilitation* **85**, 2046-2052.

Selles, R. W., Bussmann, J. B. J., Wagenaar, R. C. and Stam, H. J. (1999). Effects of prosthetic mass and mass distribution on kinematics and energetics of prosthetic gait: A systematic review. *Archives of Physical Medicine and Rehabilitation* **80**, 1593-1599.

Selles, R. W., Korteland, S., Van Soest, A. J., Bussmann, J. B. and Stam, H. J. (2003). Lower-leg inertial properties in transtibial amputees and control subjects and their influence on the swing phase during gait. *Archives of Physical Medicine and Rehabilitation* **84**, 569-577.

Seroussi, R. E., Gitter, A., Czerniecki, J. M. and Weaver, K. (1996). Mechanical work adaptations of above-knee amputee ambulation. *Archives of Physical Medicine and Rehabilitation* **77**, 1209-14.

Shemmell, J., Johansson, J., Portra, V., Gottlieb, G. L., Thomas, J. S. and Corcos, D. M. (2007). Control of interjoint coordination during the swing phase of normal gait at different speeds. *Journal of Neuroengineering and Rehabilitation* **4**, 10-10.

Silverman, A. K., Fey, N. P., Portillo, A., Walden, J. G., Bosker, G. and Neptune, R. R. (2008). Compensatory mechanisms in below-knee amputee gait in response to increasing steady-state walking speeds. *Gait & Posture* **28**, 602-9.

Singh, R., Hunter, J. and Philip, A. (2007). The rapid resolution of depression and anxiety symptoms after lower limb amputation. *Clinical Rehabilitation* **21**, 754-9.

Smith, J. D. (2008). Effects of prosthesis inertia on the mechanics and energetics of amputee locomotion. In *Kinesiology*, vol. Doctor of Philosophy: The Pennsylvania State University.

Stanish, W. D. (1984). Overuse injuries in athletes: a perspective. *Medicine and Science in Sports and Exercise* **16**, 1-7.

Stefanyshyn, D. J., Stergiou, P., Lun, V. M. Y. and Meeuwisse, W. H. (2001). Dynamic variables and injuries in running. In *5th Symposium on Footwear Biomechanics*. Zurich, Switzerland.

Su, P. F., Gard, S. A., Lipschutz, R. D. and Kuiken, T. A. (2007). Gait characteristics of persons with bilateral transtibial amputations. *Journal of Rehabilitation Research and Development* **44**, 491-501.

Taunton, J. E., Ryan, M. B., Clement, D. B., McKenzie, D. C., Lloyd-Smith, D. R. and Zumbo, B. D. (2002). A retrospective case-control analysis of 2002 running injuries. *British Journal of Sports Medicine* **36**, 95-101.

Taylor, C. R. (1994). Relating mechanics and energetics during exercise. *Advances in Veterinary Science and Comparative Medicine* **38A**, 181-215.

Taylor, J. R. (1997). An Introduction to Error Analysis: The Study of Uncertainties in Physical Measurements. Sausalito, Calif.: University Science Books.

Torburn, L., Perry, J., Ayyappa, E. and Shanfield, S. L. (1990). Below-knee amputee gait with dynamic elastic response prosthetic feet: a pilot study. *Journal of Rehabilitation Research and Development* **27**, 369-84.

van Gent, R. N., Siem, D., van Middelkoop, M., van Os, A. G., Bierma-Zeinstra, S. M. and Koes, B. W. (2007). Incidence and determinants of lower extremity running injuries in long distance runners: a systematic review. *British Journal of Sports Medicine* **41**, 469-80; discussion 480.

Ventura, J. D., Segal, A. D., Klute, G. K. and Neptune, R. R. (2011). Compensatory mechanisms of transtibial amputees during circular turning. *Gait & Posture* **34**, 307-12.

Walter, S. D., Hart, L. E., McIntosh, J. M. and Sutton, J. R. (1989). The Ontario cohort study of running-related injuries. *Archives of Internal Medicine* **149**, 2561-4.

Wells, R. P. (1988). Mechanical energy costs of human movement: an approach to evaluating the transfer possibilities of two-joint muscles. *Journal of Biomechanics* **21**, 955-64.

Weyand, P. G. and Bundle, M. W. (2010a). Last Word on Point:Counterpoint: Artificial limbs do make artificially fast running speeds possible. *Journal of Applied Physiology* **108**, 1019.

Weyand, P. G. and Bundle, M. W. (2010b). Point: Counterpoint: Artificial limbs do make artificially fast running speeds possible. *Journal of Applied Physiology* **108**, 1011-1012.

Weyand, P. G. and Bundle, M. W. (2010c). Point:Counterpoint Rebuttal from Weyand and Bundle. *Journal of Applied Physiology* **108**, 1014.

Weyand, P. G., Bundle, M. W., McGowan, C. P., Grabowski, A., Brown, M. B., Kram, R. and Herr, H. (2009). The fastest runner on artificial legs: different limbs, similar function? *Journal of Applied Physiology* **107**, 903.

Weyand, P. G., Sandell, R. F., Prime, D. N. L. and Bundle, M. W. (2010). The biological limits to running speed are imposed from the ground up. *Journal of Applied Physiology*, 950-961.

Weyand, P. G., Sternlight, D. B., Bellizzi, M. J. and Wright, S. (2000). Faster top running speeds are achieved with greater ground forces not more rapid leg movements. *Journal of Applied Physiology* **89**, 1991-9.

Williams, K. R., Cavanagh, P. R. and Ziff, J. L. (1987). Biomechanical studies of elite female distance runners. *International Journal of Sports Medicine* **8 Suppl 2**, 107-18.

Wilson, J. R., Asfour, S., Abdelrahman, K. Z. and Gailey, R. (2009). A new methodology to measure the running biomechanics of amputees. *Prosthetics and Orthotics International* **33**, 218-29.

Wing, D. C. and Hittenberger, D. A. (1989). Energy-storing prosthetic feet. *Archives of Physical Medicine and Rehabilitation* **70**, 330-5.

Winter, D. A. (1983a). Energy generation and absorption at the ankle and knee during fast, natural, and slow cadences. *Clinical Orthopaedics and Related Research*, 147-54.

Winter, D. A. (1983b). Moments of force and mechanical power in jogging. *Journal of Biomechanics* **16**, 91-7.

Winter, D. A. (2005). Biomechanics and Motor Control of Human Movement. Hoboken, N.J.: John Wiley & Sons.

Winter, D. A. and Sienko, S. E. (1988). Biomechanics of below-knee amputee gait. *Journal of Biomechanics* **21**, 361-7.

Yap, T. L. and Davis, L. S. (2008). Physical activity: the science of health promotion through tailored messages. *Rehabilitation Nursing* **33**, 55-62.

Zatsiorsky, V. M. (2002). Kinetics of Human Motion. Champaign, IL: Human Kinetics.

Zatsiorsky, V. M., Seluyanov, V. N. and Chugunova, L. G. (1990a). In vivo body segment inertial parameters determination using a gamma-scanner method. In *Biomechanics of Human Movement: Applications in Rehabilitation, Sports, and Ergonomics*, eds. N. Berme and A. Cappozzo), pp. 186-202. Worthington, Ohio: Bertec Corp.

Zatsiorsky, V. M., Seluyanov, V. N. and Chugunova, L. G. (1990b). Methods of determining mass-inertial characteristics of human body segments. In *Contemporary Problems of Biomechanics*, eds. G. G. Chernyi and S. A. Regirer), pp. 272-291. Boca Raton, Florida: CRC Press.

Ziegler-Graham, K., MacKenzie, E. J., Ephraim, P. L., Travison, T. G. and Brookmeyer, R. (2008). Estimating the prevalence of limb loss in the United States: 2005 to 2050. *Archives of Physical Medicine and Rehabilitation* **89**, 422-9.